Instituto de Neurociencias de Alicante
Consejo Superior de Investigaciones Científicas
Universidad Miguel Hernández

Thesis manuscript for:

Ph.D. in Neurosciences title

SYNAPTIC EFFECTS OF GLUK4 SUBUNIT OVEREXPRESSION

Valeria Pecoraro

Supervised by:

Prof. Juan Lerma

Year 2017

UNIVERSITAS
Miguel
Hernández

“Las ideas no se muestran fecundas con quien las sugiere o las aplica por primera vez, sino con los tenaces que las sienten con vehemencia y en cuya virtualidad ponen toda su fe y todo su amor. Bajo este aspecto, bien puede afirmarse que las conquistas científicas son creaciones de la voluntad y ofrendas de la pasión”

Santiago Ramón y Cajal

UNIVERSITAS
Miguel
Hernández

ACKNOWLEDGMENTS

First and foremost I want to express my gratitude to my advisor Prof. Juan Lerma for providing me the chance to carry out this work. I appreciate all his contributions of time and ideas to make my Ph.D. experience productive and stimulating. He contributed to this rewarding experience by giving me intellectual freedom in my work, engaging me in new ideas, and demanding a high quality in all my endeavors, including this manuscript. I gratefully acknowledge the funding sources that allowed me to pursue this work: SANTIAGO-GRISIOLIA fellowship from the “Generalitat Valenciana”.
Besides my advisor, I would like to thank the rest of my thesis committee: for being here, this is going to incent me to widen my research from various perspectives. My sincere thanks also go to all the members of the Lab. with whom I had the pleasure to work. They provided a friendly and cooperative atmosphere at work and also useful feedback and insightful comments on my work. Particularly, I am grateful to Ana for her help in *in vitro* electrophysiology, data analysis and for our “therapy sessions” especially in times of stress; to Isabel for our talk and discussion about the project in its development. I thank my labmates Sergio, Vinette, Amr and Alvaro for the stimulating discussions, for the weekends we were working together before deadlines, and for all the ideas resources and constructive questions, we have had in the last four years. Thanks also to Monica Llinares (for me *Monic*) for her everyday precious help and motivation, when all seemed to go in the wrong way she had always nice words for me. I thank my friends in the IN of Alicante. Particularly, I really want to thank Maribel, *“mi amiga del alma española”,* for our coffee times, for her continuous support, and for her patience in listening all my doubts, preoccupations and new ideas about my work. Her precious endorsement made my everyday life, here in Alicante, better than I expected. She made me feel at home in every circumstance and I thank her for her friendship, love, and unyielding support. I could not have imagined having a better friend during my stay in Alicante. I would also to thank Maria for her advice, I hope we’ll have the opportunity to better get know each other, she is a really nice and good person.

I also would like to express my gratitude to all my lifelong friends Federica, Serafina, Claudia, and Sara for our updates about our life abroad, which made me feel not alone outside Sicily, our motherland that keep our happy and special times together. I really thank them for always being there for me despite the distance.

I would like to express my sincerest and warm thanks to my family. I most thank my parents for all they always do for me, for teaching me good values, those important and essential values which guide my life and support all my pursuits, throughout writing this thesis. I am where I am today because of them. I also wish to thank my brother, whose calls arrived always at the right moment, like our

fraternal tune was attracting his support, even at 3000 miles away. You, Family, mean so much to me.

Last, but not least, a very special gratitude goes to Davide for being a supportive and patient boyfriend; for encouraging me in all my decisions, including the one to start a Ph.D. abroad and with it a long distance relationship. He has never made me feel being away. I want to thank him for his endlessly commitment and belief in us, that belief which could endure any circumstance and reach across any distance. Thank you, Amore Mio!

Thank you all so much again

ABSTRACT

Kainate receptors (KARs) are members of the family of ionotropic glutamate receptors (iGluRs) which also includes NMDA and AMPA receptors. They are critically important molecules for normal brain function and constitute a complex signaling system at most of the excitatory synapses in the brain. Five separate genes (*GRIK*1-5) encode the different receptor subunits, GluK1-GluK5, (previously known as GluR5-7, KA1 and KA2), which assemble to form both homomeric and heteromeric receptors. The structural and functional diversity of these receptors is also achieved by alternative splicing and RNA editing of the subunits. KARs not only mediate but also modulate synaptic transmission and they use both canonical and non-canonical (metabotropic) modes of signaling. Furthermore, KARs play an instrumental role in the functional and activity-dependent development of neuronal activity in many areas of the brain. Different brain pathologies involving KARs dysfunction have been also described. For instance, some abnormalities in the *GRIK*4 gene (coding for the GluK4 human subunit) are present in individuals with schizophrenia and learning disability.

The rationale for the present study was based on recent findings indicating that common variants in the *GRIK*4 gene, as well as the duplication of the chromosomal region encompassing the *GRIK*4 locus, are associated with numerous developmental problems including bipolar disorders, schizophrenia, and autism.

To investigate the role of GluK4-containing KARs in brain physiology and disease, our lab has generated mice overexpressing *grik*4 gene in the forebrain. These mice have an excess of GluK4 protein, which is expected to occur in humans carrying an In-Del variant of *GRIK*4 associated to resistance to bipolar disorders. Also, a de novo duplication of the segment containing *GRIK*4 in the chromosome 11 has been found is cases of autism. Indeed, behavioral studies revealed that these mice display anhedonia, enhanced anxiety, and depression, as well as impaired social interaction, which are common endophenotypes associated with Autism Spectrum Disorders (ASDs).

In this work, we show that overexpression of *grik*4 gene in mice causes an abnormality in the neuronal activity likely affecting global information processing in the hippocampus, mainly affecting the mossy fiber-CA3 (MFs-CA3) neuron synapses, where the GluK4 protein is abundantly expressed. Indeed, the excess of GluK4 protein alters the information transfer through the hippocampal circuit.

The analysis of synaptic transmission in the hippocampal MFs-CA3 synapses reveled that overexpressed GluK4 protein participates of functional KARs at both sides of the synapse. Presynaptically, GluK4-containing KA autoreceptors set a higher amount of neurotransmitter to be released, caused by their tonic activation. This leads to a marked alteration of short-term synaptic plasticity.

Postsynaptically, an excess of GluK4 protein produces the enlargement of KARs- and AMPARs-mediated currents concomitant to a depression of NMDARs-mediated currents.

The larger amplitude observed both in the evoked and elementary AMPARs/KARs-mediated EPSC ($EPSC_{AMPARs/KARs}$) is accounted for the both an increase in the KAR-mediated synaptic component and the enhanced presence of AMPARs lacking GluA2 in $GluK4^{Over}$ mice. These data led us to conclude that in $GluK4^{Over}$ mice there should be an impairment of the normal synapse maturation, where AMPARs-subunits trafficking is altered.

Finally, we showed that the normalization of the levels of GluK4 protein restores the synaptic phenotype observed in $GluK4^{Over}$ mice. Also, the antidepressant, Tianeptine, reverts some behavioral deficits and reestablishes the synaptic normality in $GluK4^{Over}$ mice in slices exposed to this drug.

In summary, the present results shed new light on the function of GluK4-containing KARs in establishing the properties of synaptic information flow through the trisynaptic hippocampal circuit as well as a role in the proper maturation of MFs–CA3 synapses, demonstrating the functional importance of these receptors for plasticity in the hippocampus.

This work also suggests that GluK4 may be relevant for the understanding of the role played by glutamatergic neurotransmission in ASDs and for the development of potential therapeutic approaches for this neurodevelopmental/psychiatric disorder.

RESUMEN

Los receptores de kainato (KARs) pertenecen a la familia de receptores Ionotrópicos de glutamato (iGluRs) que incluye también a los receptores NMDA y AMPA. Son moléculas con una importancia crítica para la función fisiológica cerebral y constituyen un sistema de señalización complejo en la mayoría de las sinapsis excitatorias del cerebro. Cinco genes distintos (*GRIK*1-5) codifican las diferentes subunidades del receptor, GluK1-GluK5, (conocidas anteriormente como GluR5-7, KA1 y KA2), las cuales se asocian para formar receptores homoméricos y heteroméricos. La diversidad estructural y funcional de los receptores también se logra mediante el splicing alternativo y la edición del ARN de estas subunidades. Los KARs no sólo median, sino que también modulan la transmisión sináptica y usan modos de señalización canónicos y no canónicos (metabotrópicos). Además, los KARs juegan un papel instrumental en el desarrollo funcional y dependiente de actividad neuronal, en muchas áreas del cerebro.

Igualmente, se han descrito diferentes patologías cerebrales que implican la disfuncionalidad de KARs. Por ejemplo, algunas anomalías en el gen *GRIK4* (que

codifica para la subunidad GluK4 humana) están presentes en individuos con esquizofrenia y discapacidad de aprendizaje.

La justificación del presente estudio se basa en recientes hallazgos genéticos humanos, que indican que las variantes comunes en el gen *GRIK4*, así como la duplicación cromosómica de una región que abarca el locus *GRIK4*, se asocian a numerosos problemas incluyendo trastornos bipolares, esquizofrenia y autismo.

Para investigar el papel de los KARs que contienen GluK4 en condiciones fisiológicas y patológicas, nuestro laboratorio ha generado ratones que sobreexpresan el gen *grik*4 en el Telencéfalo. Estos ratones contienen un exceso de proteína GluK4, lo cual se espera que ocurra en seres humanos que portan una variante In-Del de *GRIK*4 asociada a mayor resistencia a trastornos bipolares. Además, se ha encontrado una duplicación “de novo” en el cromosoma 11 del segmento que contiene *GRIK*4, en niños con autismo. De hecho, los ensayos conductuales revelaron que estos ratones exhiben anhedonia, ansiedad aumentada, y depresión, así como interacción social disminuida, los cuales son endofenotipos comunes asociados con trastornos del espectro autista (ASDs).

En este trabajo, hemos demostrado que la sobreexpresión del gen *grik*4 en ratones, provoca anomalías en la actividad neuronal que afecta el procesamiento de información en el hipocampo, afectando principalmente a las sinapsis de las neuronas de las fibras musgosas con las neuronas de CA3 (MFs-CA3), donde la proteína GluK4 se expresa abundantemente. El exceso de proteína GluK4 altera la transferencia de información a través del circuito del hipocampo.

La transmisión sináptica en MFs-CA3 del hipocampo, reveló que la proteína GluK4 sobreexpresada, forma parte de los KARs funcionales en ambos lados de la sinapsis. Presinápticamente, los autoreceptores KARs que contienen GluK4 aumentan la liberación de mayor cantidad de neurotransmisor, causada por su propia activación tónica. Esto conduce a una marcada alteración de la plasticidad sináptica a corto plazo. Postsinápticamente, un exceso de la proteína GluK4 produce un aumento de las corrientes mediadas por KARs y AMPARs, concomitante con una depresión de la corriente mediada por NMDARs.

El aumento de la amplitud observada en los EPSC mediados por AMPARs /KARs ($EPSC_{AMPARs/KARs}$) basales y evocadas, se explica por la mayor presencia tanto de KARs como de AMPARs que carecen de la subunidad GluA2 en los ratones $GluK4^{Over}$, y en parte, por la elevada probabilidad de liberación de glutamato causada por los KARs presinápticos. Estos datos nos llevaron a concluir que en los ratones $GluK4^{Over}$ debería haber una alteración de la maduración normal de la sinapsis, en las cuales el tráfico de subunidades AMPARs se ve modificado.

Finalmente, hemos demostrado que la normalización de los niveles de proteína GluK4 restaura el fenotipo sináptico observado en ratones $GluK4^{Over}$. Además,

el antidepresivo Tianeptine, revierte algunos déficits de comportamiento y restablece la normalidad sináptica en rodajas de ratones GluK4^{Over} expuestas a este medicamento.

En resumen, estos resultados arrojan nueva luz sobre la función de los KARs que contienen GluK4 en el establecimiento de las propiedades del flujo de información sináptica desde el giro dentado a las células piramidales CA3 y su papel en la apropiada maduración de las sinapsis MFs-CA3, demostrando la importancia funcional de estos receptores para la plasticidad hipocámpica.

Este trabajo también sugiere que GluK4 puede ser relevante para la comprensión del papel que desempeña la neurotransmisión glutamatérgica en el ASDs y para el desarrollo de posibles enfoques terapéuticos para este trastorno psiquiátrico y del desarrollo.

WORK COMMUNICATIONS

Pecoraro V, Paternain AV, Aller MI, and Lerma J. Overexpression of *grik4* modifies synaptic transmission flow through mossy fiber-CA3 synapses. 16th Congress of the Spanish Society for Neuroscience, 23-25 September 2015, Granada Spain.

Pecoraro V, Aller MI, and Lerma J. Overexpression of *grik4* alters glutamatergic transmission at mossy fiber-CA3 synapses. 10th FENS Forum of Neuroscience, 2-6 July 2016, Copenhagen, Denmark.

PUBBLICATION

Aller MI, Pecoraro V, Paternain AV, Canals S, Lerma J (2015). Increased dosage of high-affinity kainate receptor gene GRIK4 alters synaptic transmission and reproduces Autism Spectrum Disorder feature. J Neurosci. 35: 13619-13628.

UNIVERSITAS
Miguel
Hernández

LIST OF ABBREVIATIONS

A/C	Associational/Commissural
ACSF	Artificial Cerebrospinal Fluid
AMPA	α-amino-3-hydroxy-5- methyl-4-isoxazole proprionic acid
AMPAR	α-amino3-hydroxy-5-methyl-4-isoxazolepropionic acid receptors
AP	Action Potential
ASDs	Autism Spectrum Disorders
ATP	Adenosine Triphosphate
AZ	Active Zone
CA	Cornu Ammonis or Ammun's horn
CaMKII	Calcium/Calmodulin-dependent protein Kinase II
cAMP	Cyclic Adenosine Mono Phosphate
CI-AMPARs	Ca^{2+}-impermeable AMPARs
CNVs	Copy Number Variation
CP-AMPARs	Ca^{2+}-permeable AMPARs
CNS	Central Nervous System
CNQX	6-cyano-7-nitroquinoxaline
D-APV	(2*R*)-amino-5-phosphonovaleric acid; (2*R*)-amino-5-phosphonopentanoate
DG	Dentate Gyrus
DNA	Deoxyribonucleic Acid
DRG	Dorsal Root Ganglion
DNQX	Dinitroquinoxaline-2,3-dione
EC	Enthorinal Cortex

eEPSC	evoked Excitatory PostSynaptic Current
EPSC	Excitatory PostSynaptic Current
EGTA	Ethylene glycol-bis(β-aminoethyl ether)-N,N,N',N'-tetraacetic acid
fEPSP	field Excitatory Post Synaptic Potentials
FF	Frequency Facilitation
GABA	Gamma-AminoButyric Acid
GC	Granule Cell
G.C.L.	Granular Cell Layer
GFP	Green Fluorescent Protein
GluK4	Glutamatergic iontropic Kainate Receptor subunit 4
GluK4-KARs	GluK4-containing Kainate Receptors
GPCR	G-protein-coupled receptors
GTP	GuanosineTriphosphate
HFS	High Frequency Stimulation
ID	Intellectual Disability
iGluR	ionotropic Glutamate Receptors
IQ	Intelligence Quotient
KARs	Kainate Receptor
KA	Kainate
LFP	Local Field Potential

LFS	Low Frequency Stimulation
LTD	Long-Term Depression
LTP	Long-Term Potentiation
Lu	Stratum lucidum
mEPSCs	Miniature Excitatory PostSynaptic Currents
MFBs	Mossy Fiber Boutons
MFs	Mossy Fibers
mGluR	metabotropic Glutamate Receptors
mRNA	messenger RiboNucleic Acid
NBQX	2,3-dihydroxy-6-nitro-7-sulphamoyl-benzo(F)quinoxaline
NMDA	N-methyl-D-aspartate
NMDAR	N-methyl-D-aspartate receptors
NTD	N-Terminal Domain
PCR	Polymerase Chain Reaction
PhTx	Philanthotoxin
PKC	Protein Kinase C
PP	Perforant Path
PPR	Paired-Pulse Ratio
Pr	Probability of Release
PSD	Post Synaptic Density
PSD-95	Post Synaptic Density Protein 95
PTP	Post-Tetanic Potentiation
P.C.L.	Purkinje Cell Layer
Py	Pyramidal cells
Or	Stratum oriens

R_a	Stratum radiatum
RI	Rectification Index
Rpm	rounds per minute
RNA	Ribo Nucleic Acid
S_C	Schaffer Collaterals
sEPSC	spontaneous Inhibitory Post Synaptic Currents
sI_{AHP}	Slow afterhyperpolarisation
SNPs	Single-Nucleotide Polymorphism
T_{LE}	Temporal-Lobe Epilepsy
TM	Trans Membrane domain
TTx	Tetrodoxin
U_{BP310}	S)-1-(2-Amino-2-carboxyethyl)-3-(2-carboxy-thiophene-3-yl-methyl)-5-methylpyrimidine-2,4-dione

TABLE OF CONTENTS

UNIVERSITAS
Miguel
Hernández

1. Introduction

UNIVERSITAS
Miguel
Hernández

1.1 NEUROTRANSMISSION

The nervous system counts on synapses to perform a fast communication between cells. The synapse constitutes the structural unit with a pre synaptic terminal juxtaposed to a post synaptic cell. Depending on the structure of apposition zone, synapses can be categorized in two mainly groups: electrical and chemical. In the electrical synapses the pre- and post-synaptic membranes are not separated (distance about 3.5 nm) and the current flows through gap junction proteins. At a chemical synapse the distance between neurons is much larger (20 to 40 nm) and the electrical impulses, which propagate along nerve fibers to their terminals, initiate a series of events that produces the release of chemical neurotransmitters. Released neurotransmitters bind to their receptors on the post synaptic cell membrane, which activation either excites or inhibits the post synaptic cell. Any alteration in this process can interfere in the proper function of neurons leading to aberrant consequences. Thus, the analysis of such processes is of fundamental importance to understand neurological disorders.

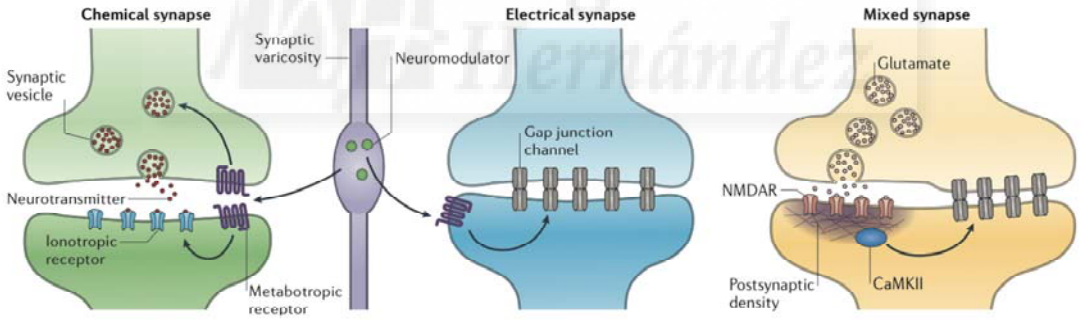

Figure 1: Synapse types according to transmission nature *(Modified from Pereda, 2014)*. Chemical synapses communication between pre- and postsynaptic cells is unidirectional with a certain delay necessary for the arrival of information at the presynaptic terminal and its transfer to the postsynaptic cell. Instead in the electrical synapses communication can be both bidirectional and/or unidirectional and instantaneous electronic transmission is provide by gap junctions. Finally, neurons coupled with electrical synapses may also form chemical synapses resulting in the so-called “Mixed synapses”.

1.1.1 GLUTAMATERGIC TRANSMISSION

The amino acid glutamate is the principal excitatory neurotransmitter in the mammalian central nervous system and exerts its actions on cells via activation of glutamate receptors, critically important molecules for normal brain function. Glutamate receptors transduce the vast majority of excitatory neurotransmission and regulate the strength of both excitatory and inhibitory transmission in the nervous system. Two class of these receptors exist: one class, known as the ionotropic glutamate receptors, includes a diverse group of ion channels that are permeable to cations (Ca^{2+}, Na^{+}), the second class of glutamate receptors, and known as metabotropic glutamate receptors, activate or inhibit second messenger systems via interactions with G-proteins.

Ionotropic Glutamate Receptors (iGluRs)

Ionotropic glutamate receptors are grouped in four receptor families, named on the basis of agonist selectivity: kainate (KA), α-amino-3-hydroxy-5- methyl-4-isoxazole proprionic acid (AMPA), N-methyl-D-aspartate (NMDA) and delta receptors. Ionotropic glutamate receptors are tetrameric protein complexes composed by four subunits, whose composition and expression profile confer them different ion-channel properties. Each subunit shows a characteristic organization consisting in: 1) a large extracellular N-terminal domain (~380 amino acids); 2) an agonist binding domain (~ 300 amino acids); a transmembran domain formed by three membrane spanning-segments (M1, M2, M4) and a membrane reentrant loop (M2); 4) a cytoplasmatic carboxy-terminal domain interacting with numerous intracellular scaffolding and trafficking proteins.

Metabotropic Glutamate Receptors (mGluRs)

mGluRs are members of G-protein-coupled receptors (GPCR) superfamily. They are membrane spanning proteins that transduce intracellular signals via interactions with G proteins. Activated G-protein subunits then modulate the function of various effector molecules such as enzymes, ion channels, and transcription factors. As other GPCRs, mGluRs consist of an extracellular N-terminal domain, seven transmembrane spanning domains separated by an extracellular loops, and an intracellular C-terminus.

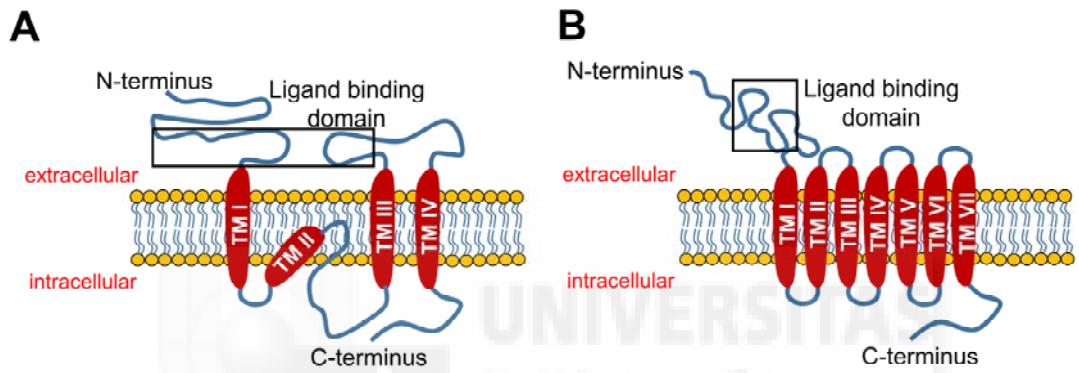

Figure 2: General structure of ionotropic and metabotropic glutamate receptors. A) All ionotropic glutamate receptor (iGluR) subunits possess four hydrophobic regions within the central portion of the sequence. Only the TMII domain forms a re-entrant loop giving these receptor subunits an extracellular N-terminus and intracellular C-terminus. In addition, the long loop between TMIII and TMIV, which is intracellular in other ligand gated ion channel subunits, is exposed to the cell surface, and forms part of the binding domain with half of the N-terminus. **B)** Metabotropic glutamate receptors (mGluRs) possess a 7-transmembrane domain motif (TM), with a larger N-terminal domain and an intracellular C-terminus and they have not large inter-helical loops.

1.2 THE HIPPOCAMPUS

The earliest description of the hippocampus comes from the Venetian anatomist Julius Caesar Aranzi (1587), who initially likened it to a seahorse, using the Latin *hippocampus* because of its shape. The hippocampus is an important limbic system structure of the vertebrate brains located in the medial temporal lobe, between septal and hypothalamic region, to which is connected by the fornix. In rodents, in which it has been well studied, the hippocampus has roughly the shape of a banana. In humans it has a curved and convoluted shape.

1.2.1 ANATOMICAL STRUCTURE AND LOCAL CIRCUITS

The hippocampus proper and its neighboring cortical regions, the dentate gyrus (DG), subiculum and enthorinal cortex (EC), are collectively termed “hippocampal formation”. The hippocampus proper, also called Ammon’s horn or Cornu Ammonis (CA) is divided into 3 distinct areas known as CA3, CA2 and CA1.

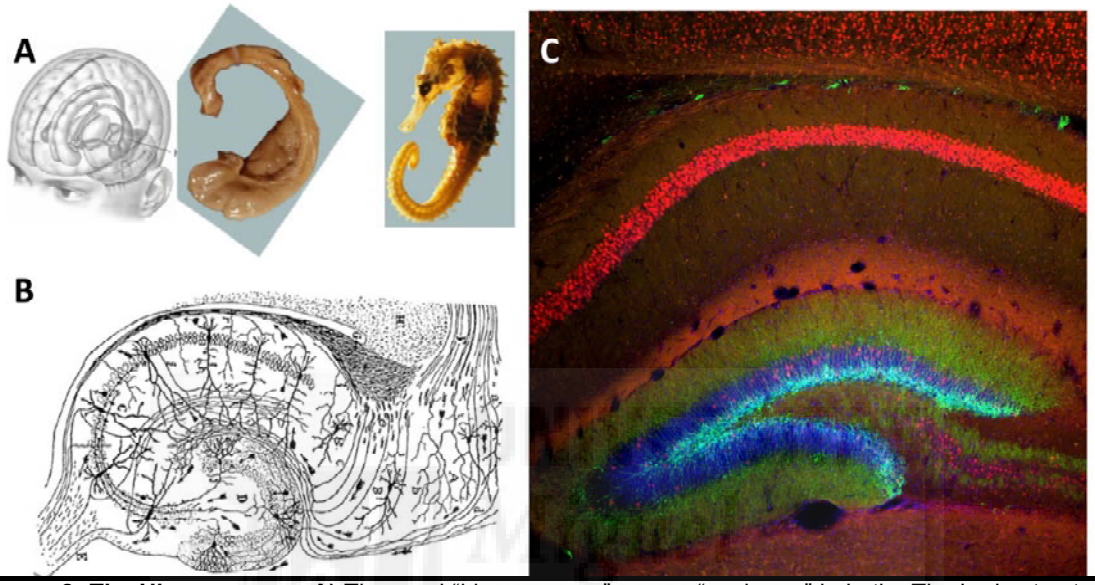

Figure 2: The Hippocampus. A) The word “hippocampus” means “seahorse” in Latin. The brain structure was so named because of its resemblance to the marine creature. **B)** Drawing of the basic circuit of the Hippocampus by Santiago Ramon y Cajal (1884). **C)** Confocal micrograph of young mouse hippocampus.

Thanks to the work of Camillo Golgi on the hippocampus in 1883 great details of this brain structure were revealed, followed by Santiago Ramon y Cajal who culminated in the Neuron Doctrine, establishing modern Neuroscience. In CA1 and CA3 regions, pyramidal neurons are glutamatergic excitatory neurons whose cell bodies are arranged in one continuous layer (pyramidal layer). Most of the afferent projection to the hippocampus originates from the EC, which has a columnar structure and is mutually interconnected with vast areas of the cerebral cortex. The EC is connected to the DG and CA3 area through extensive and disseminated projections (the Perforant Pathway, PP), while DG is connected with the CA3 area in a focused and topographic manner through the Mossy Fibers pathway (MFs). Neurons located in CA3 area are widely connected to each other forming a recurrent network, and, as already mentioned, send axons (the Shaffer Collaterals, SC) to pyramidal CA1 neurons, allowing an extended and rapid connection between the two areas. From CA1 area nerve fibers are sent to the

subiculum; from this area all efferent fibers originated from the hippocampus are directed to the EC and to the mammillary bodies. Thus, the receiving portion of the hippocampal formation consists of the dentate gyrus, while the sending portion consists of the subiculum. Lastly, the information returns to the sensory cortical areas from which it came to be processed by the hippocampus. Taking into account the main hippocampal characteristics and the signal transmission pathways, it is necessary to report how the information is processed at this level and in particular, I will pay attention to the MFs-CA3 synapses that are generally known to be the second link in the classical trisynaptic pathway from the EC to the CA1 hippocampal subfield.

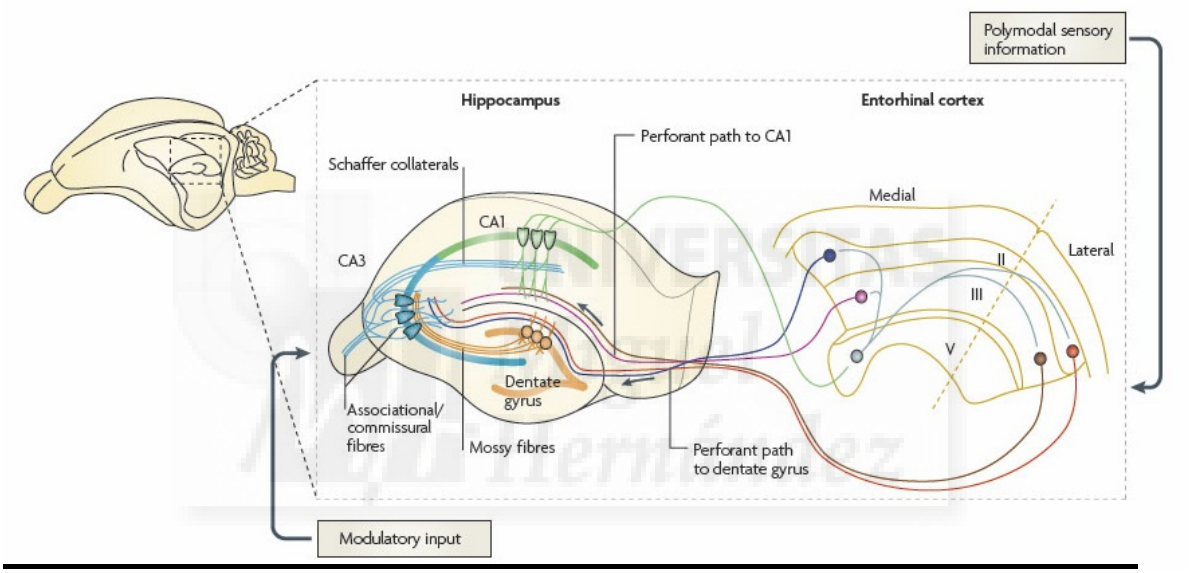

Figure 3: Long-range network of the hippocampus. Information enters via the axons, of neurons in layer II and III, of the EC, known as PP, to the DG. These axons make the loop's first connection with the granule cells of the DG; from these cells, the MFs in turn project to make the loop's second connection, with the dendrites of the CA3 pyramidal cells. The axons of these cells divide into two branches: one branch forms the commissural fibers that project to the contralateral hippocampus via the corpus callosum and the other branch forms the SC pathways making the third connection in the loop, with the CA1 cells. Lastly the CA1 axons project to the neurons of the subiculum and of the EC. Axons from the EC make also contacts with the distal dendrites of pyramidal cells in areas CA3 and CA1. Source: (Neves et al., 2008).

1.2.2 MOSSY FIBER-CA3 SYNAPSES (MFS-CA3)

Synaptic information between the DG and area CA3 of the hippocampus proper flows via axons of granule cells — the MFs pathway. They are so named after the large (up to 5 mm diameter) varicosities present all along the axon, giving them the appearance of being covered in moss (Ramon y Cajal 1911). MFs are organized in a laminar fashion along the pyramidal cell layer and their projection is limited to the stratum lucidum.

The MFs form three types of synaptic contacts onto its target neurons. First, and most notably, are the large expansions that synapse onto CA3 pyramidal neurons, the large mossy boutons (MFB). The large MFs terminals, which contain up to 35 individual release sites enclose the postsynaptic thorny excrescences of CA3 pyramidal neuron dendrites. A single granule cell contacts approximately 15 pyramidal neurons (Amaral et al., 1990) (each terminal synapses onto a single pyramidal neuron).

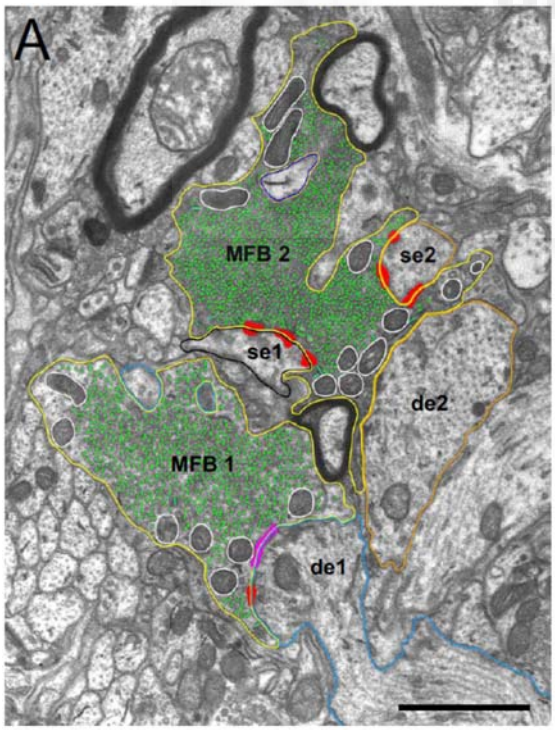

Figure 4: Electron microscopic image of two MFBs (MFB1, MFB2) taken from a P28 rat. Both MFBs outlined in yellow terminate on different dendritic segments (de1, blue contour; de2, orange contour), but especially on CA3 spiny excrescences (se1, black contour; se2, orange contour). Several active zones, AZs, for each synapse are given as red spots and mitochondria are given as white contours. Scale bar: 1µm. Adapted from Rollenhagen et al., 2007.

One CA3 pyramidal neuron may receive up to a total of approximately 50 MFs inputs only (Amaral et al., 1990). Second, 2-4 filopodial extensions arising from these large MFB make synaptic contacts onto interneurons (Acsady et al., 1998). These so-called filopodia are motile and regulated by glutamate (Tashiro et al., 2003). Third, small en passant varicosities, resembling boutons of other hippocampal neurons, also contact CA3 interneurons. The consequence of MFs input into CA3 may be inhibitory or excitatory, conditionally dependent on the frequency of input and modulators regulation. This is further complicated by the characteristics of

transmitter release from MFs where a large number of co-localized transmitters, including GABA; Zn2+, ATP and peptides may effect and modulate transmitter release. Large MFBs forming excitatory inputs on CA3 cells exhibit several unique properties shaping neurotransmission of these synapses, and MFBs have multiple release sites (Rollenhagen et al., 2007).

1.2.3 FUNCTIONS AND SYNAPTIC TRANSMISSION

The first functional description of hippocampal circuits was provided by Santiago Ramón y Cajal at the end of the 19th century. Historically, the earliest widely hypothesis is that the hippocampus was involved in olfactory functions, because of its localization. There is still a particular interest in the involvement of the hippocampus in olfactory functions, but it is now well established that the hippocampal primary function is not the smell. Over the years, the behavioral inhibition theory was very popular up to the 1960s. It derived much of its justification from two observations: first, that animals with hippocampal damage tend to be hyperactive; second, that animals with hippocampal damage often have difficulty in remembering tasks that they had previously learnt, especially if the response requires remaining quiet as in a passive avoidance test. The inhibition theory is currently the least popular of the three, since this and other functions are currently attributed to the amygdala, a structure in the limbic system and anatomically connected to hippocampus.

The second major line of thought relates the hippocampus to the mnemonic system. Russian Vladimir Bechterev noted the role of the hippocampus in memory around 1900, based on the observation of a patient with severe memory disorders. The importance of the hippocampus in memory processes was brought to the general attention thanks to the patient HM, who underwent bilateral removal of the hippocampus for the treatment of an intractable form of epilepsy. Particularly relevant was the observation that HM was still able to learn procedural tasks (associated to the functioning of basal ganglia) and that his intelligence quotient *(IQ)* was above the average. This case demonstrated a clear separation between declarative memory, procedural

memory and intelligence. This and subsequent studies have suggested that the deep structures of the temporal lobe, including the hippocampus (Amaral and Witter, 1989), are involved in the storage of long-term memory traces (Milner et al., 1998; Burgess et al., 2002). Nowadays there is almost universal agreement about the important role of the hippocampus, considered almost universally as the entrance gate of new information that, if properly consolidated, will be sent to the cortical areas, seat of long-term memory.

The third important theory of hippocampal function relates the hippocampus to space. Evidence has been provided that the hippocampus is involved in storing and processing spatial information. Studies on rodents have demonstrated that some neurons in the hippocampus possess spatial firing fields. These cells, called “place cells” (O'Keefe j, D. J., 1971), fire when the animal finds itself in a particular location in the space regardless the direction of navigation. Place cells have been also seen in humans involved in finding their way around a virtual reality town (Ekstrom et al., 2003). The discovery of place cells led to the idea that the hippocampus may represent a “cognitive map”. Since the hippocampus is a structure of great importance for the preservation of memory traces and learning processes, it is helpful to see the general lines which explain the basis of these processes emphasizing the complex molecular mechanism that govern them.

1.2.4 Learning and Memory

Learning and memory are two of the most important aspects of the nervous system function: they allow adaption to the environment, expand cultural background, and create your own individual history. Humans have something valuable: the ability to learn from experience, to modify thoughts and behavior as a function of what they experienced. In fact, learning is the process by which experience modifies the nervous system and the subsequent individual behavior. Memory is the process by which previously learned information is stored and kept. Many types of information arrive to the hippocampus, from extensive cortical areas that provide a representative input of the environment state at all times.

These information are very dense and need to be processed into a sparse code, which is indispensable for the efficient storage and recall of multiple, multidimentional memory items.

After processing cortical noisy inputs, the hippocampus creates new associations, record information on different levels, selects some, leaves decaying other ones (for example those that interfere) and finally refers the representation to the EC, from which it received the initial input. The EC is, therefore, both the main entrance and the main output of the hippocampus. The hippocampal system operates essentially through two mechanisms that are competing each other:

- Pattern separation: is the mechanism used for encoding new information: activation input from EC arrives to the DG and CA3 area; here they are processed and represented through scattered neural units and separated to be more dissimilar. The storage capacity of such network (the number of patterns they can store and retrieve reliably) is roughly inversely proportional to the sparsity of individual patterns, and generally increases as the overlap between different stored pattern decreases. The EC input is sent concomitantly to the CA1 area and there is an association between representations of CA1 and CA3. From the CA1 area then, the representation, after processing and associating, can return to the EC.
- Pattern completion or autoassociative memory: is the mechanism that, starting from small fragments of memories, allows you to recall and complete representations of events and situations. The fragmented representation, consisted of cortical input from EC arrives to the dentate gyrus and CA3; here, through the many existing connections, the representation may be supplemented and renewed. The complete representation in CA3 activates the corresponding CA1; and from there, it goes back to the EC no longer fragmented.

There is a natural competition between these two mechanisms. When the brain external inputs arrive, it does not distinguish immediately if the information arising is new (pattern separation), or instead it has to be completed because of existing memory fragments (pattern completion). The role of the hippocampus is to

optimize this ambiguity by creating as many as possible connections to better contextualize information and episodes. Several authors (McNaughton and Morris, 1987; Rolls and Treves, 1998; Rolls and Kesner, 2006) have suggested that the DG cell/MFs to CA3 may be important during the *learning* of new associations in the CA3 network, and that part of the circuit guarantees relatively sparse and orthogonal representations in CA3, by the pattern separation phenomenon. In contrast, the theory predicts that the direct PP input to CA3 is important in initiating *retrieval* from the CA3 autoassociation network, especially with an incomplete retrieval cue.

Short-term plasticity

An attractive feature of synapses is their plastic behavior, provided by their highly dynamic nature, and characterized by changes in the synaptic strength. Short-term synaptic plasticity is referred to changes in the synaptic efficacy that usually occurs on a timescale of milliseconds to minutes. Synaptic changes shape dramatically the pattern selectivity of synapses and the information transfer they mediate. Short-term plasticity typically reflects a presynaptic change in neurotransmitter release, even if also postsynaptic mechanisms may contribute to this phenomenon. Short-term plasticity can result in synaptic enhancement (through three processes: facilitation, augmentation and post-tetanic potentiation) or in synaptic depression (Zucker and Regehr, 2002).

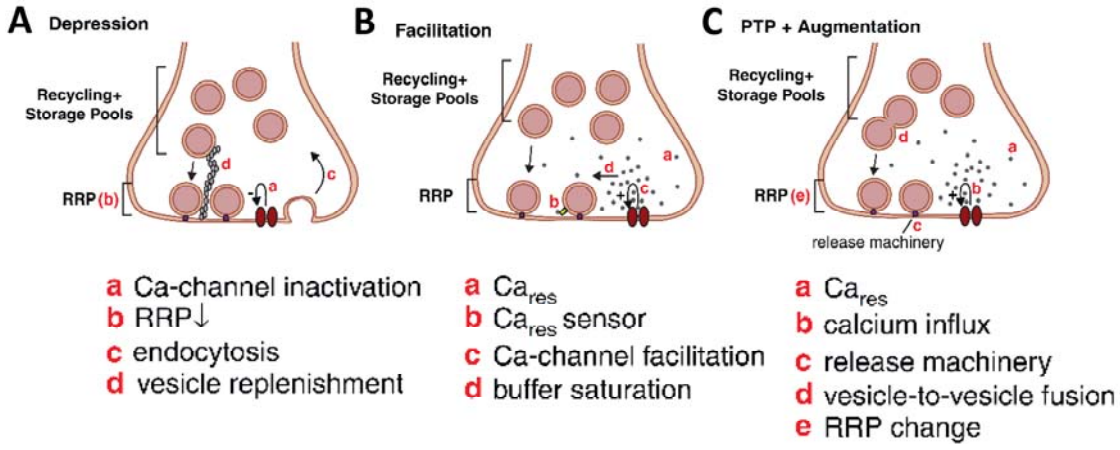

Figure 5: Different use-dependent mechanisms of short-term plasticity. Schematic diagrams illustrate proposed mechanisms for depression **(a)**, facilitation **(b)**, and post-tetanic potentiation (PTP) and Augmentation **(c)**. RRP: readily releasable pool of vesicles; Ca_{res}: residual calcium. Adapted from Fioravante and Regehr (2011).

For most synapses with a low initial probability of release, repeated stimulation at short time intervals leads to a transient increase in transmitter release probability (Hallermann et al., 2010). Several mechanisms have been proposed to account for this facilitation. One proposed mechanism for facilitation involves residual calcium (Ca^{2+}res) that persists in the presynaptic terminal following synaptic activation (Zucker and Regehr, 2002). Another potential mechanism for facilitation involves calcium-binding proteins within presynaptic terminals that normally intercept calcium ions between calcium channels and release sites; in this case vesicle docking sites and Ca^{2+} channels are clustered together and when a Ca^{2+} channel opens, Ca^{2+} entering the cell create a local microdomain of elevated Ca^{2+} that should be highly effective in triggering the exocytosis of the local vesicle (Neher 1998). Post-tetanic Potentiation (PTP) and Augmentation are two closely related forms of enhancement that are observed following sustained, high frequency synaptic activation (Zucker and Regehr, 2002). PTP lasts for tens of seconds to minutes, and becomes longer lasting when the stimulus frequency and duration are increased. Instead, a less prolonged stimulation induced Augmentation, lasting for 5–10 s. Paired Pulse Facilitation (PPF) and Frequency Facilitation (FF) are two well know form of short-term synaptic plasticity: PPF is defined as an increase in the size of the synaptic response to a second pulse delivered within a short interval of time following the first pulse. It is well established that PPF is a purely presynaptic phenomenon and is often used to control or monitor presynaptic performance. FF occurs when the stimulation frequency is changed from a very low rate (e.g., 0.025 Hz) to a low rate (1 Hz) and typically is only sustained for as long as the stimulation is applied at that frequency. This is a striking characteristic of the MFs synapse and is not seen with that prominence at any other hippocampal synapses (Dobrunz and Stevens 1999). At many synapses, synaptic depression reduces the synaptic strength during repeated stimuli, delivered as closely paired stimuli (paired-pulse depression) or trains of stimuli. Several factors can account for reduced release, including but not limited to vesicle depletion, inactivation of release sites, and decreased presynaptic Ca^{2+} influx (see Fig. 5). Therefore, like facilitation, augmentation, and PTP, multiple mechanisms contribute to synaptic depression, and their relative roles are still under debate.

Postsynaptic mechanisms also contributing to short-term plasticity. In fact, postsynaptic receptors saturations can prevent an increase in synaptic strength also if the neurotransmitter release is enhanced (Foster et al., 2002; 2005). A similar situation is represented by receptor desensitization following repetitive activation of presynaptic terminals (Jones and Westbrook, 1996; Overstreet et al., 2000). A fundamental consequence of short term synaptic plasticity is to influence the information processing function of synapses, enabling them to act as filters. For instance synapses with a low intrinsic probability of neurotransmitter release function as *high-pass* filters, since they will facilitate during high frequency action potential bursts while low-frequency bursts will not be transmitted with the same efficacy. In contrast, synapses with high initial probability of release function as *low-pass* filters in that they will depress during high-frequency bursts but will reliably relay low frequency activity (Abbott and Regehr, 2004). The filtering features of a synapse can be modified trough modulation of the initial release probability, commonly via activation of presynaptic receptors. The MFs–CA3 circuit represents a high pass filter for the information reaching the hippocampus. In case of repetitive stimulus presentation or autonomous memory trace replay, presynaptic MFs plasticity may help the orthogonalization process, creating an opportunity for the faithful information transfer (pattern separation) or for the reactivation of the same CA3 circuit pattern (pattern completion). Only at high frequencies CA3 pyramidal neurons follow granule cells firing, meaning that only the strongest entorhinal excitatory, reaching the postsynaptic spike threshold, will participate to the information transfer to CA3, assuring a sparse code transformation. Hence et al., (2002) suggested that granule cells can act as a “conditional detonator” since the very low spontaneous firing rates, observed in the freely moving condition, rapidly increase to 40 Hz (Jung and McNaughton, 1993) as the animal enters the place field of the neuron. In this case the probability of spike transmission to CA3 becomes very high, providing the faithful transfer of an orthogonalized dentate signal, filtering out non coding spontaneous activity and overcoming the strong feedforward inhibition, which at low frequency blocks the spike transmission from granule cells to pyramidal cells. Long lasting processes such as long term potentiation or depression build on these shorter processes to span the gap between synaptic plasticity and permanent structural changes involved in long term memory.

Long term-plasticity

Bliss and Lomo (1973) showed that the application of a short burst of high-frequency stimulation to the Perforant Pathway, determines a long lasting potentiation of the transmission in the DG. This phenomenon was called Long Term Potentiation (LTP). Ultimately the phenomenon of LTP was found in all the synapses of the hippocampal trisynaptic circuit, rendering it an extremely plastic structure, enable to modify itself in response to changes in the afferent electrical activity pattern and to maintain the modification over the time. This important plasticity was consistent with the hypothesis that hippocampus was the site of changes in synaptic efficacy required for the memory trace formation and this has led to the hypothesis that LTP was the cellular mechanism responsible for such changes.

Based on its pre- and post-synaptic inducing requirement LTP can be classified into Hebbian, non-Hebbian and anti Hebbian type. Borrowing its name from the Hebb's postulate, Hebbian LTP requires simultaneous pre- and post-synaptic depolarization for its induction. Instead, non- Hebbian LTP does not require such simultaneous depolarization of pre- and post-synaptic cells. A special case of non-Hebbian LTP, the anti-Hebbian LTP, explicitly requires simultaneous presynaptic depolarization and relative postsynaptic hyperpolarization for its induction. In the Hebbian LTP, AMPARs became sufficiently excited flowing Na^+ into the cell, determining a dramatic depolarization of the postsynaptic cell. This phenomenon releases the magnesium ion blocking the NMDARs, and allows Ca^{2+} to enter the cell. Importantly, unlike AMPARs channels, the NMDARs channel allows Ca^{2+} as well as Na^+ to enter the postsynaptic dendritic spine. Increase in intracellular Ca^{2+} concentration leads to the activation of intracellular signaling cascades involving a number of protein kinases, most importantly CaMKII. Once activated, CaMKII phophorylates AMPARs, increasing their single channel conductance and, promoting incorporation of additional AMPARs into the postsynaptic density. The result is a durable increase of the synaptic strength after incorporation of new AMPARs into the synapses.

Up to now, it is clear that a mechanistically distinct forms of plasticity coexist in the hippocampus: while in the CA1 region the LTP is closely dependent on the activation of ionotropic NMDARs, in the CA3 region the phenomenon is largely NMDARs-independent. In contrast to NMDARs-dependent LTP, the triggering and the expression of this form of LTP is thought to be solely or predominantly presynaptic. Most experimental evidence suggests that presynaptic LTP is triggered by high frequency tetanic stimulation, which causes a large, activity-dependent increase in Ca^{2+} concentration within the presynaptic terminals. Ca^{2+} entry into the presynaptic terminal may occur through presynaptic voltage-dependent calcium channels, although the activation of presynaptic KARs, particularly those containing GluK2 subunit (Lauri et al, 2001; Schmitz et al, 2003), has been reported as well. Nowadays, there is a general agreement about the presynaptic origin of long term changes in MFs-CA3, meaning they do not depend neither on post synaptic NMDARs and AMPARs activation nor on postsynaptic Ca^{2+} influx, but they are manifested as long term changes in the probability of glutamate release.

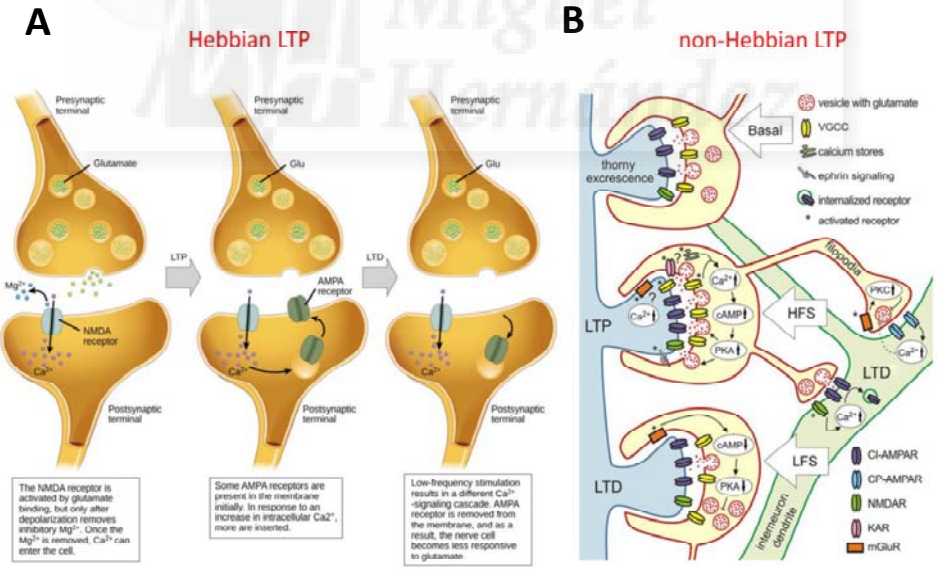

Figure 6: Long-term plasticity, Hebbian and non-Hebbain type: A) in Hebbian synaptic plasticity, calcium entry through postsynaptic NMDARs can initiate two different forms of synaptic plasticity: long-term potentiation (LTP) and long-term depression (LTD). LTP results in the insertion of more AMPARs into the postsynaptic membrane. LTD occurs when NMDARs initiate a different intracellular cascade, which results in the endocytosis of AMPARs. **B)** In non-Hebbian synaptic plasticity, likely MFs-CA3 and MF-interneurons synapses, high frequency stimulation (HFS) induces LTP and low frequency stimulation (LFS) induces LTD. LTP at pyramidal cell synapses is NMDARs-independent and expressed at the presynaptic site, where KARs and Ca^{2+} release from stores may be involved. Same type of stimulation evokes LTD at filopodial synapses onto interneurons. Adapted from Evstratova and Tóth (2014).

In the hippocampus, a form of anti-Hebbian, NMDA receptor-independent, LTP occurs at excitatory synapses made on some inhibitory neurons. This is preferentially induced when postsynaptic interneurons are hyperpolarized and depends on Ca^{2+} entry through Ca^{2+}-permeable AMPARs (CP-AMPARs). Activation of group I metabotropic receptors (mGluRs) is required for anti-Hebbian LTP induction in interneurons with cell bodies in the CA1 stratum oriens concomitant to muscarinic acetylcholine receptors (mAChRs) activation as shown by Le Duigou et al. (2015).

Low-frequency stimulation, around a few Hz, causes a long-term effect completely opposite to the LTP. This phenomenon is known as Long Term Depression (LTD) and consists in an activity-dependent reduction in the efficacy of neuronal synapses lasting hours or longer. Likely LTP, LTD occurs in many areas of the CNS with varying mechanisms depending upon brain region and developmental progress. LTD at the hippocampal Schaffer collateral-CA1 synapses occurs when Schaffer collaterals are stimulated repetitively for extended time periods (10–15 minutes) at a low frequency (approximately 1Hz) (Malenka, 1994). Depressed excitatory postsynaptic potentials (EPSPs) result from this particular stimulation pattern. Because low-frequency stimulation causes the LTD, the Ca^{2+} influx in postsynaptic termination must be quite small compared to that required to induce LTP with high frequency.

While LTP is in part due to the activation of protein kinases, which subsequently phosphorylate target proteins, LTD arises from activation of Ca^{2+} -dependent phosphatases that dephosphorylate the target proteins. Selective activation of these phosphatases by varying Ca^{2+} levels might be responsible for the different effects of Ca^{2+} observed during LTD. The activation of postsynaptic phosphatases causes internalization of synaptic AMPARs into the postsynaptic cell.

Similar protocols of stimulation commonly used to trigger NMDARs-dependent LTD at Shaffer collateral-CA1 synapses also induce a MFs-CA3 homosynaptic LTD expressed as a pre synaptic reduction in glutamate release (Kobayashi et al. 1996). Presynaptic MFs-LTD induction is NMDARs-independent and seems to require presynaptic mGluR2 (Yokoi et al. 1996; Tzounopoulos et al., 1998).

MFs-LTD induced in mGluR2/3 double knockout mice was abolished by pharmacologically blocking KARs (Lyon et al. 2011), raising the intriguing possibility that these receptors, via a metabotropic action, could be involved in the induction of presynaptic MFs-LTD.

The observation of LTP and LTD from the hippocampus has quickly shifted to other brain structures involved in memory and learning.

1.3 IONOTROPIC GLUTAMATE RECEPTORS (iGluR)

1.3.1 AMPA RECEPTORS

AMPA receptors (AMPARs) represent, among the distinct ionotropic glutamate receptors subtypes, the primary driving force for postsynaptic depolarization. They conduct the majority of fast synaptic transmission and their abundance is a crucial factor in determining synaptic efficacy. AMPARs, as well as all glutamate channel receptors, are composed of four types of subunits, designated as GluA1, GuA2, GluA3, and GluA4, each of which has an identical membrane topology and core structure comprising ~900 amino acids with a molecular weight of ~105 kDa. Each subunit has four hydrophobic transmembrane segments (M1-M4). The M2 segment does not cross entirely the membrane but forms an intracellular loop that makes the C-terminal intracellular side facing, while the N-terminal domain located on the extracellular matrix. AMPARs are permeable to Na^+, K^+ and Ca^{2+}, but in this respect what occurs is a significant difference in the Ca^{2+}-conductance, due to a particular position of the M2 segment of the GluA2 subunit. At 586 position of the non-NMDA receptor, DNA codifies for a glutamine (Q), but the residue often found is an arginine (R). This position is then called Q/R and it render the channel impermeable to Ca^{2+}.

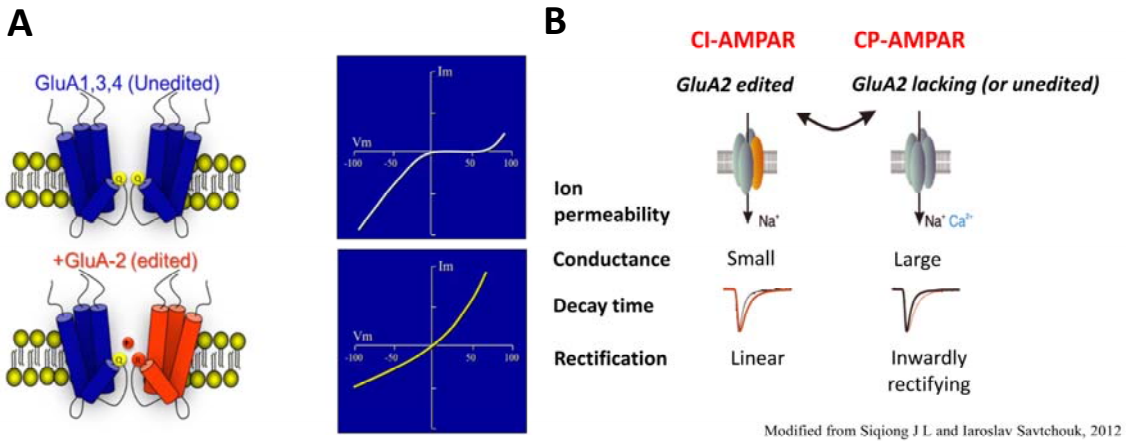

Figure 7: AMPAR topology and properties. A) Unedited CP-AMPARs contain a Glutamine (Q) in M2 segment, they are inwardly rectifying owing to voltage-dependent block by intracellular polyamine, while edited CI-AMPARs contain an Arginine (R) showing a linear current-voltage relationship. **B)** CI-AMPAR containing edited GluA2 are Ca^{2+} impermeable and exhibit a lower single-channel conductance with slower kinetics; but CP-AMPAR either lacking GluA2 or containing an unedited GluA2 are Ca^{2+} permeable, show higher single-channel conductance.

So, the presence of GluA2 subunit has a profound impact on the biophysical property of AMPARs heteromeric complexes such that the GluA2-containing AMPARs are Ca^{2+}-impermeable (CI-AMPARs) with linear current-voltage relationship while GluA2-lacking receptors are Ca^{2+}-permeable (CP-AMPARs) and have an inwardly rectifying current-voltage relationship (Fig.7). The profile of AMPARs stoichiometry changes markedly during development: early in development, many synapses contain GluA2-lacking CP-AMPARs, which are exchanged for GluA2 containing CI-AMPARs after the second postnatal week (Pelligrini et al., 1992). Predominant expression of GluA1 is also developmentally restricted and in the adult brain the majority of AMPARs contain GluA2 edited and/or less amount of GluA1. A transient expression of CP-AMPARs has been also documented during plastic phenomena where their activity-dependent trafficking tunes neuronal excitability. CP-AMPARs mediate also the initial phase of the homeostatic synaptic scaling, where AMPARs increase during synaptic activity suppression. In these circumstances, GluA1 is more recruited to synapses than GluA2, providing a rapid source of GluA1 homomers CP-AMPARs (Thiagarajan et al., 2005; Sutton et al., 2006).

AMPARs are crucial for many aspects of brain function, including learning, memory and cognition. The number, synaptic localization and subunit composition of synaptic AMPARs are tightly regulated by network activity and by

the history of activity at individual synapses. Synaptic plasticity can be regulated at the presynaptic side by altering the efficacy of neurotransmitter release or on the postsynaptic side by changing the density, types and properties of neurotransmitter receptors. The best understood postsynaptic modification involves a change in the number or phosphorylation state of AMPARs, so altering the amplitude of the synaptic current and giving rise to long-term potentiation and depression (Barry and Ziff, 2002; Malinow and Malenka, 2002; Song and Huganir, 2002). However, neuronal activity can also alter the subunit composition of synaptic AMPARs and thereby change the kinetics of the synaptic current (Geiger et al., 1995). The most commonly observed AMPARs subtype remodeling involves changes in the abundance of GluA1 subunits. Such changes can occur through an activity-dependent mechanism delivering GluA1-containing AMPARs directly to the postsynaptic membrane (Gerges et al., 2006; Boehm et al., 2006)

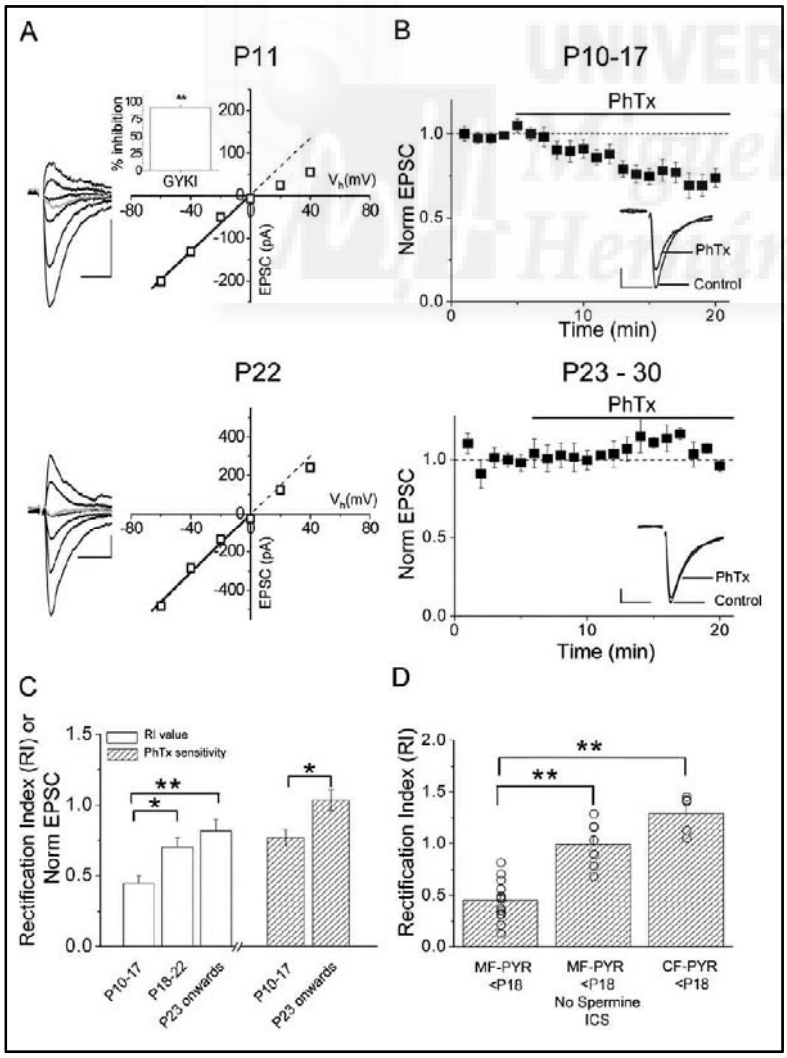

Figure 8: Changes in the properties of AMPARs during MFs-CA3 synapses development. A) Top, deviation of the current-voltage relationship at P11 from linearity compared to the bottom showing a linear relationship in adult mice (P22) and **B)** their sensitivity to the specific CP-AMPARs antagonist philanthotoxin-433 (PhTx) show the Ca^{2+} permeability of AMPARs at P11 but not at P23-30; **C)** summary histogram illustrating the averaged Rectification Index (RI) values for MF-CA3 transmission at different ages and the effect of PhTx. **D)** comparison between RI from P10-17 in the absence and presence of Spermine, consistent with a specific role for polyamines in mediating the rectification; and also from collateral fiber- CA3 synapses (CF-PYR). Adapted from Ho et al., 2007.

1.3.2 NMDA RECEPTORS

NMDARs are heteromeric complexes incorporating different subunits within a repertoire of 3 subtypes: NR1, NR2 and NR3. There are eight different NR1 subunits generated by alternative splicing from a single gene, four different NR2 subunits (A, B, C and D) and two NR3 subunits (A and B) (Dingledine et al., 1999). Functional NMDARs always contain NR1 that is combined with one or two subunits of NR2 or NR3. NMDARs are permeable to Na^+, K^+ and Ca^{2+}. However, at a resting membrane potential, these receptors do not determine current flux because they are blocked, in a voltage dependent manner, by a magnesium ion. The channel represents an important access way for Ca^{2+} only when cell is depolarized, thus, removal of magnesium requires depolarization (~40 mV) of the postsynaptic neuron, which typically occurs after glutamate binds AMPARs or KARs. The NMDARs activation requires the binding of glutamate and coagonist, glycine (Lerma et al., 1990, Hennebergen et al., 2010). Although the GluN2 subunits consist of GluN2A-D, adult CA1 pyramidal neurons predominantly express GluN2A and GluN2B. During development, the ratio of GluN2A/GluN2B-containing receptors increases, and GluN2A containing receptors come to predominate at adult synapses, whereas GluN2B predominates within extrasynaptic compartments. Functionally, the identity of the GluN2 subunit within NMDARs imparts distinct properties to the resulting receptor channel. For example, GluN1/GluN2B receptors have a higher affinity for glutamate and glycine compared to GluN1/GluN2A. In addition, GluN1/GluN2A-mediated currents exhibit faster rise and decay kinetics than those by generated GluN1/GluN2B channels (Lau and Zukin 2007). The longer time constants of decay for currents generated by GluN1/GluN2B receptors allows a greater relative contribution of Ca^{2+} influx compared to GluN1/GluN2A receptors.

1.3.3 DELTA RECEPTORS

The delta receptors, GluD1 and GluD2, are regarded as a subfamily of the ionotropic glutamate receptors solely because of their sequence homology, which is ~76%. GluD1 and GluD2 are not coexpressed in the same neurons in most brain regions, whereas they are often coexpressed with other iGluRs. They play important roles in cerebellar function and high-frequency hearing and appear to

serve structural functions at synapses. In addition, although delta receptors have functional gating machineries and ion permeation pathways similar to those of AMPARs and KARs (Orth et al., 2013), they are not gated by glutamate.

1.4 KAINATE RECEPTORS

KARs are highly expressed in the central nervous system (CNS) and have been implicated in various functions (Lerma et al., 2001; Lerma, 2003; Pinheiro and Mulle, 2006). As ionotropic receptors, KARs have been characterized, pre and postsynaptically, in several brain region. Presynaptically KARs influence the strength of both excitatory and inhibitory transmission, modulating transmitter release and fine tune synaptic plasticity at a subset of central synapses (Rodriguez-Moreno et al, 1997; Kamiya and Ozawa, 2000; Contractor et al., 2001; Lauri et al., 2001; Schmitz et al., 2001), whereas postsynaptic KARs carry part of the synaptic charge, similar to the well-characterized function of AMPARs and NMDARs, influencing neuronal excitability through effects on voltage gated ion channels (Castillo et al., 1997; Vignes and Collingridge, 1997).

1.4.1 STRUCTURE AND DISTRIBUTION OF KAINATE RECEPTORS

Five separate genes (*GRIK*1-5) encode the different receptor subunits, which are categorized into two separate groups based upon their ability to form functional homomeric receptors and their similar primary sequence homology. KARs are tetrameric combination of five subunits (proteins with molecular masses of ~ 100 kDa): the principal subunits, GluK1, GluK2, and GluK3 (previously known as GluR5-7), form functional plasma membrane-localized receptors in recombinant expression systems. GluK4 (KA1) and GluK5 (KA2) subunits are often termed the high-affinity subunits, because of their low nanomolar affinity for the marine toxin kainic acid, or auxiliary subunits, because they do not assemble as functional homomeric receptors. Instead, they modify the biophysical function and pharmacological properties of KARs when coexpressed with GluK1-3 subunits. Moreover, binding assays on recombinant receptors have shown that GluK4 and GluK5 have a significantly higher affinity for kainate than GluK1-GluK3 (Lerma et al., 2001).

Each KARs subunit begin with a 400-residue extracellular N-terminal domain, which play a key role in assembly, followed by the first segment of the neurotransmitter-binding cleft, called S1. This segment then passes through the cell membrane, forming the first of three membrane spanning regions, M1. The M2 segment then begins on the cytoplasmatic face of the membrane, pushes into the cell membrane, and then dips back out to the cytoplasm. The M2 segment, termed the “p loop”, determines the calcium permeability of the receptor. M2 turns into M3, another transmembrane segment which emerges on the extracellular face to complete the neurotransmitter binding site (a portion called S2). M4 begins extracellularly, and passes again through the membrane into the cytoplasm, forming the C-terminal of the protein, responsible of the receptor trafficking (Fig.9).

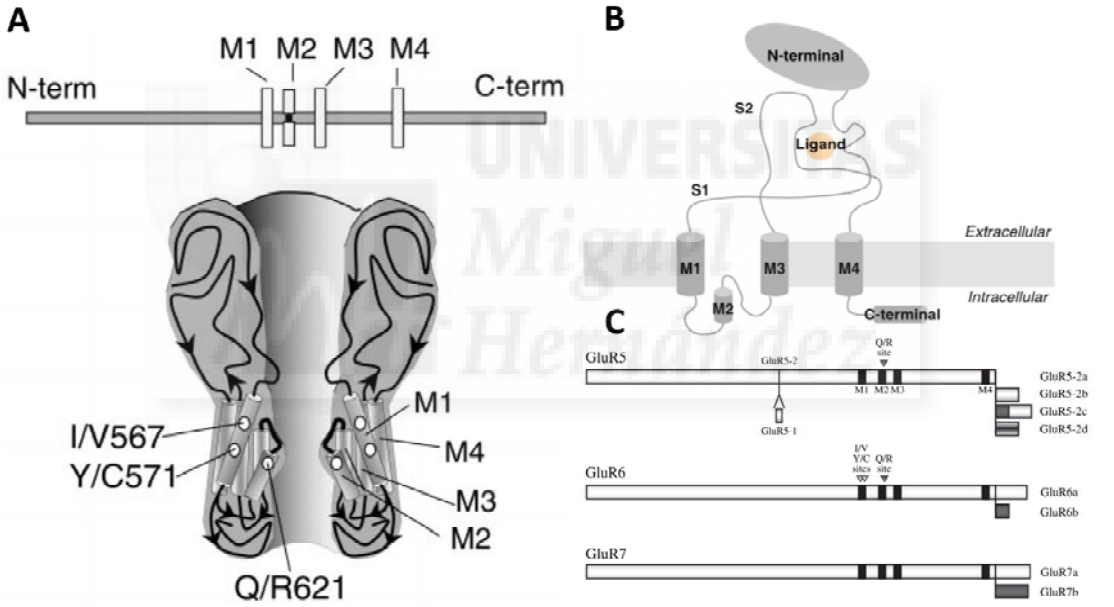

Figure 9: General KARs subunit structure and alternative splicing. A) KARs subunits have three transmembrane domains, M1, M3, and M4. Interspersed between M1 and M3 is the pore-forming p-loop domain, M2. The three highlighted residues correspond to sites susceptible to editing in the mRNA of GluR6 subunits. **B)** The N-terminal domain regulates the assembly of tetrameric receptors. The extracellular ligand binding domain (LBD) formed by S1 the region of the protein preceding the first membrane domain M1, and S2, the region between M3 and M4. Finally the C-terminal mediates receptor trafficking. **C)** Cartoons illustrating the splice isoforms of GluR5, GluR6, and GluR7 KARs subunits. The sites of RNA editing of the membrane domains of GluR5 and GluR6 are shown as well. A and C are adapted from Lerma (2001); B is adapted from Oswald et al. (2007)

The identification of different isoforms derived from *alternative splicing* has revealed that the structural repertoire of the KARs is not limited to the five proteins GluK1-GluK5. GluK1-3 are present with an altered primary sequence of the subunit cytoplasmic C-termini. GluK1 mRNA also contains a splice site that inserts an additional 15 amino acids stretch immediately preceding the S1 domain. Two C-terminal splice variants have been isolated for the GluK2 subunit. The two GluK3 subunits isoforms also differ in their cytoplasmic domains. There are no known splice isoforms of GluK4 and GluK5.

Another structural mechanism characterizing the diversity in the stoichiometry and channel properties of these receptors is the *mRNA editing*. GluK1 and GluK2 (but not GluK3, GluK4 and GluK5) are susceptible to undergoing posttranscriptional modification at a specific position of their M2 segment, the so-called glutamine-arginine (Q/R) site. The Q to R substitution decreases the calcium permeability, whilst increasing their chloride permeability, and reduces their unitary conductance modifying their rectification properties from inwardly rectifying to linear or slightly outwardly rectifying. This mRNA editing is regulated both developmentally and regionally and influences the pharmacologic properties of the channel.

The unique physiological and pharmacological properties displayed by neuronal KARs are determined largely by their subunit composition and distribution. Therefore, KARs subunit expression in distinct neuronal cell types is an important indicator of functional contribution of these receptors to synaptic signaling. The analysis by *in situ* hybridization of the distribution of KARs has revealed that they are widely expressed throughout the nervous system. GluK1 transcript is mainly present in DRG neurons, in the subiculum, in the septal nuclei, in the piriform and cingulate cortices, an in the Purkinje cells of the cerebellum (Fig 10). GluK2 is most abundant in the cerebellar granule cells, in the DG and CA3 and CA1 regions of the hippocampus (Fig 10), and in the striatum. The GluK3 mRNA is expressed at low levels throughout the brain but particularly in the deep layer of the cerebral cortex, in the striatum, and in the inhibitory neurons of the molecular layer of the cerebellum.

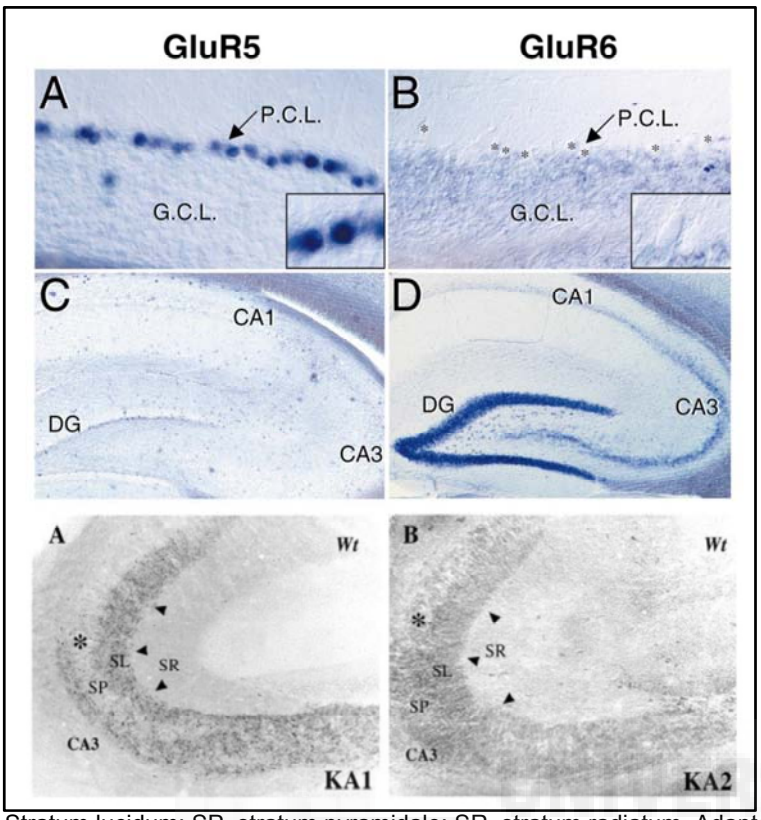

Figure 10: Expression pattern of GluR5 and GluR6 in the cerebellum and in the hippocampus. A) GluR5 (GluK1) is expressed in the Purkinje cell layer (P.C.L.) and in the granular cell layer (G.C.L.). **B)** GluR6 (GluK2) is expressed in the G.C.L., but not in P.C.L. **C)** In the hippocampus, GluR5 is mainly expressed by interneurons, and **D)** GluR6 is predominantly expressed in the principal cells. Adapted from Paternain et al. (2000).

Figure 11: Distribution of some KARs-subunits in the hippocampal MFs-CA3 synapses. A) KA1 immunoperoxidase staining in the stratum lucidum (arrowheads) of the hippocampus in wild-type mice. CA3 pyramidal cells (asterisk) are devoid of staining. **B)** KA2-immunopositive staining in the stratum lucidum and the pyramidal cell layer of the CA3 area in wild-type mice. SL, Stratum lucidum; SP, stratum pyramidale; SR, stratum radiatum. Adapted from Darstein et al. (2003).

GluK4 transcripts appear with the development of the hippocampus and remain largely confined to discrete areas (Bahn et al., 1994): GluK4 shows very limited and well-defined expression at high levels in the CA3 pyramidal neurons and at low levels in granule cells in the DG (Werner et al., 1991). Previous studies have failed to detect *grik4* mRNA in other regions than CA3 and DG. However, a recent study in our lab using non-radioactive *in situ* hybridization, revealed that *grik4* is abundantly expressed also in CA1 field and striatum, and even in many hippocampal interneurons. The Purkinje neurons in the cerebellum express significant amounts of mRNA and GluK4 protein (Darstein et al., 2003; Herb et al., 1992; Werner et al., 1991). GluK4 protein is also present, in lower extent, in the amygdala and in the entorhinal cortex. The significance of this regionalized expression pattern of GluK4 is unclear but it is expected that heteromeric receptors containing GluK4 subunits will have distinct properties.

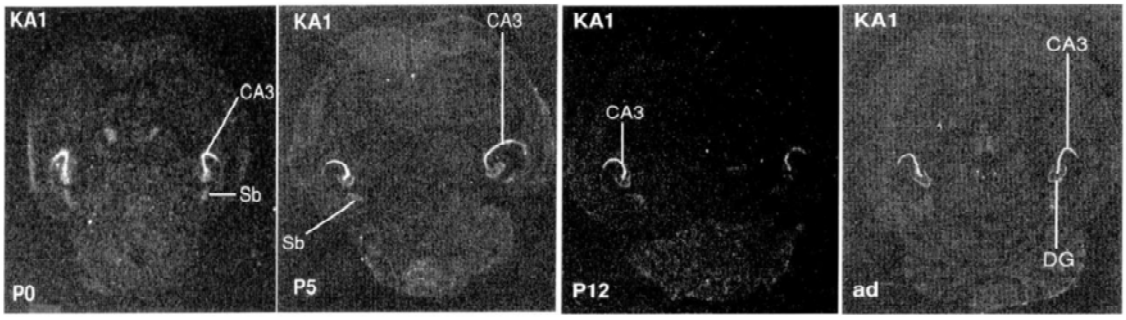

Figure 12: GluK4 distribution in developing rat brain. X-ray film autoradiographs illustrating distribution of kainate-receptor subunit mRNAs encoding GluK4 (KA1) in horizontal section from P0, P5, P12 and adult rat brain. Adapted from Bahn et al. (1994).

Finally GluK5 is ubiquitously expressed in the nervous system, suggesting that it is a constituent of most heteromeric neuronal KARs assemblies (Herb et al., 1992).

1.4.2 PHARMACOLOGICAL PROFILE

KARs are activated by kainate in a way dependent on the subunit composition: the high-affinity subunits GluK4 and GluK5 have a dissociation constant, *Kd*, of ~4-15 nM, while the low-affinity subunits GluK1-3, show a *Kd* of ~50-100 nM. A similar situation has been found for glutamate, the endogenous agonist. In addition to kainate and glutamate, different molecules have been shown to activate KARs with a certain degree of specificity, such as ATPA (2-Amino-3-(3-hydroxy-5-*tert*-butylisoxazol-4-yl) propanoic acid). The lack of specific agonist and antagonist of KARs made their understanding very difficult. Although a clear pharmacological demarcation has been traced between NMDARs and other ionotropic glutamate receptor classes, through the classic non-NMDARs antagonists, such as 6-cyano-7-nitroquinoxaline- 2,3-dione (CNQX), 6,7-dinitroquinoxaline-2,3-dione (DNQX), and 6-nitro-7-sulfamoylbenzoquinoxaline-2,3-dione (NBQX), the separation between KARs and AMPARs became possible only with the advent of GYKI53655 (Paternain et al. 1995), and other selective AMPARs and KARs antagonists. Between them, LY382884 displays high affinity for human GluK1 but not GluA1-4, GluK2 or GluK3-containing receptors. In a functional assay, LY382884 acted as an antagonist of heteromeric KARs containing a GluK1 subunit, such as GluK1/GluK2 and GluK1/GluK5 with similar potency to that for GluK1 alone (Ki ~ 7 μM for GluK1 homomers, ~3.6μM heteromers and Ki>100 μM for AMPARs) (Christensen et al. 2004; Bortolotto et

al., 1999, 2003; Lauri et al., 2001). The compound UBP310 was originally developed as a GluK1-selective antagonist (Dolman et al., 2007) and later found that it also potently antagonize GluK3 homomers (Perrais et al., 2009). However, these molecules were much less effective on GluK2/3 heteromeric receptors. It has been also shown that UBP310 is an antagonist of recombinant GluK2/5 receptors, the major population of KARs in the brain.

1.4.3 Neuronal function of Kainate Receptors

KARs receptors play significant roles in the brain at three main levels. In the first place, they mediate postsynaptic depolarization and they are responsible for carrying some of the synaptic current, although this only happens at some synapses. Second, KARs can modulate the synaptic release of neurotransmitters such as GABA and glutamate at different sites. Third, they play an influential role in the maturation of neural circuits during development. These roles are frequently fulfilled in an unconventional way given that KARs can signal by activating a G protein, behaving more like a metabotropic receptor than an ion channel. I will briefly review KARs functions only at hippocampal excitatory synapses, since this work has been focused on MFs-CA3 cells synapses.

Postsynaptic receptors at hippocampal excitatory synapses

The activation of postsynaptic KARs by synaptically released glutamate yields small amplitude excitatory postsynaptic currents (EPSCs), with slow activation and deactivation kinetics (Castillo et al., 1997). The first recordings of KARs-mediated EPSCs were reported simultaneously by the groups of Roger Nicoll and Graham Collingridge. They showed that the repetitive stimulation of the MFs in the presence of GYKI 53655 and 2-amino-5-phosphonovalerate (APV), antagonists of AMPARs and NMDARs, respectively, revealed the existence of a current with slow rise and decay kinetics that disappeared when CNQX was added to the bath. This evidence was not observed at other excitatory connection received by the CA3 neurons, as the associational-commissural path way.

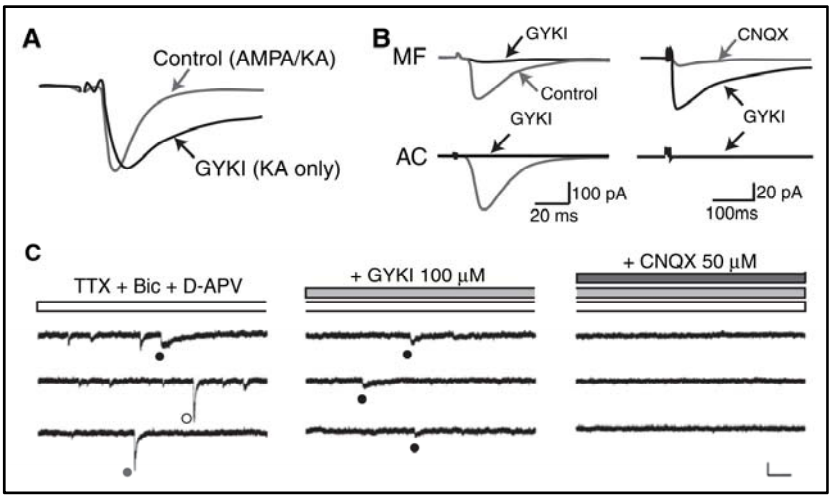

Figure 13: MFs KARs-mediated excitatory postsynaptic currents. **A)** KARs-EPSCs was scaled to the peak of the AMPA receptor component and showed a slower decay time **B)** GYKI blocks the response to single MFs and associated/commissural (AC) stimulation. Repetitive stimulation (4 stimuli at 200 Hz) evoked a slow inward current at MFs that is blocked by CNQX, but fails to restore a response at AC fibers (Castillo et al., 1997). **C)** Miniature EPSCs recorded from CA3 pyramidal neurons have relatively slow decay kinetics (black circles), mixed fast and slow components to the decay (gray circle), or only fast decay kinetics (open circles). GYKI 52466 eliminates the fast and mixed miniature EPSCs, suggesting that those with slow kinetics arise from synaptic KARs. This was confirmed by inhibition with a high concentration of the non-selective antagonist CNQX. Adapted from Cossart et al. (2002).

Later, KARs-mediated EPSCs have been found in contacts between Schaffer collaterals and CA1 hippocampal interneurons, and other brain regions such as the cerebellum, the striatum, the spinal cord, and the amygdala. The common characteristic of KARs present in all these regions is their slow kinetic, first attributed to their extracellular localization but finally associated to the intrinsic properties of these postsynaptic receptors, feature that probably provides integrative capacities to information transfer clearly unfulfilled by other glutamate receptors. In support of this idea, it has been shown that KARs-mediated EPSCs in hippocampal CA1 interneurons is sufficiently slow to allow substantial tonic depolarization bringing the cell to the spike threshold, during even modest activation (Frerking and Ohliger, 2002). In contrast to CA1 interneurons, the search for postsynaptic KARs in the CA1 pyramidal cells has been unsuccessful (Lerma et al., 1997; reviewed by Lerma et al., 2001), although application of exogenous KARs agonists does evoke KARs-mediated currents in CA1 pyramidal cells (Chittajallu et al., 1996; Bureau et al., 1999). Furthermore, KARs have been shown to be subject to homeostatic plasticity (Yan et al., 2013) in that the KARs-mediated EPSCs at MFs to cerebellar granule cell synapses was enhanced after network activity blockade (either by TTx or genetically removing AMPARs).

This phenomenon relies on the enhanced expression of GluK5 subunits that produces receptors with a higher affinity for glutamate, efficiently maintaining spike generation at granule cells.

The subunit composition of MFs KARs has been the subject of some debate, but multiple lines of evidence support a growing consensus that postsynaptic KARs are predominantly heteromeric combinations of, GluK2, GluK4 and GluK5 subunits. Moreover, in mouse hippocampus, granule neurons express high levels of GluK2, GluK3, and GluK5 mRNA, whereas pyramidal neurons express GluK2, GluK4, and GluK5 mRNA (Bureau et al., 1999).

An early pharmacological study suggested that the postsynaptic KARs were comprised of the GluK1 subunit (Vignes et al., 1998), even if mRNA for GluK1 is expressed only weakly in hippocampal principal neurons after the first week of postnatal development (Bahn et al., 1994) and others pharmacological experiments failed to reproduce the demonstration of a role for GluK1-containing receptors in mediating the $EPSC_{KARs}$ (Lauri et al., 2001). Subsequent studies in knockout mice instead demonstrated a critical role for the GluK2 subunit because the MFs $EPSC_{KARs}$ was absent in these animals (Mulle et al., 1998). This hypothesis is consistent with the robust expression of GluK2 mRNA in the CA3 region (Bahn et al., 1994). mRNAs for GluK4 and GluK5 subunits are also expressed at high levels in CA3 pyramidal neurons. The $EPSC_{KARs}$ in GluK5 knockout mice has significantly faster decay kinetics, suggesting that the inclusion of this subunit contributes to the biophysical properties of synaptic KARs (Contractor et al., 2003). The subunit composition of MFs KARs as determined from knockout studies remains to be confirmed with a complementary pharmacological analysis because antagonists that selectively inhibit GluK2 and other subunits have not been developed.

Presynaptic receptors at hippocampal excitatory synapses

Apart from their postsynaptic role, KARs have been shown to modulate synaptic transmission by a presynaptic mechanism at a subset of both excitatory and inhibitory terminals. The physiological outcome of presynaptic KARs activation varies depending on the synapse type: facilitation, depression as well as biphasic concentration–dependent actions on transmission have been characterized at numerous synapses in the central nervous system.

At the MFs-CA3 synapses of the hippocampus, Ca^{2+}-permeable presynaptic KARs are implicated in the characteristic frequency-dependent facilitation of mossy fiber excitatory transmission (Schmitz et al., 2001; Lauri et al., 2001; Contractor et al., 2001; Pinheiro et al., 2007). Facilitation of glutamate release at MFs-CA3 synapses is mimicked by applying low concentration of exogenous kainate (Schmitz et al., 2000; Kamiya and Ozawa, 2000), whereas higher concentrations depress MFs synaptic transmission. This inhibition is accompanied by a reduction in presynaptic Ca^{2+} and occurs through a metabotropic signaling and is not only seen at MFs-CA3 synapses but also at synapses between Schaffer collateral and CA1 pyramidal cells, where it was demonstrated a presynaptic reduction in transmitter release upon the activation of KARs in acute hippocampal slices (Chittajallu et al., 1996). As is the case with bath application of kainate, synaptically released glutamate also can cause a bidirectional modification of MFs synaptic transmission acting on these presynaptic autoreceptors (Schmitz et al., 2000). Incongruity between pharmacologic and gene knockout approaches has generated debate regarding the subunit composition of presynaptic MFs KARs. Pharmacologic reagents apparently selective for GluK1-containing KARs occluded presynaptic facilitation (Lauri et al., 2001), a result at odds with data from GluK1$^{-/-}$ mice, which exhibit normal frequency KARs–mediated facilitation (Contractor et al., 2001) and with a subsequent study unable to replicate key effects on MFs short-term plasticity with the GluK1 antagonist (Breustedt and Schmitz at al., 2004). mRNA localization suggests that the GluK2 receptor subunit is the most likely candidate for the principal subunit of presynaptic KARs, and this is supported by studies in knockout mice (Contractor et al., 2000). Knockout mice lacking the GluK3 subunit exhibited marked reduction in short-term plasticity at MFs synapses, demonstrating that this subunit contributes to the presynaptic KARs (Pinheiro et al., 2007). The evidence for presynaptic targeting of GluK4 is weaker as compared to the other subunits. Some immunohistological and biochemical evidence support presynaptic localization of GluK4 and GluK5 receptor subunits at MFs synapses (Darstein et al.,2003) and in the central terminals of dorsal root ganglion (DRG) neurons (Lucifora et al., 2006). GluK4-containing KARs are positioned near release sites to respond to single release events, and with the

other high affinity subunit GluK5 regulate the incorporation of GluK2 subunit at its localization (Fernandes et al., 2009). Fernandes and his group demonstrated also the role of the high affinity subunits showing that both synaptic and extrasynaptic KARs lacking GluK4 and GluK5 do not function efficiently as ligand gated ion channel, but remain capable of activating metabotropic pathway to modulate neuronal excitability and that facilitation of MFs synaptic transmission is in part mediated by facilitatory KARs autoreceptors. The GluK5 subunit clearly contributes to presynaptic KARs because gene-targeted mice lacking this subunit have reduced sensitivity to heterosynaptic facilitation by glutamate released following stimulation of associational/commissural inputs (Contractor et al., 2003). It remains to be clarified whether distinct receptor populations exist and perform distinct functions in MFs axons and terminals, given that all five KARs subunits have been implicated in the formation of presynaptic KARs.

Metabotropic action of KARs

Several evidences for metabotropic actions of KARs have been accumulated, acting both pre- and postsynaptically in several region of the CNS. KARs can signal through G-proteins and others second messengers independently of ion flux (Rozas et al., 2003). One way through which KARs act on G-protein activated signaling is provided by their action on voltage sensitive Ca^{2+}-dependent K^+ channels, regulating the slow afterhyperpolazitation current (sI_{AHP}). KARs activation inhibits sI_{AHP} in CA1 pyramidal cells (Melyan et al., 2002), increasing neuronal excitability. Postsynaptic regulation of neuronal excitability by KARs activation has also been observed in CA3 pyramidal cells, where a short train of stimuli to the MFs could not only directly depolarize the postsynaptic membrane but also increase neuronal excitability by preventing spike adaptation (Fisahn et al., 2005; Ruiz et al., 2005). Metabotrobic presynaptic KARs are involved in the control of neurotransmitter release at the two GABAergic and glutamatergic synapses. Presynaptic KARs could modulate GABA release in a bidirectional manner through their dual signaling in that GABA release would be facilitated through canonical ionotropic KARs while depression would be achieved by a non-canonical metabotropic pathway (Rodríguez-Moreno and Lerma 1998; Frerking et al., 1998; Christensen et al., 2004).

The KARs mode to modulate neurotransmitter release shows its duality also in the case of glutamatergic synapses. Close to the general agreement on the facilitation of glutamate release by presynaptic KARs acting through their classic ionotropic activity, there is growing evidence that the inhibitory effects of presynaptic KARs on glutamate release are mediated by G-protein coupling. This metabotropic action has been shown in the hippocampus at both MFs-CA3 and Schaffer collateral-CA1 synapses. The effect of activating presynaptic KARs with endogenous glutamate may depend on the glutamate concentrations actually reaching these presynaptic KARs. Indeed, glutamate spill over from nearby synaptic terminals may be distinct under different conditions. Whether specific subunit are responsible for the metabotropic and ionotropic activity need more detailed elucidations.

1.4.4 KARs IN DEVELOPMENT

The expression, activation, and signaling of KARs is significant during early postnatal development and functional and structural regulation of KARs subunits is documented in different brain regions, including the barrel cortex, spinal cord the cerebellar granule cells. For instance, KARs are highly expressed throughout the neonatal brain. The KAR-EPSCs switch to AMPAR-EPSCs during development and after LTP at thalamocortical synapses (Kidd and Isaac, 1999). Developmentally restricted functions have also been described for presynaptically located KARs in both areas CA3 and CA1 of the hippocampus. At MFs connections presynaptic KARs are functional at early developmental stages, while postsynaptic KARs-mediated EPSCs starts appearing during the second postnatal week when MFs acquire the classical glutamatergic phenotype. Different roles of presynaptic KARs exerted at immature hippocampal formation are summarized in Fig. 14.

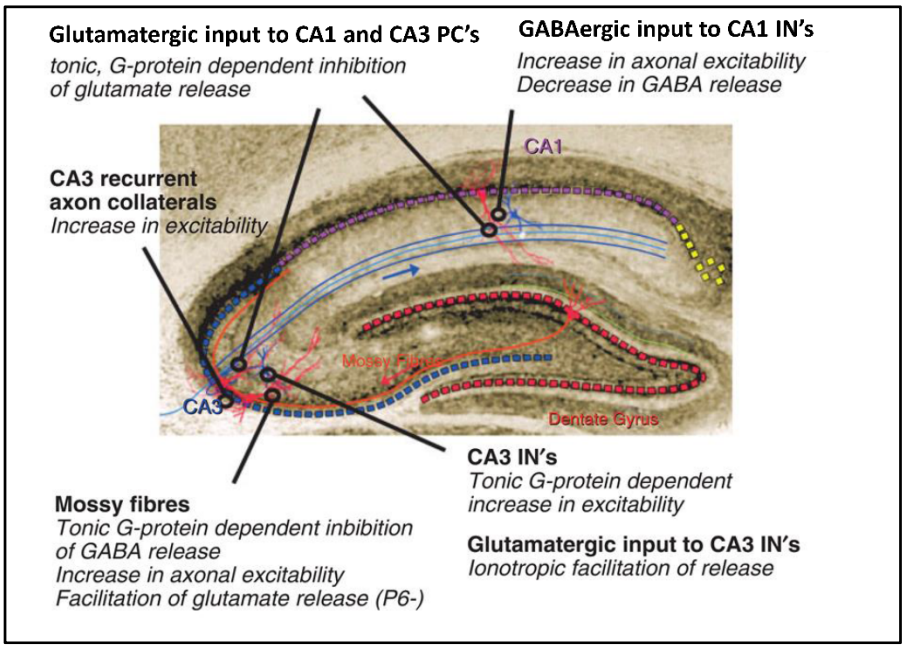

Figure 14: Diverse functions of KARs in the developing hippocampus: in immature MF-CA3 synapses it has been shown that KARs modulate GABA release increasing axonal excitability in a G-protein dependent manner (Caiati et al., 2010), while facilitation of glutamate release appears from postnatal day 6 (Marchal et al., 2004). At glutamatergic terminal onto CA3 interneurons (CA3 IN's), presynaptic KARs facilitate release in a G-protein-independent mechanism; the same input to CA3 cells (CA3 PC's) KARs inhibit glutamate via a G-protein and PKC-dependent mechanism with a final upregulation of the inhibitory transmission (Lauri et al., 2005). In CA1 area presynaptic KARs tonically inhibit glutamate release through their metabotropic way of action (Lauri et al., 2006). In CA1 interneurons (CA1 IN's) GluK1-KARs inhibit GABA release (Segerstrale et al., 2010). Finally, activation of high-affinity KA receptors leads to dramatic increase in network bursts in CA3 cells, receiving afferents from axon collaterals (Juuri et al., 2010). Adapted from Lauri and Taira.

KARs are also necessary for the proper functional maturation of MFs-CA3 synapses, also regulating AMPARs-currents (Marchal and Mulle, 2004). Apart from their functional role in neural network development, KARs have been related to the enhanced motility at MFs axons in younger hippocampal slice culture, suggesting a key role for KARs for establishing synaptic contacts and for stabilizing new formed ones (Tashiro et al., 2003).

1.4.5 NEUROPATHOLOGIES AND KARS

Over the past three decades, genetic manipulations in mice have been used in neuroscience as a major approach to investigate the function of genes and their alterations. The identification of numerous disease-linked gene mutations has led to the creation of various transgenic mouse models that replicate the phenotypes of human patients. A number of publications report that genetic variants in *GRIK* genes influence KARs ion channel function in humans. Given their central role in synaptic transmission, KARs have been linked to a number of human brain diseases.

Gene	Data	Linked Disease	Behavioral Test in KO	References
Grik1	Upregulated expression	Epilepsy	No	Sander et al., 1997; Izzi et al., 2002; Li et al., 2010; Lucarini et al., 2007
Grik2	Modest linkage	Autism	No	Jamain et al. 2002; Shuang et al., 2004; Szatmari et al., 2007; Freitag 2007; but see Dutta et al., 2007
Grik2	Deletion of exons 7 and 8	Mania, mild mental retardation	No	Motazacker et al., 2007; Shaltiel et al., 2008; Lanore et al., 2012
Grik2	Mapping susceptibility locus	Schizophrenia	Yes	Beneyto et al., 2007; Shaltiel et al., 2008; but see Shibata et al., 2002, 2006
Grik2	mapping	Huntington	No	MacDonald et al., 1999; Chattopadhyay et al., 2003; but see Lee et al., 2012 and Diguet et al., 2004
Grik3	SNP T928G (rs6691840)	Schizophrenia	No	Begni et al., 2002; Kilic et al., 2010; Ahmad et al., 2009;
Grik3	SNP T928G (rs6691840)	Major depression	No	Schiffer and Heinemann, 2007; Wilson et al., 2006
Grik4	Treatment response	Depression	No	Paddock et al., 2007
Grik4	14 bp deletion/insertion variant	Bipolar disorder	Yes	Pickard et al., 2008; Catches et al., 2012; Lowry et al., 2013
Grik4	SNPs rs2282586 and rs1944522	Protection against Schizophrenia	Yes	Pickard et al., 2006

Table 1: Several kainate genes are linked to different diseases. Adapt from Lerma J and Marques JM 2013.

Kainate has a long and successful history as a model of seizure disorders, most notably, temporal-lobe epilepsy (TLE). More recent work has revealed that KARs may have a role in other brain disorders such as Autism Spectrum Disorders (ASDs) (Gilman et al., 2011; Levy et al., 2011; De Rubeis et al., 2014), intellectual disability (ID), schizophrenia and mood disorder, yet their role in brain pathologies appears at times contradictory. An evidence in favor of the involvement of KARs in epilepsy was the finding of upregulated GluK1 in the hippocampus of TLE patients. In this region, GluK1 function could be linked to neuronal damage and mossy fiber sprouting causing the formation of a recurrent excitatory circuit, causing seizures (Li et al., 2010). Different studies that potentially connect KARs with schizophrenia and bipolar disorders, have also been published. For instance, postmortem gene expression profiling indicated that in the hippocampus, parahippocampus, and the prefrontal cortex, there is a decrease in the mRNA encoding GluK1 subunit (Scarr et al., 2005). *GRIK*1 gene, encoding GluK1, localizes in the chromosome 21 whose triplication it is known being the origin of Down syndrome, the most frequent genetic cause of intellectual disability. It is therefore possible that excess of function of KARs may also contribute to Down syndrome phenotype, even when nothing is known on the effect of GluK1 overexpression.

The use of GluK2 KO mice demonstrated that acute seizure induced in vivo by systemic administration of low doses of kainate depends, at least in part, on GluK2-containing KARs (Mulle et al., 1998).

Among the cascade of events generated by status epilepticus cell loss, sprouting and formation of aberrant synapses have been described. Aberrant MFs synapses onto dentate gyrus cells induce the recruitment of KARs in chronic epileptic rats. It has been studied that some mutations of *grik2* are related to deficits in cognition and mental retardation (Motazacker et al., 2007). Single nucleotides polymorphism (SNP) association studies on various populations support a role of *GRIK2* in autism (Shuang et al., 2004; Dutta et al., 2007; Griswold et al., 2012). Although the sole contribution of GluK2 to the glutamate pathway may not reflect the abnormalities in glutamatergic neurotransmission in autism (Dutta et al., 2007). A mutation in *GRIK*2 causing a partial deletion of the amino-terminal domain and transmembrane domain and resulting in loss of function was reported in patients with intellectual disability (Motazacker et al., 2007). Similarly, a reported microdeletion involving the *GRIK3* gene was detected in a patient diagnosed with severe developmental delay (Takenouchi et al., 2014). As *grik3*$^{-/-}$ mice exhibit impaired synaptic transmission, the functional deletion of the *grik3* gene may lead to development delay (Pinheiro et al., 2007). The glutamatergic dysfunction hypothesis suggests genes involved in glutamatergic transmission are candidates for schizophrenia susceptibility genes. The *GRIK3* variant that encodes GluK3S310A showed a significant association with schizophrenia (Begni et al., 2002; Minelli et al., 2009; Lai et al., 2005).

The gene *grik4* might also take part in many disorders. The ablation of *grik4* in mice results in marked hyperactivity and impairments in memory acquisition suggesting a role for KARs in spatial memory (Lowry et al., 2013). Interestingly, a recent study described a chromosome abnormality disrupting the kainate class ionotropic glutamate receptor gene, *GRIK*4, in an individual with schizophrenia and learning disability (mental retardation) (Chatches et al., 2012). It has been demonstrated in a tagging SNP case-control study that three physically separated haplotypes within *GRIK*4 gene in the wider Scottish population were significantly associated with increased risk of schizophrenia and decreased risk of bipolar disorder, respectively. One of the haplotypes predisposes carrier individuals to schizophrenia; the other two demonstrated a greater statistical significance and exhibited a protective effect against bipolar disorder for carrier individuals (Pickard et al, 2006).

Furthermore, an interesting study identified an insertion/deletion (indel) variant in the 3′ untranslated region (3′UTR) of the *GRIK*4 gene. In subjects carrying the protective haplotype (Pickard et al, 2008), this was associated to the presence of the deletion, which resulted in a higher cellular transcript level of *GRIK4*.

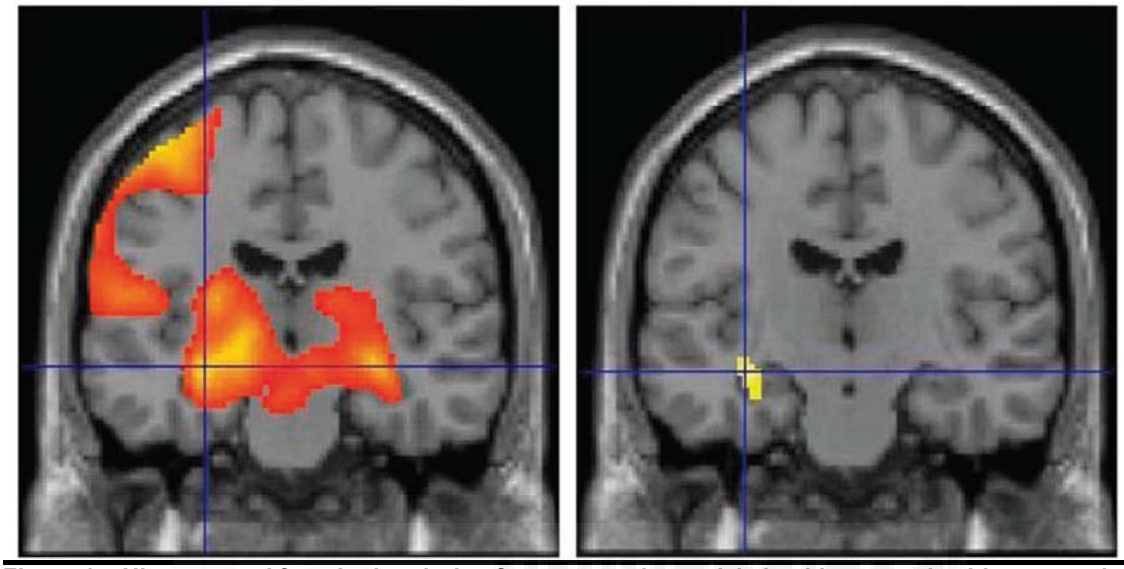

Figure 15: Hippocampal functioning during face processing task in healthy control subjects carrying the (indel) variant in the 3′UTR of the *GRIK*4 gene. Left) carriers of the protective deletion show greater hippocampal activation than non-carriers (right). Adapted from Pickard et al., 2008.

Follow-up studies showed positive correlation between the deletion variant and increased hippocampal activities (Fig.15) in humans via magnetic resonance imaging as well as significantly higher GluK4 protein distribution in the frontal cortex and hippocampus of the postmortem human brain tissue in the deletion group (Whalley et al., 2009; Knight et al., 2012). The importance of genes related to synaptic function in brain disease has been implied in studies describing *de novo* germline mutations and copy number variants. De novo copy number variation, CNVs (deletion or duplication of a chromosomal region) of synaptic genes has been recently implicated as risk factors for mental retardation or autism. A duplication of *GRIK4* was found in a case of autism. SNPs in *GRIK5* have also shown association with bipolar disorder (Gratacòs et al., 2009)

1.5 AIM OF THE THESIS PROJECT

The main objective of this work was to study the significance of GluK4-KARs in the physiology and pathology of the brain and determine if higher dosage of *grik4* reproduces in a mice model any kind of mental disorder like autism or schizophrenia. We wanted to determine the role of GluK4- containing KARs in neurotransmission, plasticity and maturation of glutamatergic synapses in the area CA3 of the mouse hippocampus.

The specific aims were:

1. To study the physiological function of GluK4-containing KARs in the hippocampal glutamatergic transmission.
2. To characterise presynaptic and postsynaptic GluK4-containing KARs.
3. To study if a change in KARs composition has any action on long-term synaptic plasticity in MFs-CA3 synapses, as LTP and LTD constitute the cellular basis of information storage in the brain.
4. To evaluate the impact of GluK4 protein overexpression in AMPARs and NMDARs-mediated transmission.

UNIVERSITAS
Miguel
Hernández

2. Materials & Methods

UNIVERSITAS
Miguel
Hernández

2.1 ANIMAL USE

For all experiments, mice were housed in ventilated cages in a temperature-controlled, standard pathogen-free environment (23°C), at humidity between 40 and 60%, and on a 12 h light/dark cycle. Mice had *ad libitum* access to food and water and the cages were changed weekly. Experimental procedures involving use of live mice were performed in accordance with Spanish and European Union regulations (2010/63/EU), and bioethical committees at both the Instituto de Neurociencias and at the Consejo Superior de Investigaciones Científicas approved them. The experiments were performed on postnatal day (P) 18–P21 and P13-14 mice for electrophysiological analysis and on > 4 week-old mice for biochemical characterization. All the procedures were done after extensive backcrossing to C57BL/6J. All analyses were performed on mice whose genotype was unknown before to collect all data.

2.2 GENOTYPING

grik4 recombination was assessed in DNA preparations from tail samples of wild-type and GluK4^{Over} animals using the primers detailed in Table 2.1 and the following polymerase chain reaction (PCR) conditions: 3 minutes at 94°C; 30 seconds at 94°C, 30 seconds at 62°C, and 30 seconds at 72°C repeated for 35 consecutive cycles; and finally 8 minutes at 72°C.

2.3 GENERATION OF MOUSE LINES

The transgenic lines overexpressing *grik*4 were generated as described in Aller et al. 2015. Briefly, a tag containing 5 myc epitopes was added to the cDNA of rat *grik*4, just after the signal peptide (first 20 aa). The functionality of the pcDNA3 myc *grik*4 plasmid was assayed through electrophysiological recordings when expressed in HEK293 cells. The *myc-grik*4 construct to generate the transgenic mice was cloned in two consecutive steps. First, *myc-grik*4 was cloned as an EcoRV-SmaI fragment into the pNN265 plasmid that contains an intron sequence necessary for the correct functioning of the CaMKII promoter. Subsequently, a NotI fragment containing *myc-grik*4 and the intronic sequence was introduced into the PMM403 plasmid that has the CaMKII promoter inserted in pBluescript (Mayford et al., 1996). The construct, cut with *SfI I* restriction enzyme to remove the pBluescript backbone, was injected into the pronucleus of fertilized eggs

(performed at the Unitat Animals Transge`nics Centre de Biotecnologia Animal i Tera`pia Ge`nica, Universitat Auto`noma de Barcelona). Of the nine founders obtained, one was discarded due to integration into the Y chromosome. The levels of *myc-grik*4 expression were analyzed in the first generation by *in situ* hybridization, immunohistochemistry, and Western blots. Two different lines with similar expression levels were chosen for further studies.

2.4 WESTERN BLOTS

Western Blotting to detect KARs- and AMPARs-subunits

Fresh-dissected hippocampi and neocortex from wild-type and GluK4^{Over} mice were homogenized in 2X volume of sheep buffer containing protease inhibitors and then centrifuged (4,000 rpm at 4ºC). Then supernatant was transferred to a new tube and centrifuged (18,000rpm at 4ºC). From there, the supernatant was removed and the bottom pellet resuspended with MKM buffer containing protease inhibitors and agitated to dissolve protein pellet (1h at 4ºC in a rotator). This solution was then centrifuged (4,000 rpm, 10 min, 4ºC) to pellet out undissolved fractions. Protein concentrations were determined by Bradford quantification (Pierce™ BCA Protein Assay Kit) and samples concentrations were normalized (10 µg/µl). Samples were treated with mercaptoethanol and boiled for 5 minutes at 100°C. Proteins were separated by electrophoresis (1h 30 min at 30 mA) and transferred overnight to nitrocellulose membranes. Correct protein transfer was confirmed by staining membranes with Ponceau red. Membranes containing the proteins were blocked for 1 h at room temperature with 5% milk in TBS containing Tween 20 (TBS/T) and incubated overnight at 4°C with one of the following primary antibodies: blots probed with the following primary antibodies: mouse anti-α-tubulin (1:1000; Abcam), mouse anti-myc (1:500; Santa Cruz Biotechnology), rabbit anti-GluR6/7 and rabbit anti-KA2 (1:1000; Millipore), rabbit anti-GluR2/3 (1:1000; Novus Biological), and rabbit anti-KA1 (1:1000; gently provided by Dr. Melanie Darstein; Darstein et al., 2003). Following overnight incubation in primary antibody, blots were washed in TBS/T, incubated for 2 hours in the appropriate secondary antibody, washed again, and incubated in chemiluminescent reagent (SuperSignal® West Pico Chemiluminescent Substrate, ThermoScientific).

Antibody binding was detected on a luminescent image analyzer (LAS-1000PLUS, Fuji) and quantified with Quantity One 1D Analysis Software (Bio-Rad Laboratories). For quantifications, all densities were normalized to the respective tubulin signal.

2.5 IMMUNOFLUORESCENCE

Brains were fixed as described previously (Schneider Gasser et al., 2006) and sectioned in 20 µm slices, which were incubated overnight at 4°C with rabbit anti-myc (1:500; Abcam) and mouse anti-PSD95 (1:500; NeuroMab) in blocking solution (PBS, 0.2% Triton X-100, and 10% NGS). Afterward, sections were incubated with secondary antibodies Alexa 555-conjugated anti-rabbit and Alexa 488- conjugated anti-mouse, both used at 1:1000. Evaluation of immunofluorescence staining where performed using a Leica DMLFSA confocal microscope and the image analysis software Imaris (Bitplane). A lowpass filter was applied to subtract background.

Deglycosylation. EndoH/PNGaseF was assayed as described previously (Fernandes et al., 2009), whereby 500 units of EndoH (P0702, New England Biolabs) were used to remove high-mannose-containing oligosaccharides, and an equal amount of PNGaseF (P0704, New England Biolabs) was used to remove all N-linked oligosaccharides. After a 1 h digestion, the lysates were analyzed by Western blots probed with mouse anti-myc (1:500; Santa Cruz Biotechnology) and rabbit anti-KA1 (1:1000).

2.6 *In situ* HYBRIDIZATION

In situ hybridization was performed with ^{35}S-labeled specific oligonucleotide probes as described previously (Wisden and Morris, 2002). As a control for specificity, two independent oligonucleotides for the *grik*4 gene were hybridized in parallel, producing identical results. The oligonucleotide sequences used were as follows:

*Grik*4 a:

5´-CTTGTAGTTGAACCGTAGGATCTCAGCCAACTCCTTGAGCATGTC-3´;

Grik4 b: 5´-TAGCCCGGTCTGCGTCCCATATGAACTCTGTAAAGAATACTA-3´;
Myc: 5´-CTCCATTTCATTCAAGTCCTCTTCAGAAATGAGCTTTTGCTCCAT-3´.

2.7 In vitro ELECTROPHYSIOLOGY

2.7.1 SET-UP

Electrophysiological recordings were performed in a dedicated rig with the following elements:

- Pneumatic anti-vibration table to prevent vibrations, where inverted microscope, mechanical and piezoelectric micromanipulators (Burleigh PCS-6000) are mounted.
- A patch-clamp amplifier (Axopatch 200A)
- Gravity perfusion system. General Valve Corporation.
- Visualization system (Sony CCD-IRIS camera and Hamamatsu Argus50 + Monitor).
- Oscilloscope (Tektronik model).
- Data acquisition system (Digidata 1400A Axon instruments) coupled to pClamp10 acquisition software on a personal computer
- Stimulation system (Cibertec CS20 and ISU165)
- Noise eliminator (HumBug Quest Scientific).
- Faraday cage shielding the patch clamp recordings from surrounding electrical noise

2.7.2 PATCH CLAMP RECORDINGS

Membrane currents were recorded by the patch-clamp technique using the, whole cell configuration. Mouse brain slices (age 13-14 days and 18/21 days) were used to record both spontaneous and evoked synaptic currents from CA3 pyramidal neurons, by stimulating the Mossy fiber pathway (MFs) and from CA1 pyramidal neurons, by stimulating Shaffer collateral fibers (SC).

Slice preparation

Animals were deeply anaesthetized using Isoflurane (IsoVet®) and decapitated. The brain was dissected and immediately place in an ice-cold high sucrose buffer (in mM: 124 NaCl, 8 $NaHCO_3$, 10 Glucose, 3 KCl, 1.25 NaH_2PO_4, 1 $MgSO_4$, 2 $CaCl_2$, saturated with 95% O_2/5% CO_2). Cerebellum/pons/medulla were removed and the brain was cut on the sagittal lane. Right and left hemispheres were glued on the brain holder and cut by a vibroslicer (Leica VT1200S) in ice-cold sucrose buffer. Hippocampal slices (300 µm) were cut in an anteroposterior direction and directly transferred into a 37ºC bath of extracellular solution artificial cerebrospinal fluid (aCSF) with the composition (in mM): 124 NaCl, 3 KCl, 1.25 KH_2PO4, 1 $MgSO_4$, 2 $CaCl_2$, 26 $NaHCO_3$, and 10 glucose, equilibrated with 95% O_2/5% CO_2, pH 7.3 (300 mOsm). Slices were allowed to recover for at least 45 min in a holding chamber before recording and used for the experiment typically ~6 hours after slicing. Brain slices were transferred to a recording chamber filled with oxygenated aCSF, supplemented with drugs depending on the experiment protocol, constantly renewed at a speed of 1 ml/min. Recordings were made on a classical *in vitro* setup to record bioelectrical activity in hippocampal slices at room temperature (22º-25º C). Once the slice was under the microscope objective, it was gently anchored by a platinum grid in the recording chamber to avoid slice movement during recording due to fluid streaming. The area CA3 and CA1 (different experiments) were located under a 10X objective, but cells were visually identified at higher magnification (40X), water immersion objective. I recorded pyramidal cells located in the pyramidal layer. Somatic whole-cell patch-clamp recordings in visually identified cells were carried out using borosilicate glass pipettes (Kwik-Fil™, WPI) of 3-5 MΩ resistance, filled with a specific internal solution depending on experiment type.

Spontaneous KARs-mediated Excitatory Post Synaptic Currents ($sEPSC_{KARs}$) from CA3 neurons

$sEPSC_{KARs}$ were recorded after at least 2 min of forming a stable whole cell patch clamping to assure the entrance of the intracellular solution composed by

(in mM): 135 K-Gluconate, 10 NaCl, 10 Hepes, 0.3 EGTA, 2 ATP-Mg and 0.5 GTP, pH=7.3. Recordings were performed by holding the cell at -65mV and perfused with aCSF supplied with the following compound cocktail: 25μM D-APV (Abcam), 100 μM picrotoxin (Tocris) to antagonize NMDARs, $GABA_A$ respectively; 0.5 μM tetrodoxin (TTX, Tocris) to record action potential-independent events and 25 μM LY303070 (the active isomer of GYKI53655) to block AMPAR-currents.

Miniature AMPARs/KARs-mediated Excitatory Postsynaptic Currents ($mEPSC_{AMPARs/KARs}$)

$mEPSC_{AMPARs}$ were collected after at least 3 min of forming a stable whole cell patch clamping, recordings were performed by holding the CA3 cells at -75 mV and perfused with aCSF supplied with the following cocktail compound: 25μM D-APV, 100 μM picrotoxin to antagonize NMDARs, $GABA_A$ respectively; and 0.5 μM TTX to record action potential-independent events.
All drugs, 10μM LY382884, 50 μM IEM-1460 and 0.5μM Calphostin C were dissolved in aCSF in addition to the cocktail compound described and applied by gravity. The exchange from aCSF to drug-containing aCSF was achieved using a switch valve (General Valve Corporation®, valve driver II). Following switchover it required approximately 1 min for the drug-containing solution to reach the recording chamber and 2-3 min before stabilization of the drug effect. After a 2 min of baseline, recording of 3 min were done to check the effect of the drug, except the case of recordings with Calphostin C, made after 7 min of perfusion, enough time to activate the intracellular signaling cascade mediated by PKC. The recording electrode was filled with intracellular solution composed by (in mM): 135 K-Gluconate, 10 NaCl, 10 Hepes, 0.3 EGTA, 2 ATP-Mg and 0.5 GTP, pH 7.3. Drugs were applied by gravity, switching between four perfusion lines.

Evoked excitatory postsynaptic current from MFs-CA3 synapses

To evoke mossy fiber $EPSC_{AMPARsKARs}$, electric shocks were applied through a monopolar electrode made from a glass pipette placed in the stratum lucidum to stimulate mossy fiber pathway.

Recording of AMPARs/KARs-currents were conducted in the presence of 25 μM D-APV , 100 μM picrotoxin to antagonize NMDARs, $GABA_A$ respectively. Each evoked response was repeated for 20 times with an inter-stimulus interval of 15 s (0.06Hz). CA3 cells were clamped at -65mV for ~5 min to ensure stable response.

Recording of NMDARs-currents were conducted with aCSF containing 100 μM picrotoxin and each evoked response was repeated for 20 times with an inter-stimulus interval of 15 s for all CA3 cells recorded. CA3 cells were first clamped at -70 mV for ~5 min, followed by switching the holding potential to +40mV for an additional 5 min to obtain AMPAR and NMDAR component. Averaged NMDARs-mediated EPSCs was calculated 50 ms after the onset of the current, point where AMPAR contribution was null. NMDAR to AMPAR current ratio was calculated by dividing the peak of NMDARs-current with peak of AMPARs-current.

Same procedure was done to calculate the AMPARs-rectification index (RI), with the only difference that cell were clamped at -65mV and in the presence of 25 μM of D-APV.

A double pulse delivered every 15 s was applied to calculate paired-pulse ratio (PPR). The effect on PPR of different compounds were studied (LY382884, UBP310, IEM-1460 and Tianeptine) in different group of neurons. Each compound was dissolved in aCSF, previously supplied with 25μM D-APV, 100 μM picrotoxin, and applied by bath perfusion. Frequency Facilitation (FF) was elicited delivering ~ 20 pulses every 15 s followed by other ~ 20 pulses at 1 Hz. Thus, after baseline recordings at 0.06 Hz, 30 pulses at 1 Hz were applied to afferent fibers and facilitation was calculated as the percentage increase of the $EPSC_{AMPARs}$ observed at 1 Hz relative to the $EPSC_{AMPARs}$ recorded at 0.06 Hz. The recording of all evoked responses were done with the following intracellular solution (in mM):130 $CsMeSO_3$, 4 NaCl, 10 HEPES, 0.2 EGTA, 10 tetraethylamonium, 2 Na_2ATP, 0.5 Na_3GTP, 5 QX314, pH 7.3 (287 mOsm).

Extracellular field recording experiments from MFs-CA3 synapses

Field excitatory post synaptic potentials (fEPSP) were recorded with 3-5MΩ borosilicate electrodes filled with 1M NaCl placed in the stratum lucidum of the CA3 area. fEPSP were evoked at the frequency of 0.06 Hz with a monopolar stimulation electrode. The duration of the stimulus was 100μs; the stimulation intensity corresponded to that necessary to obtain a response equal to 50 % of the maximal fEPSP.

For long term potentiation (LTP) protocol, after a stable 10 minutes baseline was recorded, high frequency stimulation (HFS) potentiation protocol (1 trains of 1 sec pulses at 100Hz) was applied, resulting in a persistent increase of fEPSP size (Bortolotto et al., 2011).

Long term depression (LTD) was obtained by stimulating the same afferent pathway at 1 Hz for 15 min trough low-frequency stimulation (LFS) protocol. In both HFS and LFS protocols, 25μM D-APV was included in the aCSF solution.

The mossy fiber origin was distinguished at the beginning of each experiment because they were characterized by a marked facilitation of EPSCs after switching stimulus frequency from 0.06 to 1 Hz. However, this was also assessed by the depression induced by 10 μM, (2*S*,1′*S*,2′*S*)-2-(carboxycyclopropyl) glycine (LCCG-1), applied at the end of each experiment. The rare cells with an inhibition by LCCG-I <80% were not included in the study.

Evoked excitatory postsynaptic current from Shaffer Collateral-CA1 synapses

Recording of evoked $EPSC_{AMPARs}$, PPR and FF were made positioning the stimulation pipette in the Shaffer Collateral pathway, recording were made from CA1 pyramidal neurons and each experiment protocol was applied as already described for MFs-CA3 synapses. Slices were continuously perfused with aCSF solution. The recording electrode was filled with intracellular solution composed by (in mM): 135 K-Gluconate, 10 NaCl, 10 Hepes, 0.3 EGTA, 2 ATP-Mg and 0.5 GTP, pH 7.

2.8 DATA ANALYSIS

Electrophysiological data were acquired using Clampex 10.6. Evoked EpsC were analyzed by Clampfit 10.6 and mEPSC measurements were analyzed with MiniAnalysis program (Synaptosoft Inc.). For the analysis of EPSCs-decay, one or two exponentials were fitted to the decay phase of the current curve. Statistical analyses were run with the analysis tools provided with SigmaPlot 12.5 analysis software.

We mainly used ANOVA test for comparisons among more than 2 groups of data; Student t-test (confidence interval 95%), when comparison was between two groups presenting a normal distribution, or Mann Withney test on ranks in the case of no normal distribution of data.

UNIVERSITAS
Miguel
Hernández

3. Results

UNIVERSITAS
Miguel
Hernández

3.1 GENERATION OF MOUSE LINES

In order to delineate the function of the high-affinity KARs subunit GluK4, we generated mice overexpressing *grik*4 gene in the forebrain. For that purpose, rat *grik*4 cDNA was tagged with 5 myc epitopes and inserted into the PMM403 plasmid that had the CaMKII promoter (Fig.16A). Out of 9 mice lines in which different levels of *grik*4 expression was evident (GluK4^{Over} lines), we selected 2 with similar level of expression for further work (C57BL/6J-Tg(camk2-grik4)2 and C57BL/6J-Tg(camk2-grik4)3). In Fig.16 B glutamate 1mM activated the whole population of KARs and 0.1 mM ATPA revealed the formation of functional hetoromeric GluK2/GluK4 receptors in HEK293 cells. *In situ* hybridization and myc immunocytochemistry (Fig. 16C and D) illustrated that, as expected, the transgene was expressed in the forebrain, particularly in the neocortex and hippocampus but also in the striatum. Furthermore, the glycolytic processing of exogenous GluK4 protein in GluK4^{Over} mice was entirely normal (Fig.16E).

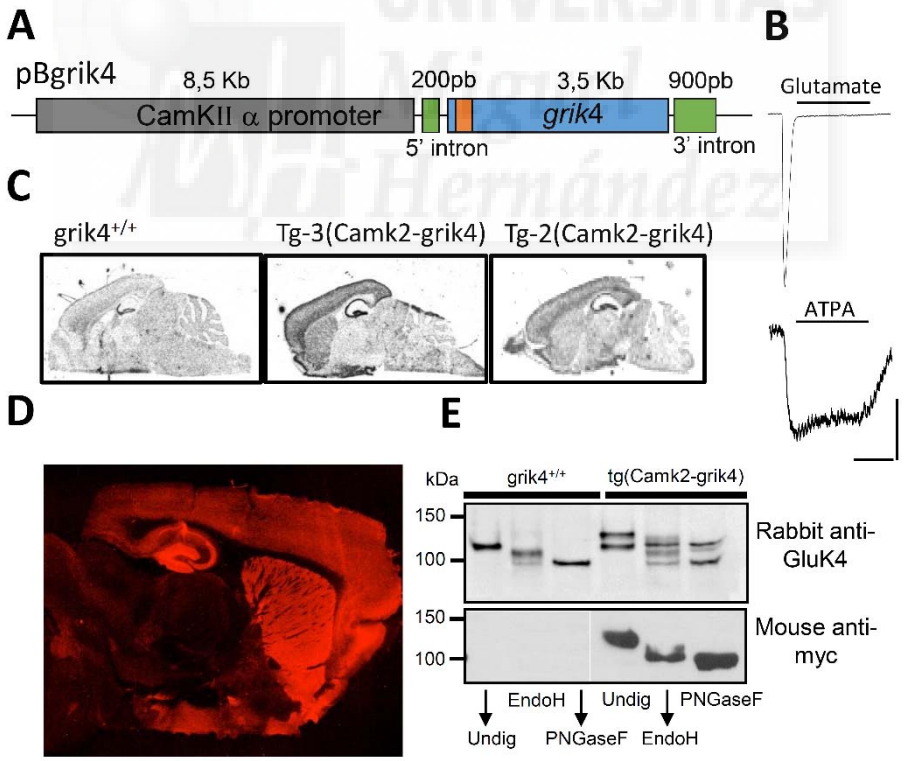

Figure 16: Exogenous GluK4 protein in the mice forebrain. A) Scheme shown the *grik4* transgene arrangement. **B**) Electrophysiological response induced by glutamate (1mM) and ATPA (0.1mM) in HEK293 cells expressing the construct plus GluK2 subunits. The response to ATPA revealed the formation of functional hetoromeric GluK2/GluK4 receptors. Vertical calibration are 100 pA (top response) and 20 pA (bottom). Horizontal bar is 200 ms. **C**) In situ hybridization of normal, GluK4$^{+/+}$ and GluK4 overexpressing, GluK4^{Over}, mice. **D**) Expression of GluK4 transcribed from the transgene in the forebrain detected by anti-myc antibody. **E**) Normal glycolytic processing of exogenous GluK4 protein in GluK4^{Over} mice.

3.2 PRESYNAPTIC AND POSTSYNAPTIC LOCALIZATION OF GluK4 PROTEIN

Neuronal KARs have been best described in the hippocampus, where they have been functionally localized to both postsynaptic densities (Castillo et al., 1997; Mulle et al., 1998; Vignes and Collingridge, 1997) and presynaptic terminals and axons (Chittajallu et al., 1996; Contractor et al., 2000; Schmitz et al., 2000, 2001). Of the several different excitatory and inhibitory synapses where KARs play a role in synaptic transmission, the MFs synapse, formed between the axons of the dentate gyrus granule cells and the pyramidal neurons in the CA3 region, is a particularly good model for studying KARs function. At this synapse, GluK4 is endogenously expressed in granule cells and CA3 pyramidal neurons, and is localized to the MFs presynaptic boutons and postsynaptic density in CA3 pyramidal cell thorny excrescence spines (Darstein et al., 2003). To see if GluK4 subunit was localized at the expected site, immunocytochemical studies were performed in C57BL/6J-Tg(camk2-grik4)3 mouse line. Myc-immunoreactivity was detected in PSD95 labeled structures (Fig. 17A-D) and in GFP-labeled MFs terminals, after crossing GluK4 overexpressing mice with transgenic mice expressing GFP in dentate gyrus granule cells (Feng et al., 2000) (Fig. 17E-H).

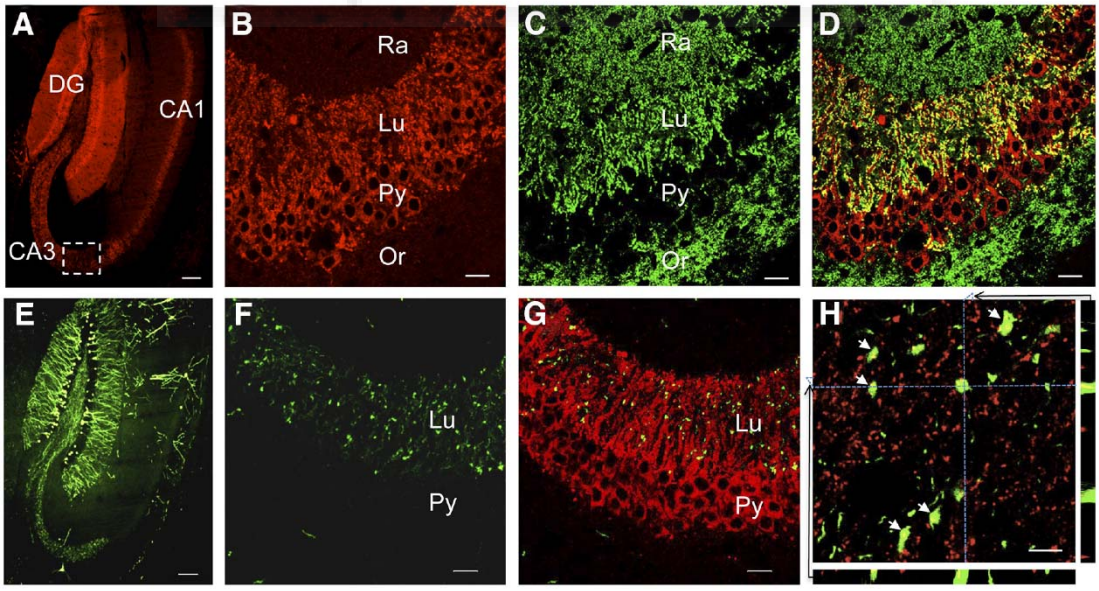

Figure 17: Distribution of myc-GluK4 subunit in hippocampal MFs synapses. GluK4^{Over} brain slices (2 months) were immunostained for myc immunoreactivity and the postsynaptic marker protein PSD95 in hippocampal MFs synapse. **A–C)**, myc-GluK4 **(A, B)** and PSD95 **(C)** expression in the hippocampus. **D)** Overlay of *B* and *C*. Colocalization of both proteins (yellow) in the stratum lucidum (Lu) suggests the presence of GluK4 in postsynaptic structures. **E)** and **F)** Reconstruction of several confocal sections through the hippocampus of a mouse expressing GFP in the granule cells of the DG **(E)** and

therefore in MFB **(F). G)** Overlay of GFP-expressing mossy fibers (*F*) and myc-GluK4 red immunoreactivity (similar section as in *B*). **H)** A detail at high-magnification from *G* showing myc-GluK4 immunoreactivity inside the synaptic buttons (arrows). The projections in three orthogonal planes at the level indicated by the dotted lines are also shown (right and bottom edges). Or, Stratum oriens; Py, pyramidal cell layer; Ra, stratum radiatum. Scale bars: *A*, *E*, 100µm; *B–D*, *F*, *G*, 20µm; *H*, 3µm.

These data revealed that exogenous GluK4 was expressed in the hippocampal CA3 field at both sides of the synapse.

3.3 CHANGES IN KARs PROTEIN LEVEL IN GluK4^{Over} MICE

GluK4 overexpressed protein was evaluated as well in C57BL/6J-Tg(camk2-grik4)3 mouse line, where the biochemical characterization of GluK4, GluK5, GluK2/3 KARs subunits and GluA2/3 AMPARs subunits was carried out. Western blots for the GluK4 protein encoded by *grik*4 revealed that this protein was over-expressed by 40-50% in the hippocampus and around 100% in the neocortex (Fig. 18A). Whereas GluK5 subunit was significantly decreased in the hippocampus (Fig. 18B), GluK2/GluK3 protein level were normal and GluA2/GluA3 protein levels showed a tendency to decrease, without reaching statistical significance.

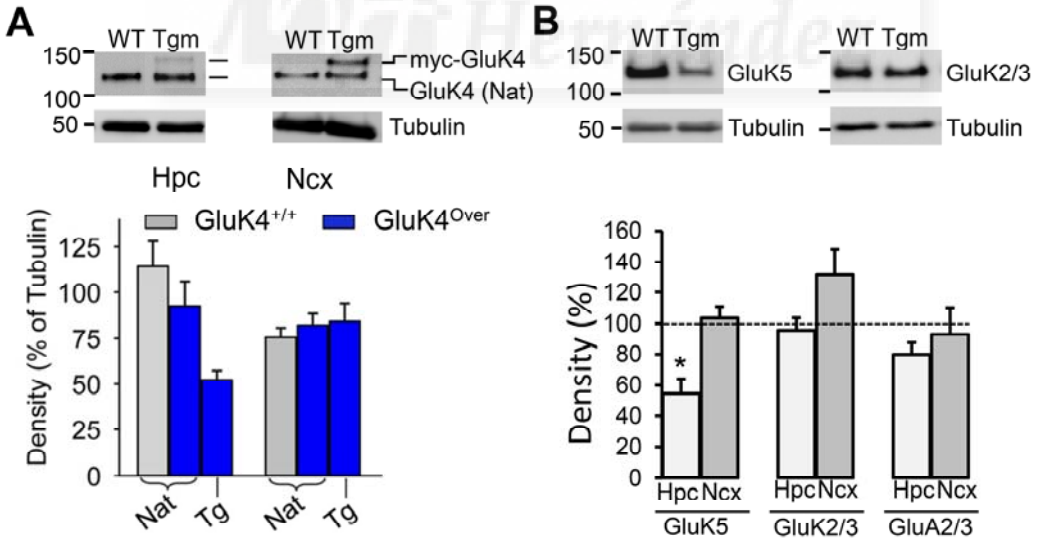

Figure 18: *grik*4 transgenic mice show increased expression of GluK4 protein. A) Quantification by Western blots of native (GluK4; Nat) and transgene-derived (myc GluK4, Tg) protein in the hippocampus (Hpc) and the neocortex (Ncx) of both GluK4^{Over} (Tgm) and GluK4$^{+/+}$ not carrying the transgene (WT). Relative levels of expression were estimated by referring GluK4 band densities to the density of tubulin in each structure **B)** Expression levels of kainate receptor subunits (GluK5 and GluK2/3) and AMPARs subunits (GluA2/3) in the GluK4^{Over} transgenic mice and their wild-type littermates in the cortex and hippocampus Histograms at the bottom reflect the mean±SEM of measurements from four (Tgm) and three (WT) independent samples run in duplicate (*p<0.05, Student's t test).

These data show that GluK4 protein expression is altered and this affects also the expression of other glutamatergic receptor subunits, probably reflecting a process to compensate for the excess of GluK4.

3.4 GluK4 OVEREXPRESSED SUBUNIT PARTICIPATES TO FUNCTIONAL KARs IN MFs-CA3 CELL SYNAPSES

Synaptic transmission was evaluated in C57BL/6J-Tg(camk2-grik4)3 mouse line overexpressing GluK4 in the hippocampal CA3, an area where KARs are expressed abundantly at both the pre- and postsynaptic sides. To directly measure the strength of KARs-mediated excitatory synaptic transmission in CA3 pyramidal neurons, we performed whole-cell intracellular recordings to study spontaneous synaptic transmission. CA3 pyramidal cells were clamped at –60 mV through a recording pipette filled with 135 mM $KMeSO_3$. Spontaneous EPSCs (sEPSCs) mediated by KARs were recorded in the presence of 50 μM picrotoxin and 25 μM D-APV to antagonize GABARs- and NMDARs-mediated current and in the additional presence of LY303070 (25 μM) to also antagonize AMPARs (Fig. 19). As examined in the MFs-CA3 synapses of the hippocampus, the presence of more GluK4 protein induced a prominent change in KARs-mediated synaptic transmission.

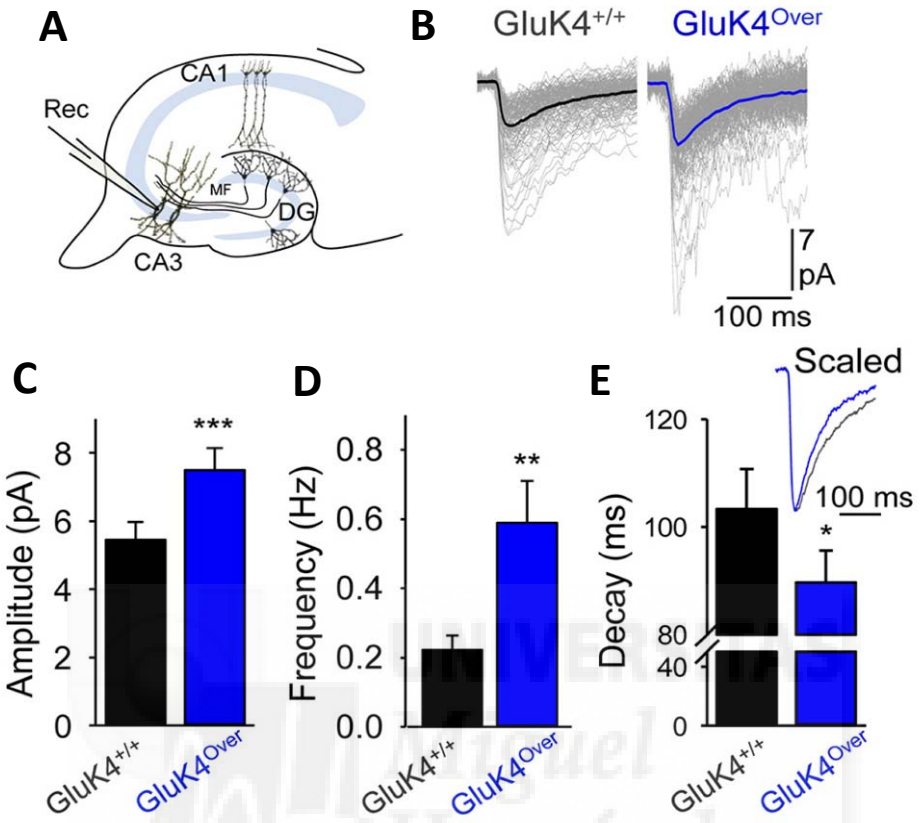

Figure 19: Exogenous GluK4 takes part of functional synaptic KARs. A) Hippocampal slice scheme with recording (Rec) electrode (MF, mossy fibers; DG, dentate gyrus). **B)** Spontaneous KAR-mediated EPSCs in CA3 pyramidal cells recorded at -60 mV of membrane potential have been alienated and superimposed (grey traces). Resulting averages of all responses are included as thick traces. The mean values for the amplitude (**C)**, frequency (**D)** and decay times (**E)** for these responses are shown for each genotype. The inset in E shows scaled and superimposed averaged KARs mediated responses in WT and transgenic mice. Data derived from 32 neurons/11 slices and 41 neurons/10 slices from 8 GluK4^{Over} and 6 GluK4$^{+/+}$mice, respectively; ***p<0.001, **p<0.01, *p<0.05 Mann–Whitney rank-sum test.

sEPSC$_{KARs}$ in CA3 pyramidal cells had 38% larger amplitude than in normal mice (5.5±0.2 pA and 7.5±0.3 pA for GluK4$^{+/+}$ and GluK4^{Over}, respectively, n=41 and 32 neurons; p<0.001), they were more frequent (0.22±0.04 Hz and 0.59±0.11 Hz for GluK4$^{+/+}$ and GluK4^{Over}, respectively; p=0.013) and presented faster deactivation rates (103.3±3.7 ms and 89.7±2.9 ms for GluK4$^{+/+}$ and GluK4^{Over}, respectively; p=0.035) (Fig. 19 C-E). These data demonstrate that exogenous subunits take part of normal synaptic receptors in MFs-CA3 pyramidal neuron synapses.

3.5 GluK4 OVEREXPRESSION AFFECTS AMPARs- AND NMDARs-MEDIATED GLUTAMATERGIC TRANSMISSION AT HIPPOCAMPAL MFs-CA3 CELL SYNAPSES

As examined in the MFs-CA3 synapses of the hippocampus, the presence of more GluK4 protein induced a prominent change in KARs-mediated synaptic transmission. To directly measure the strength of AMPARs- and NMDARs-mediated excitatory synaptic transmission in CA3 pyramidal neurons, we performed whole-cell intracellular recordings to study both spontaneous and evoked synaptic responses.

3.5.1 mEPSC FREQUENCY AND AMPLITUDE ARE HIGHER AND FASTER IN GluK4^{Over} MICE

CA3 pyramidal cells were clamped at –75 mV through a recording pipette filled with 135 mM $KMeSO_3$. Miniature EPSCs (mEPSCs) mediated by AMPARs and KARs were recorded in the presence of 0.5 μM TTX to record only AP-independent release of glutamate. Spontaneous AMPARs/KARs-mediated events presented larger amplitude and higher frequency in CA3 pyramidal neurons of GluK4^{Over} slices (Fig. 20). The cumulative probability distribution of $mEPSC_{AMPARs/KARs}$ frequencies was shifted to the left in GluK4^{Over} slices (6.32±0.59 Hz) compared with WT slices (1.61±0.25 Hz) and the cumulative probability distribution of amplitudes was similarly shifted to the right in GluK4^{Over} neurons (44.2±2.9 pA) as compared to WT neurons (29.1±2.3 pA). GluK4^{Over} mice events also presented a faster decay time compared to WT mice (5.47±0.15 ms for GluK4^{Over} mice and 6.36±0.22 ms for GluK4$^{+/+}$ mice).

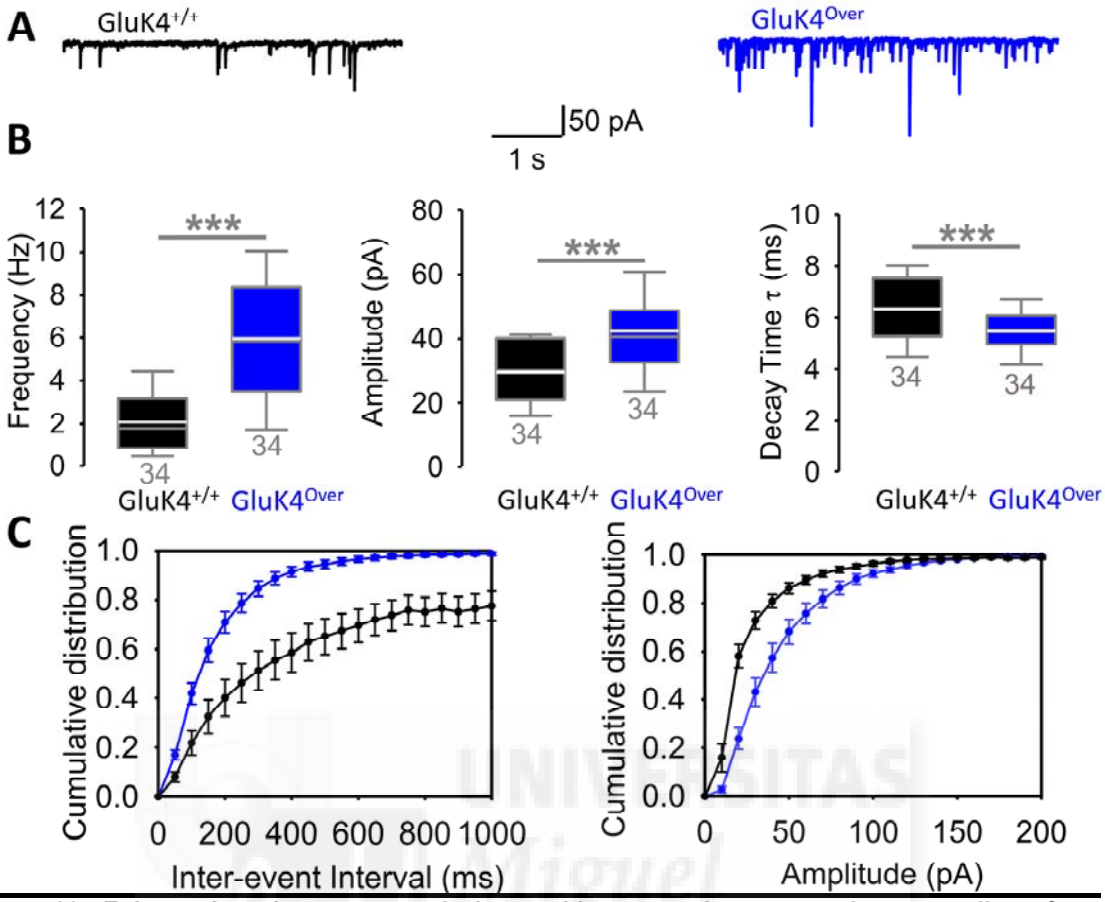

Figure 20: Enhanced excitatory transmission at hippocampal synapses in acute slices from GluK4^{Over} mice. A) Representative traces of mEPSC$_{AMPARs/KARs}$ recorded in the presence of TTX (0.5 µM), D-APV (25 µM) and picrotoxin (50 µM). **B)** Quantification of frequency, amplitude and decay time of EPSC$_{AMPARs/KARs}$ events (numbers under the box indicate the number of neurons analyzed in 7 slices from 3 WT mice and 6 slices from 3 GluK4^{Over} mice). In the box plots, horizontal grey lines denote the median and white lines represent the mean. **C)** Cumulative probability distribution of EPSC$_{AMPARs/KARs}$ amplitudes and frequencies in CA3 pyramidal neurons in acute slices from GluK4^{Over} mice and WT mice. ***p<0.001; Mann-Whitney rank-sum test.

The amplitude distributions were fitted with Gaussian curves (Fig. 21A, B): GluK4^{Over} distribution was fitted with two Gaussian curves compared to the only more skewed curve for GluK4$^{+/+}$ mice. The Gaussian fit yields mean values of 8.9 pA±3.2 pA for the GluK4$^{+/+}$ distribution, slightly shifted to the left compared to mean value of 11.3 pA±4.3 pA of the first curve in GluK4^{Over} distribution. The additional curve for GluK4^{Over} distribution showed a mean value of 20.4 pA±4.6 pA. The larger amplitude and variability of mEPSC$_{AMPARs/KARs}$ at GluK4^{Over} synapses could be attributable to both pre- and postsynaptic factors thought to contribute to large synaptic current variability at other CNS synapses. One possibility is that the simultaneous fusion of multiple transmitter vesicles occurs with a greater probability at GluK4^{Over} presynaptic boutons, possibly as a result of extracellular Ca^{2+} influx at boutons with multiple release site like MFs terminals.

This would be expected to generate broad mEPSCs amplitude distribution with multiple peaks, as we observed in GluK4^{Over} distribution. If large mEPSCs amplitude is generated by a Ca^{2+}-dependent multiquantal release mechanism, then reducing the probability of spontaneous release should result in a decrease of both mEPSCs variability and mean amplitude. To test this possibility directly, we recorded $mEPSC_{AMPARs/KARs}$ lowering the extracellular Ca^{2+} concentration $[Ca^{2+}]_e$ to 0.2 mM. The frequency of the events fell down in 0.2 mM Ca^{2+}, as a consequence of the decreased probability of release (*p*) as shown in Fig. 21C, D, whereas the mEPSCs mean amplitude was also reduced but still showed the presence of two peaks and a broader amplitude distribution in GluK4^{Over} neurons. GluK4$^{+/+}$ showed a mean amplitude value of 9.6 pA±3.3 pA and GluK4^{Over} showed two Gaussian distributions, even more evident than those observed at 2 mM Ca^{2+}, yielding values of 11.9 pA±3.9 pA and 19.9 pA±5.3 pA. Pool data of the $mEPSC_{AMPARs/KARs}$ amplitude values (insert in Fig.21) showed a significant difference between the two genotypes at both Ca^{2+} concentration (21.7 pA±1.5 pA for GluK4$^{+/+}$ *vs* 32.6 pA±1.5 pA for GluK4^{Over} at 0.2 mM Ca^{2+}, and 29.1±2.3 pA for GluK4$^{+/+}$ *vs* 44.2±2.9 pA for GluK4^{Over} at 2 mM Ca^{2+}).

These results suggest that GluK4 overexpression determines an increase in the quantal frequency. The larger $mEPSC_{AMPARs/KARs}$ amplitudes are in part derived from a Ca^{2+}-dependent multiquantal release mechanism, but also from a higher quantal amplitude (*q*) due to the presence of a new population of events having a higher conductance, mainly Ca^{2+}-independent and likely derive from factors other than multiquantal release, such as an increase in the type or number of postsynaptic receptors activated by the glutamate molecules from a quantal secretion.

Therefore, we might conclude that the total increase of the mean $mEPSC_{AMPARs/KARs}$ amplitude observed in GluK4^{Over} mice compared to GluK4$^{+/+}$ mice is mirroring not only a change in the number and/or type of activated postsynaptic receptors but also the increased probability of glutamate release .

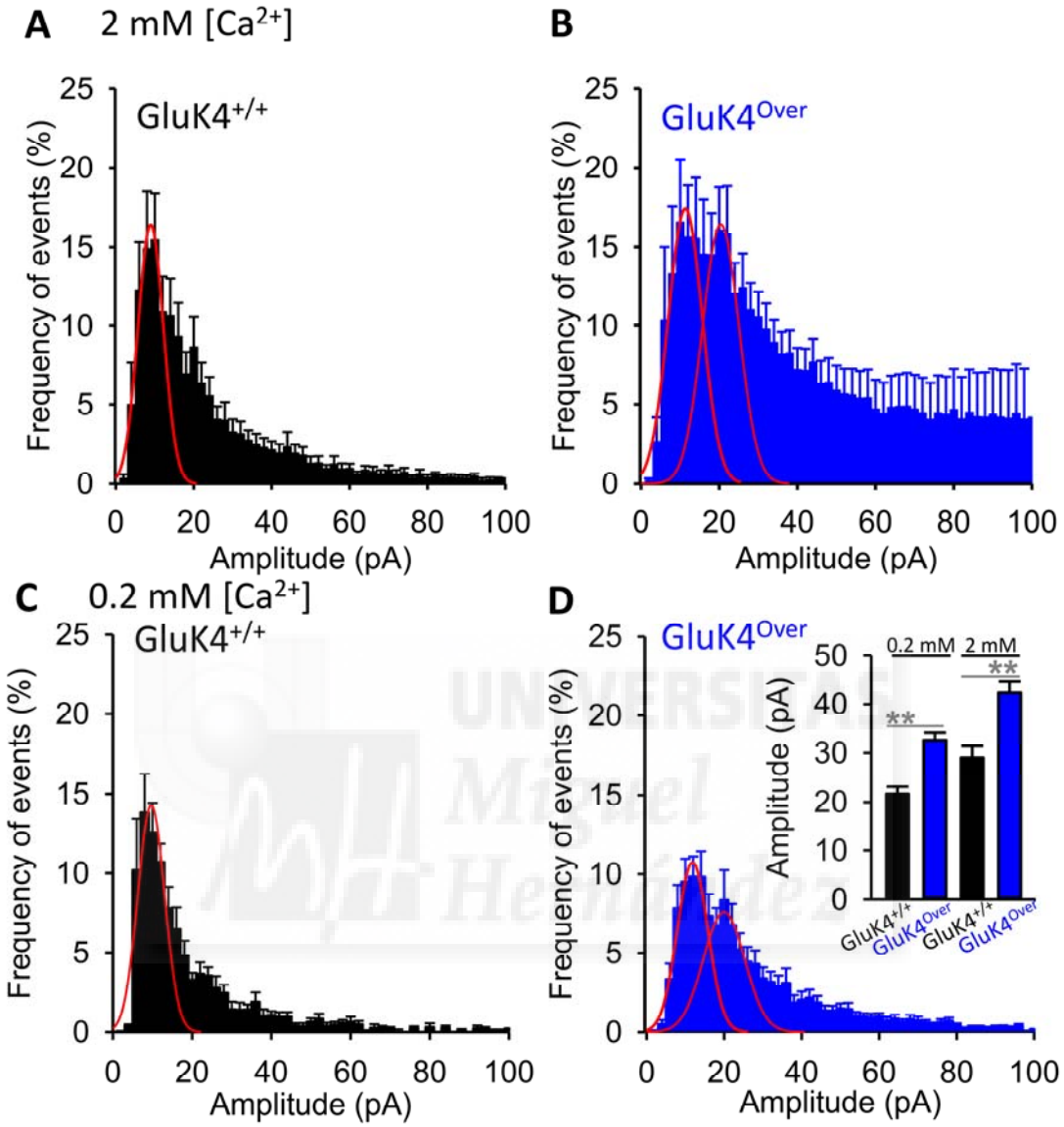

Figure 21: Changes in mEPSC$_{MPARs/KARs}$ amplitude distributions between GluK4$^{+/+}$ and GluK4^{Over} mice. A) and **B)** Average amplitude distributions of miniature events were fitted to Gaussian curves in both genotypes. The Gaussian fit yields mean value of 8.9 pA±3.2 pA for the GluK4$^{+/+}$ distribution, slightly shifted to the left compared to mean value of the first peak 11.3 pA±4.3 pA showed by the GluK4^{Over} distribution. Note the presence of a second peak in GluK4^{Over} distribution yielding a mean value of 20.4 pA±4.6 pA. **C)** and **D)** When the $[Ca^{2+}]_e$ was reduced to 0.2 mM the Gaussian fit yields mean amplitude values of 9.6 pA±3.3 pA for the GluK4$^{+/+}$ distribution, and 11.9 pA±3.9 pA and 19.9 pA±5.3 pA for the GluK4^{Over} distribution. **Insert)** Pooled data showing the significant difference in mEPSC$_{AMPARs/KARs}$ amplitude between genotypes at different Ca^{2+} concentration. Histograms are the average amplitude distributions of 16 cells (3 mice) for GluK4$^{+/+}$ and of 20 cells (3 mice) for GluK4^{Over} in the case of 2 mM $[Ca^{2+}]$ and 12 cells (2 mice) for GluK4$^{+/+}$ and of 14 cells (2 mice) for GluK4^{Over} in 0.2 mM $[Ca^{2+}]$. ***p*<0.01 Mann-Whitney rank-sum test.

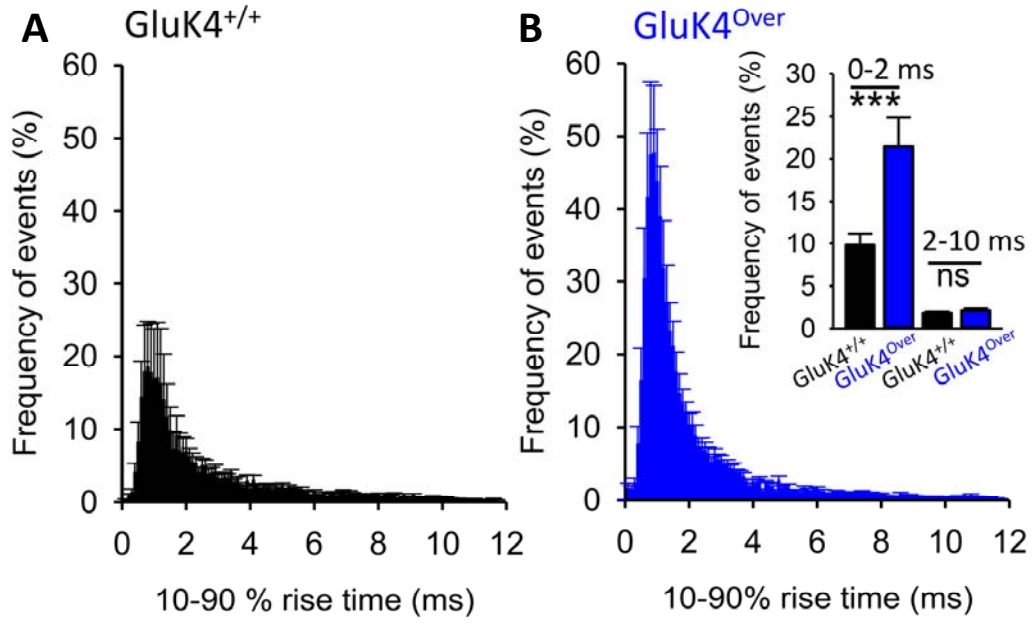

Figure 22: GluK4^{Over} mEPSC$_{AMPARs/KARs}$ show higher frequency of faster rise events. Average 10-90% Rise time distributions show heterogeneous populations with rise time centered around 1 ms in both **A)** GluK4$^{+/+}$ and **B)** GluK4^{Over} mice, however GluK4^{Over} mice show a higher frequency of events with faster rise time compared to GluK4$^{+/+}$ mice as showed by the inserted graph. Histograms are the average rise time10-90% distributions of 15 cells (3 mice) for each genotype. ****p*<0.001; Mann-Whitney rank-sum test.

Instead, 10-90 % rise time kinetic distributions (Fig. 22A) showed that GluK4^{Over} mice have a higher frequency of events with faster rise kinetic compared to GluK4$^{+/+}$ mice. Bearing in mind that MFs, and not the associational commissural (A/C) fibers, are the source of the large mEPSC recorded from CA3 pyramidal cells (Henze et al., 1997), these results suggest that more frequent mEPSCs with larger amplitude might primarily belong to a class of mEPSCs that originate at synapses located on proximal rather that distal dendrites, and thus GluK4 overexpression increases the frequency and the amplitude of miniature events from MFs terminals contacting CA3 neurons, likely leaving unchanged miniature events originating from the A/C fibers.

3.5.2 GluK4^{Over} mice show modified properties in eEPSC$_{AMPARs/KARs}$

Synaptic transmission was studied stimulating MFs pathway and recording from CA3 pyramidal neurons at 0.06 Hz. Cells were clamped at –65 mV and MFs EPSCs identified by large paired pulse facilitation and by the addition of the group II mGluR agonist LCCG 10 μM at the end of the experiment. This agonist abolished >90% of the synaptic signal, indicating that MFs were exclusively

activated. Examination of the MFs-evoked EPSCs mediated by AMPARs/KARs were consistently larger in GluK4^{Over} mice (195±13 pA; *n* = 58) than in wild-type mice (110±6 pA; *n* = 63) (Fig. 23C). Furthermore, faster decay times of evoked eEPSC$_{AMPARs/KARs}$ in GluK4^{Over} mice were also observed, as shown in Fig. 23D. Double exponential functions were fitted to the traces to measure the duration of AMPAR-EPSCs.

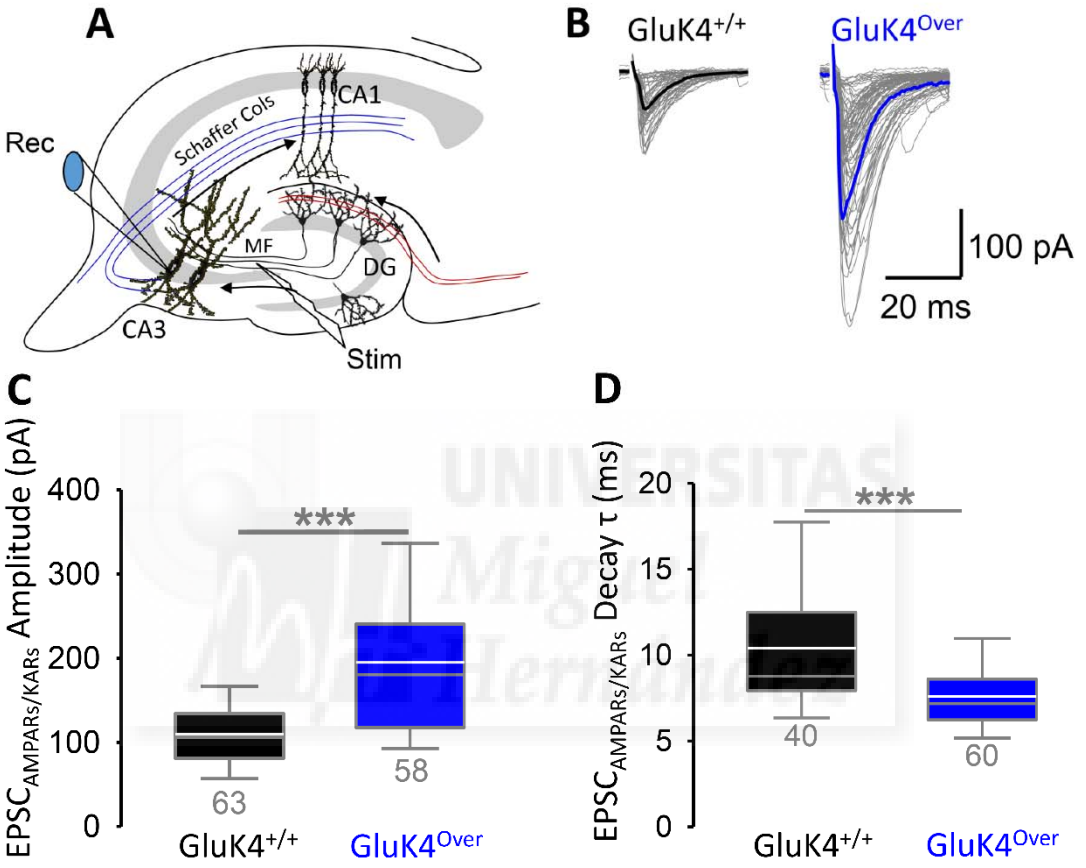

Figure 23: GluK4^{Over} mice show increased eEPSC$_{AMPARs/KARs}$ with faster kinetics. A) Hippocampal slice scheme with recording (Rec) and stimulating (Stim) electrodes (MFs, mossy fibers; DG, dentate gyrus). **B)** MFs evoked EPSCs in CA3 neurons show larger amplitude and faster decay in GluK4^{Over} as compared with GluK4$^{+/+}$ mice. **C)** Quantification of AMPARs-mediated current (n=63 neurons from 6 WT mice and n=58 neurons from 5 GluK4^{Over} mice) and **D)** their decay time for both genotypes (n=40 neurons from 6 WT mice and n=60 neurons from 5 GluK4^{Over} mice) Double-exponential functions were fitted to the curves showing a faster kinetics in GluK4^{Over} mice. In the box plots, horizontal grey lines denote the median and white lines represent the mean. ***p<0.001; Mann-Whitney rank-sum test.

These data imply that information transfer at MFs synapses is altered in mice overexpressing the GluK4 subunit of KARs.

3.5.3 GluK4^{Over} mice have enhanced rectification at MFs-CA3 synapses

The larger amplitude of both AMPARs/KARs-mediated mEPSCs and evoked AMPARs/KARs-mediated EPSCs led us to think about a change in the type of activated postsynaptic AMPARs receptors in GluK4^{Over} synapses. The type of subunit composing AMPARs influences their biophysical properties and confers different features. In fact, AMPARs lacking GluA2 subunits have two important properties, they are Ca^{2+}-permeable and present larger single channel conductance. These AMPARs also present strong inward rectification, a signature that allows identifying their presence in the synapse. To test whether this was the case, we measured the AMPARs-rectification index (RI) (Fig. 24), which gave us an idea about the relative presence of GluA2-containing and GluA2-lacking AMPARs. Channels containing edited GluA2 subunits have a linear current-voltage relationship (Boulter et al., 1990), are impermeable to Ca^{2+} and present a relatively low single-channel conductance. Cells were clamped at –65 mV and the rectification index (RI), defined as the ratio of amplitudes of AMPARs-mediated response measured at +40 and -65 mV, was calculated. The RI was significantly smaller in P17–P21 (adult) GluK4^{Over} neurons (0.35±0.06; *n* =16) than in same age GluK4$^{+/+}$ neurons (0.87±0.12; *n* = 22). Recordings at P13/P14 (juvenile) post-natal days revealed a smaller RI in GluK4^{Over} mice (0.23±0.04; *n*=18) than wild-type mice (0.51±0.04; *n* = 13). Interestingly, we observed that adult GluK4^{Over} mice had a RI very similar to that found in juvenile wild-type mice.

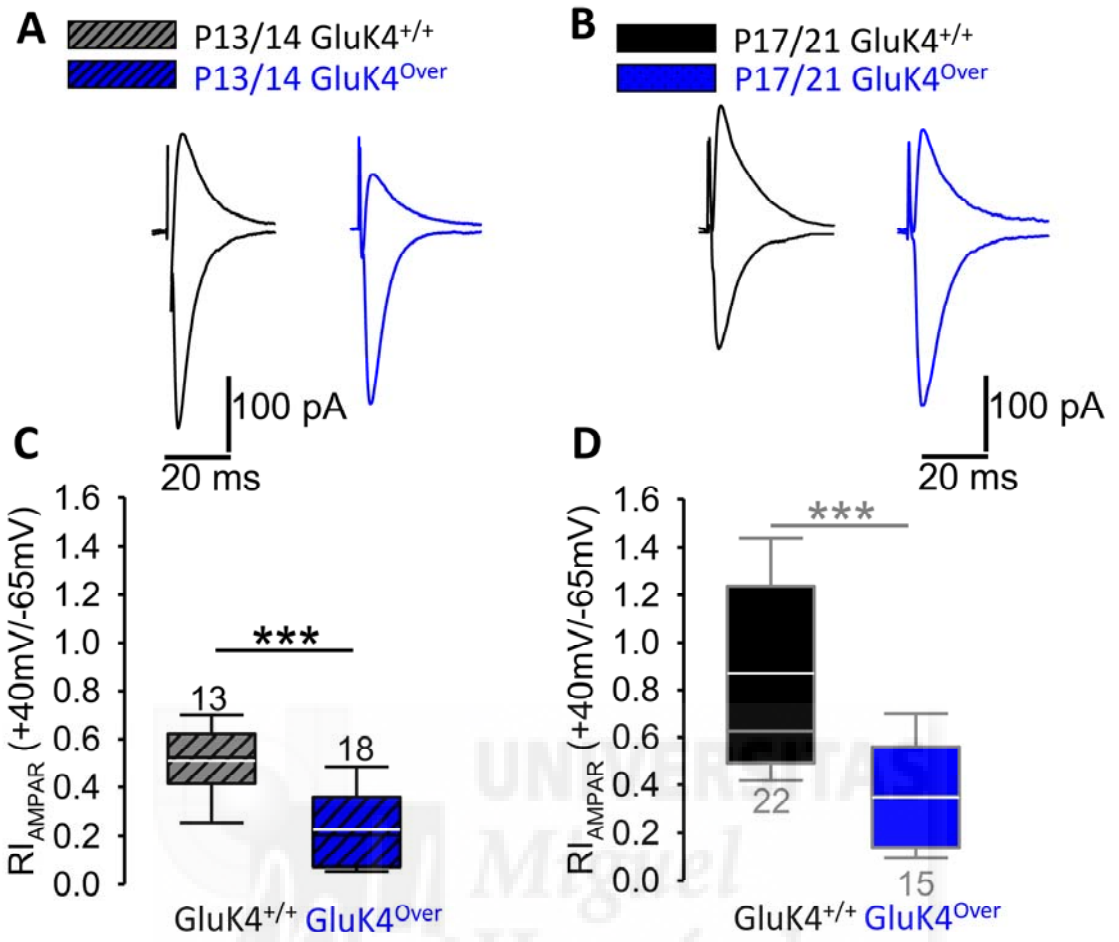

Figure 24: GluK4^{Over} mice contain Ca^{2+}-permeable AMPARs. Representative EPSC$_{AMPARs}$ currents in P13-P14 **(A)** and P17-P21 **(B)** and their respective total quantification **(C)** and **(D)**. GluK4^{Over} neurons show a lower RI than GluK4$^{+/+}$ neurons. Adult GluK4^{Over} mice neurons show a similar RI to juvenile GluK4$^{+/+}$ mice neurons. 2 juvenile mice for each genotype and 2 adult mice for each genotype were used. In the box plots, horizontal grey lines denote the median and white lines represent the mean *** p<0.001; Student's t test in **(C)** and Mann-Whitney rank-sum test in **(D)**.

These results suggest that the part of the higher conductance and the increased kinetic of the AMPARs-synaptic response are the consequence of more CP-AMPARs present in GluK4^{Over} mice than a normal MFs-CA3 synapse. An impairment of the physiological switch in the AMPARs phenotype, from CP- to CI-AMPARs, normally occurring during development, could also account for the changes observed in AMPARs-mediated transmission in GluK4^{Over} mice.

3.5.4 SMALLER NMDARS-MEDIATED EPSCS ARE ASSOCIATED WITH Ca^{2+}-PERMEABLE SYNAPSES IN GLUK4^{OVER} MICE

Dysfunctions of NMDARs have been implicated in the pathophysiology of neuropsychiatric diseases, most notably in schizophrenia but also recently in autism spectrum disorders (ASDs). In view of that, we recorded NMDARs and AMPARs-currents, at +40 mV and -70 mV respectively, to calculate the NMDA/AMPA ratio. First, the amplitude of NMDARs currents was measured at +40 mV to avoid Mg^{2+} blockade and in the presence of CNQX 50 µM to avoid KARs- and AMPARs-mediated EPSCs. Results show smaller $EPSC_{NMDARs}$ in GluK4^{Over} mice (53.3±4.0 pA; *n* = 22) as compared to wild-type control mice (75.2±4.5pA; *n* = 21). Given that both AMPARs- and NMDARs-mediated transmission were increased and decreased respectively, the NMDA/AMPA ratio, calculated from a different set of experiments was consequently decreased in GluK4^{Over} mice (0.75±0.15, *n* = 16 for GluK4$^{+/+}$ mice and 0.32±0.04, *n* = 21 for GluK4^{Over} mice).

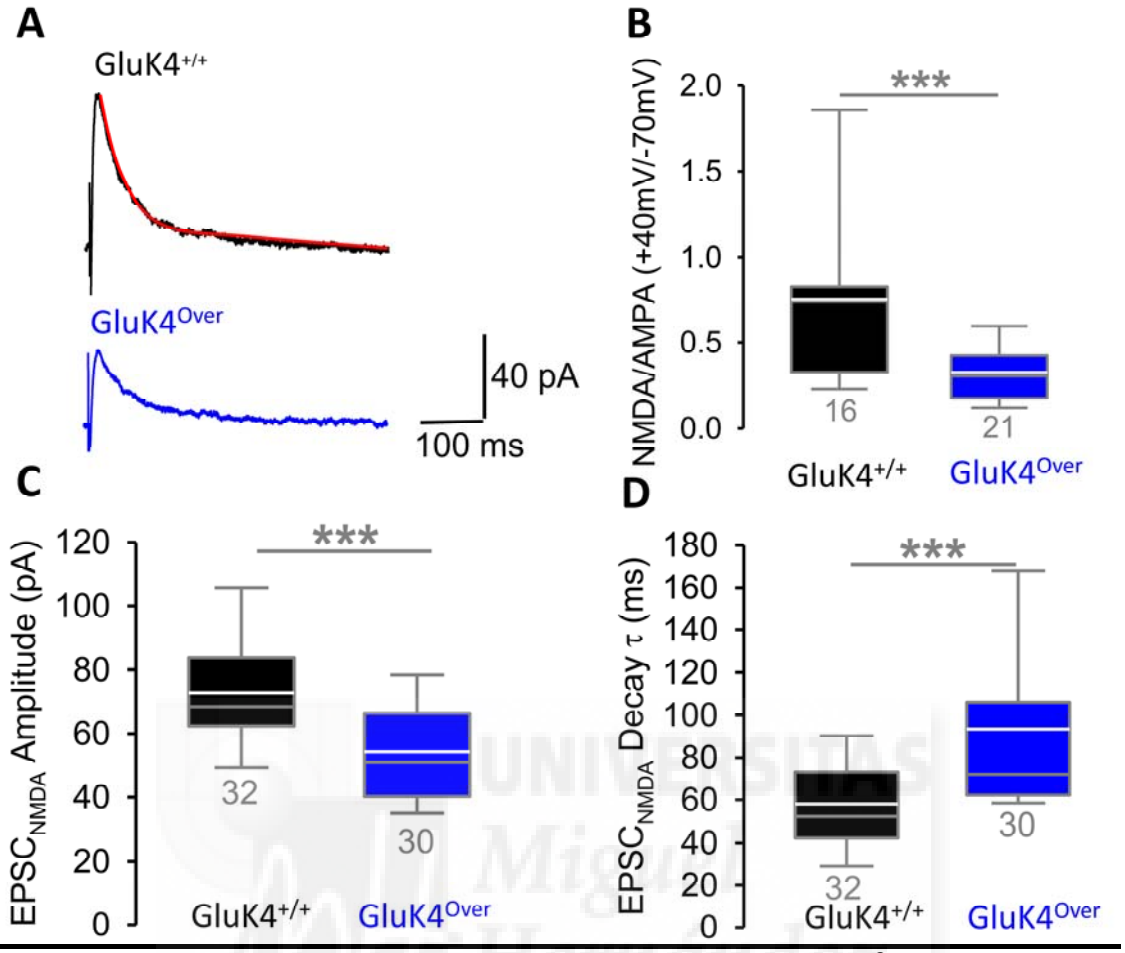

Figure 25: **Impaired NMDARs-dependent synaptic transmission in GluK4^{Over} mice. A)** Typical NMDARs-mediated EPSCs (Vm=+40 mV) in CA3 pyramidal cells in each genotype. The amplitude of NMDAR component was measured in the presence of CNQX (50 μM) and their decay time τ were obtained fitting single-exponential functions to the current curves (red line). **B)** Reduced ratio of NMDARs to AMPARs-mediated transmission was observed in GluK4^{Over} mice compared to their WT siblings. The NMDA/AMPA ratio was obtained by measuring AMPARs component at a holding potential of -70 mV, and NMDARs component at +40 mV. **C)** Summary graph of $EPSC_{NMDAR}$ amplitudes showing a NMDAR-hypofunction in GluK4^{Over} mice. **D)** Grouped data from all NMDARs currents decay time show slower kinetics in Gluk4^{Over} mice. 3 mice for each genotype were analyzed. In the box plots, horizontal grey lines denote the median and white lines represent the mean. ***p<0.001, **p<0.01; Mann-Whitney rank-sum test.

Single-exponential functions were fitted to the curves to calculate NMDARs—decay times (T). The evaluation of $EPSC_{NMDARs}$ decay time also showed a significant difference between the two genotypes (time constants of 83.6±7.8 ms for GluK4^{Over} mice compared to 60.1±4.1 ms for GluK4$^{+/+}$ mice) as shown in Fig. 25D.

These results suggest that GluK4 overexpression is determining an important change on synaptic information transfer through MFs-CA3 synapses. These experimental evidences may indicate that GluK4 overexpression provokes an

improper maturation of MFs-CA3 pyramidal cells synapses. First, it increases the glutamate release as shown by the increase in $mEPSC_{AMPARs/KARs}$ frequency which is also affecting the $mESPC_{AMPARs/KARs}$ overall amplitude; secondly, GluK4 overexpression provokes the insertion of CP-AMPARs. These receptors are responsible for the reduced decay time of $mEPSC_{AMPARs/KARs}$ and $eEPSC_{AMPARs/KARs}$, and they partially account for the conductance increase observed in $mEPSC_{AMPARs/KARs}$ and $eEPSC_{AMPARs/KARs}$. Ultimately, GluK4 overexpression determined a removal of NMDARs from the postsynaptic terminal and likely a change in their subunit composition since their slower kinetics may be due to an increase of GluN2B/GluN2A ratio.

3.6 THE SYNAPTIC RELEASE OF GLUTAMATE IS ALTERED IN GluK4^{Over} MICE

Presynaptic KARs on MFs axons and boutons modulate glutamate release (Schmitz et al., 2001). However, how these KARs autoreceptors exert this function is under debate and even more uncertain appear the subunit composition of the autoreceptors responsible for this modulation. Therefore, we examined the contribution of GluK4 to presynaptic KARs function in the overexpressing GluK4 mice, and their respective wild-type littermates by recording Paired Pulse Ratio (PPR) and Frequency Facilitation (FF) at MFs-CA3 synapses, two different types of short-term plasticity controlled by presynaptic phenomena.

PPR is defined as an increase in the size of the synaptic response to a second pulse delivered within a short interval of time following the first pulse. In the MFs-CA3 synapse, PPR is maximal at short (e.g. 40 ms) interstimulus intervals and declines exponentially over a period of 500 ms. It is well established that PPR is a purely presynaptic phenomenon and is often used to monitor presynaptic performance. Frequency facilitation occurs when the stimulation frequency is changed from a very low rate (e.g. 0.06 Hz) to a low rate (1 Hz) of synaptic activation and typically it is only sustained for as long as the stimulation is applied at that frequency. This is a striking characteristic of the MFs-CA3 synapses and is not seen with that prominence at any other hippocampal synapses (Salin et al.

1996; Dobrunz and Stevens 1999; Toth et al. 2000). To analyze short-term synaptic plasticity at this synapse and the role of GluK4-containing KARs in the neurotransmitter release from the presynaptic terminal, paired stimuli were applied to evoke MFs-EPSCs and paired-pulse ratios (PPR) measured; 25 traces for each cell were recorded and their respective mean value measured (EPSC1 and EPSC2). The PPR were calculated, as the ratio between the EPSC2 mean values over the EPSC1 mean values, at 40, 100, 200 and 500 ms of interstimulus intervals. The effect of a train of five stimuli delivered at 25 Hz on synaptic facilitation was also studied. To verify the contribution of KARs in the modulation of glutamate release from MFs terminals, PPR and FF were calculated in the presence of UBP310, a KARs antagonist. $mEPSC_{AMPARs/KARs}$ were also recorded in the presence of LY382885, a second selective KARs antagonist. Finally, Ca^{2+}-permeability of KARs was assessed applying IEM-1460, a blocker of Ca^{2+} permeable AMPARs/KARs.

3.6.1 GluK4^{Over} mice showed decreased facilitation at MFs-CA3 synapses

Decreased PPR was found in GluK4^{Over} mice compared to GluK4$^{+/+}$ mice (Fig. 26A, B). We observed a significant difference in paired-pulse ratio measurements at the shortest interstimulus intervals from 40-500 ms.

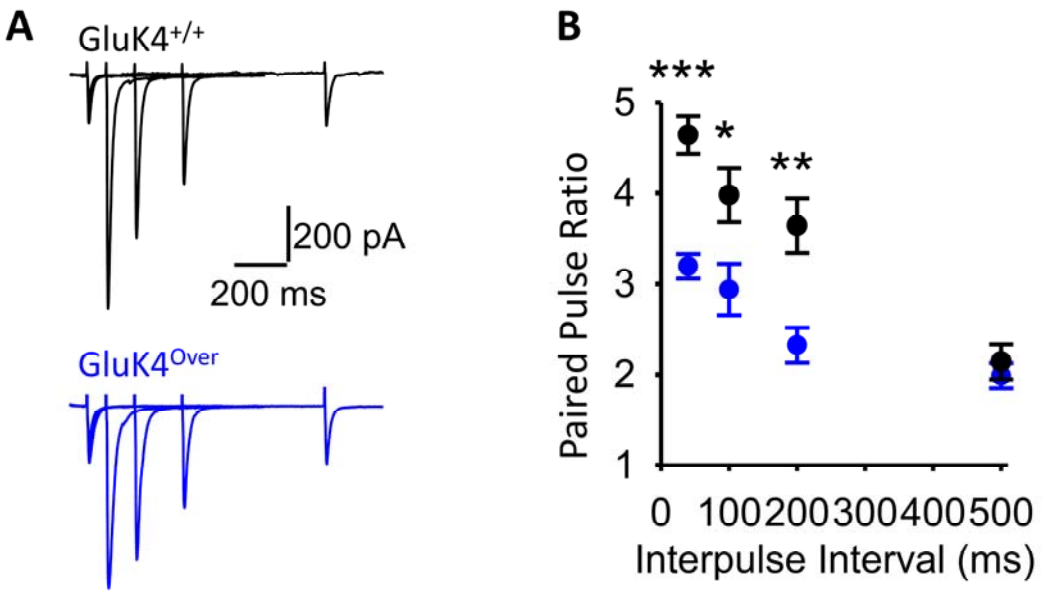

Figure 26: **GluK4 overexpression determines decreased facilitation at MFs-CA3 synapses. A)** Representative examples of paired-pulse AMPAR-mediated responses ($EPSC_{AMPARs}$) generated at intervals

of 40, 100, 200 and 500 ms in GluK4$^{+/+}$ (black) and GluK4^{Over} (blue) mice; **B)** grouped data of paired pulse ratios for both genotypes (Mean±SEM, 2-way ANOVA *post hoc* Bonferroni's test *p<005 **p<0.01 ***p<0.001).

Similarly, the frequency facilitation of EPSCs amplitudes observed when afferent stimulation frequency was increased from 0.06 Hz to 1 Hz was attenuated in GluK4^{Over} mutants compared to the WT mice (324%±20%, n = 20 for GluK4^{Over} ; 528%±31%, n = 32 for GluK4$^{+/+}$; Fig. 27B).

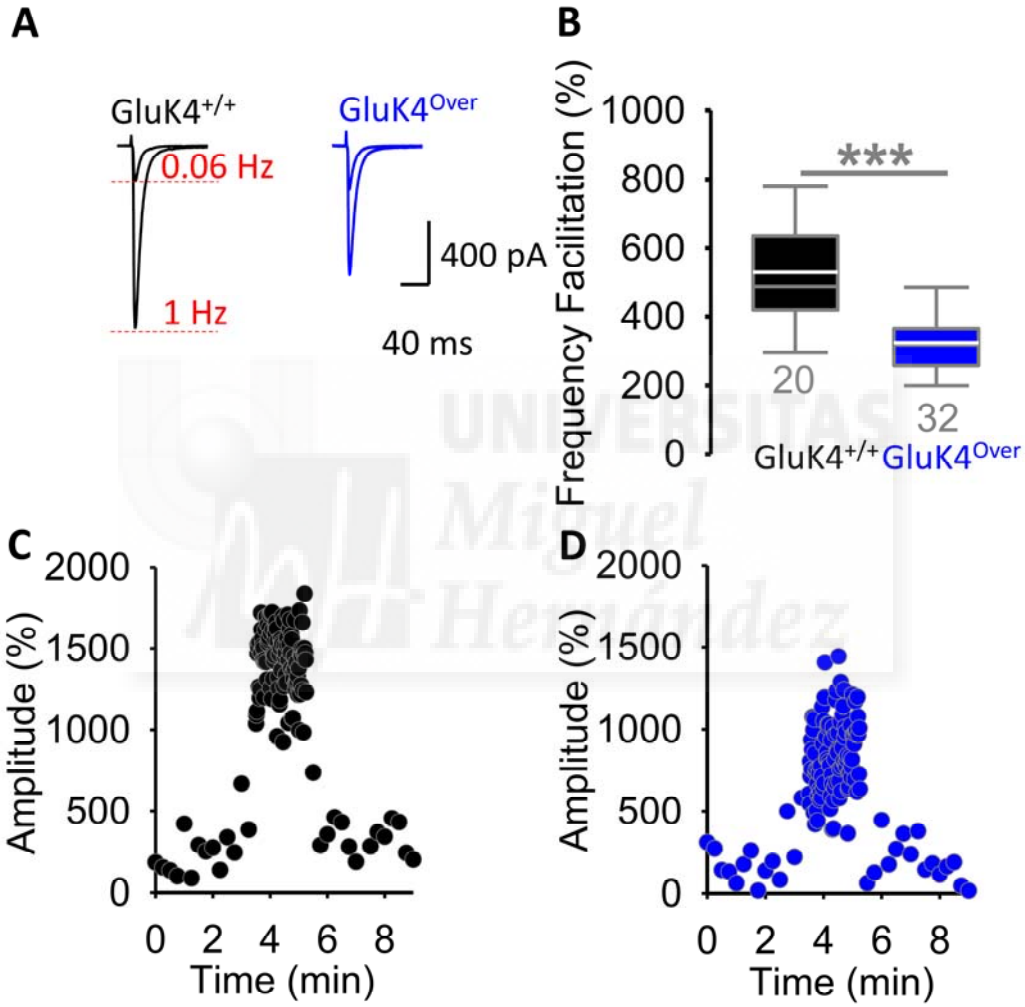

Figure 27: Frequency facilitation is altered in GluK4^{Over} mice. A) Example responses in CA3 pyramidal neurons from GluK4$^{+/+}$ and GluK4^{Over} mice to 0.06 Hz or 1Hz MFs stimulation. **B)** Average data from all recorded neurons for both genotypes (20 neurons from 3 GluK4$^{+/+}$ and 32 neurons from 4 GluK4^{Over} mice). Box plot horizontal bars: grey denotes the median and white represents the mean. ***p<0.001; Mann-Whitney rank-sum test). **C)** and **D)** panels show the time course of EPSC$_{AMPARs}$ in a single experiment when stimuli frequency was increased from 0.06 Hz to 1 Hz for each genotype.

To investigate the mechanism of facilitation, we also studied the synaptic response during brief, high-frequency stimulation of MFs, following blockade of NMDARs and GABARs conductance. Consistent with the PPR and FF data, the relative facilitation of the 5th stimulus to the 1st one was decreased in GluK4^{Over}

mice compared to GluK4$^{+/+}$ mice (492%±28% *n* = 38 for GluK4^{Over}; 646%±51%, *n* = 33 for GluK4$^{+/+}$); to study the difference in the duration of the effects of activation of the facilitatory KARs, we also delivered a test pulse at 600 ms interval following the 5 shock train (Fig. 28). Facilitation of the test EPSCs relative to the 1st stimulus did not show any substantial difference between the two genotypes, meaning that, after this lapse of time, the GluK4-KARs are not affecting anymore the facilitation properties of the MFs-CA3 cell synapses.

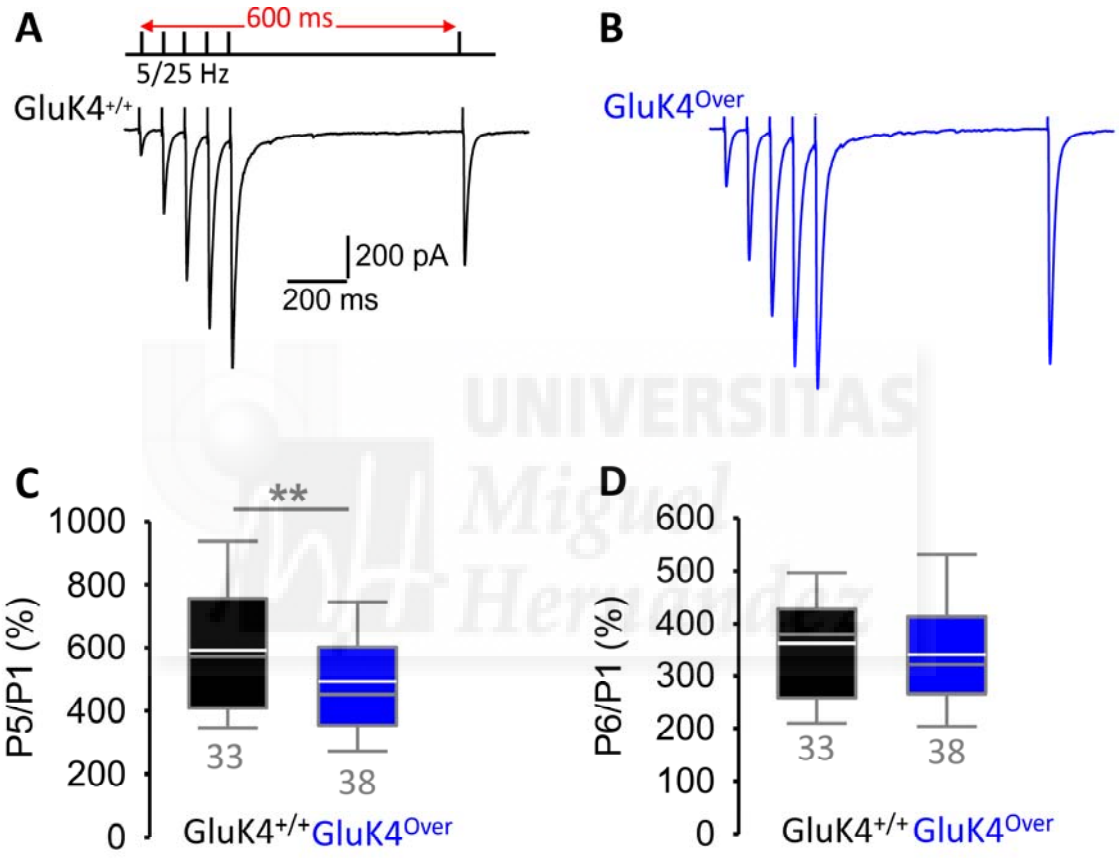

Figure 28: The effects of five stimuli delivered at 25 Hz on facilitation. A) and B) Example responses from single neurons for the 2 genotypes showing the frequency facilitation induced by the 25Hz train delivered at. MFs-CA3 synapses. **C)** Frequency facilitation P5/P1 is decreased in GluK4^{Over} mice compared to the wildtype case. **D)** Frequency facilitation P6/P1 does not change between the two genotypes. Box plot horizontal bars: grey denotes the median and white represents the mean (33 neurons from 4 GluK4$^{+/+}$ and 38 neurons from 4 GluK4^{Over} mice). ***p*<0.001; Mann-Whitney rank-sum test.

3.6.2 Application of UBP310 restores some characteristics of synaptic transmission at MFs-CA3 synapses in GluK4^{Over} mice

In control conditions, we first observed that both FF and PPR of CA3 eEPSC were significantly smaller in GluK4^{Over} compared to GluK4$^{+/+}$ mice. To deeper understand the possible role of KARs in the glutamate release modulation, we

also studied short-term synaptic plasticity after antagonizing KARs by perfusing UBP310 (10 µM). For each genotype, 5 minutes of baseline recording was followed by other 5 minutes of recording in the presence of the antagonist. UBP 310 significantly restored PPR values in GluK4^{Over} mice (3.0±0.8 in GluK4^{Over}; 3.9±0.2 after applying UBP; *n* = 15) without changing them in GluK4$^{+/+}$ mice (4.3±0.4 in GluK4$^{+/+}$; 4.1±0.4 after applying UBP; *n* = 10), as shown in Fig. 29C, D. Similarly UBP 310 reverted FF in GluK4^{Over} mice (307%±29% in GluK4^{Over}; 419%±41% after applying UBP; *n* = 8) but had no effect in GluK4$^{+/+}$ mice (456%±39% in GluK4$^{+/+}$; 452%±60% after applying UBP; *n* = 10). (Fig. 29A, B).

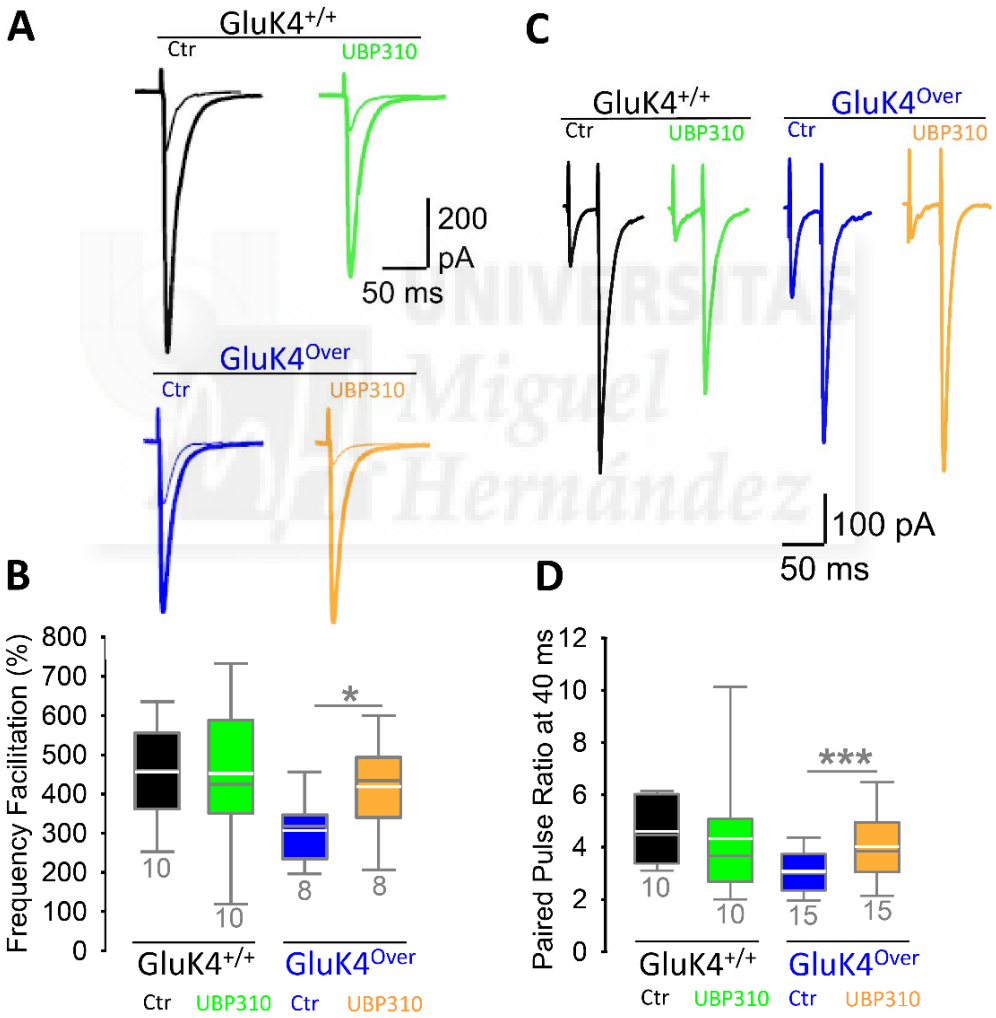

Figure 29: UBP 310 restores FF and PPR in GluK4^{Over} mice. A) Examples of responses in CA3 neurons from GluK4$^{+/+}$ and GluK4^{Over} mice to 0.06 Hz or 1 Hz MFs stimulation frequency. **B)** Summary plot showing the effect of UBP310 on FF in 10 cells from GluK4$^{+/+}$ and 8 cells from GluK4^{Over} mice; UBP 310 10µM had no effect on FF magnitude in GluK4$^{+/+}$, but restored it in GluK4^{Over} slices. **C)** Representative examples of paired-pulse responses with 40 ms interval in GluK4$^{+/+}$ and GluK4^{Over} mice. **D)** Pooled data from 10 wild-type cells/slices (3 WT mice) and 15 GluK4^{Over} cells/slices (3 GluK4^{Over} mice) show that UBP 310 restored PPR in both GluK4^{Over}. In the box plots, horizontal grey lines denote the median and white lines represent the mean. *p<0.05 ***p<0.001; Student t-test.

3.6.3 PRESYNAPTIC GLUK4-CONTAINING KARS PLAY AN IMPORTANT ROLE IN THE FACILITATION OF GLUTAMATE RELEASE

Going on with the characterization of GluK4 overexpressing mice, to deeper understand the function of GluK4-containing KARs, we analyzed the effects of the selective GluK1-containing KARs antagonist, LY382884, on spontaneous transmission at MFs-CA3 synapses (Fig. 30).

LY382884 is a compound with selectivity for GluR5-containing receptors (Ki ~ 7 μM for GluK1 homomers and ~ 3.6 μM for GluK1/GluK2 heteromers), and is largely inactive at AMPA receptor subunits (Ki > 100 μM) (Bortolotto, et al. 1999; Simmons, et al. 1998). AMPARs/KARs-mediated mEPSC were recorded as previously described. After 2 minutes of control recording, slices were perfused with LY382884 (10 μM) for 3 minutes. Frequencies of $mEPSC_{AMPARs/KARs}$ were significantly larger in $GluK4^{Over}$ neurons compared to $GluK4^{+/+}$ cells as we previously shown (see above). LY382884 drastically decreased $mEPSC_{AMPARs/KARs}$ frequency in $GluK4^{Over}$ (from 6.7±0.7 Hz to 3.5±0.3 Hz; n = 11 $p<0.005$), but did not have any effect on $mEPSC_{AMPARs/KARs}$ frequency in control $GluK4^{+/+}$ animals (from 2.0±0.4 Hz to 1.76±0.28 Hz; n = 11) (Fig. 30).

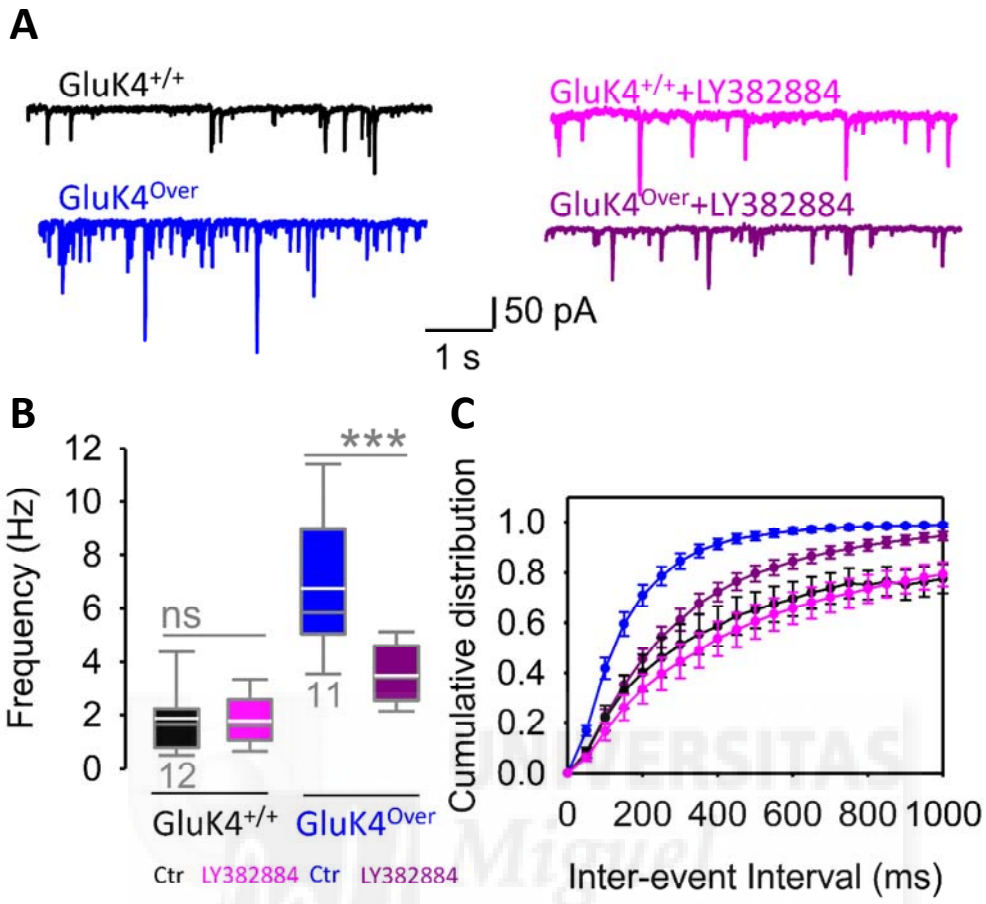

Figure 30: **Enhanced glutamate release is mediated by GluK4-KARs autoreceptors in MFs terminals. A)** Representative traces of AMPARs/KARs-mediated mEPSCs (Vm=-75mV) in CA3 pyramidal cells in each genotype before and after application of the KAR-antagonist LY382884 (10 μM). **B)** $mEPSC_{AMPAR}$ had larger frequency in the $GluK4^{Over}$ mice. LY382884 (10 μM) had no effect on transmission at synapses in $GluK4^{+/+}$, but decreased the frequency of $mEPSC_{AMPARs/KARs}$ in $GluK4^{Over}$ neurons. **C)** Cumulative distributions of $mEPSC_{AMPARs/KARs}$-frequency show well the differences between the two genotypes and the effect of LY382884 on them. (12 neurons/slices were recorded from 2 WT mice and 11 neurons/slices were recorded from 2 $GluK4^{Over}$ mice) In the box plots, horizontal grey lines denote the median and white lines represent the mean. *** p<0.001 ANOVA on ranks test.

3.6.4 PRESYNAPTIC KARS ARE BLOCKED BY IEM-1460, A CHANNEL BLOCKER OF Ca^{2+}-PERMEABLE KARS

IEM-1460, is an open channel blocker that exclusively affects CP-AMPARs or KARs. Using whole-cell patch clamp recordings from CA3 pyramidal cells, we studied the effect of IEM-1460 on mEPSCs. This was done in the presence of 25 μM of DAP-V and 50 μM of picrotoxin, to block NMDARs and GABARs respectively, keeping the cell at -75mV. After recording two minutes of baseline values, slices were perfused with IEM-1460 for 3 minutes. The frequency of spontaneous $mEPSC_{AMPARs/KARs}$ was evaluated before and after the treatment.

The degree of inhibition by 50 µM IEM-1460 was estimated to be 42.6%±4.8% of $mEPSC_{AMPARs/KARs}$ frequency in $GluK4^{Over}$ mice, and IEM-1460 did not altered these parameters in $GluK4^{+/+}$ mice. Particularly, in $GluK4^{Over}$, IEM-1460 restored $mEPSC_{AMPARs/KARs}$ frequencies to control values (Fig. 31).

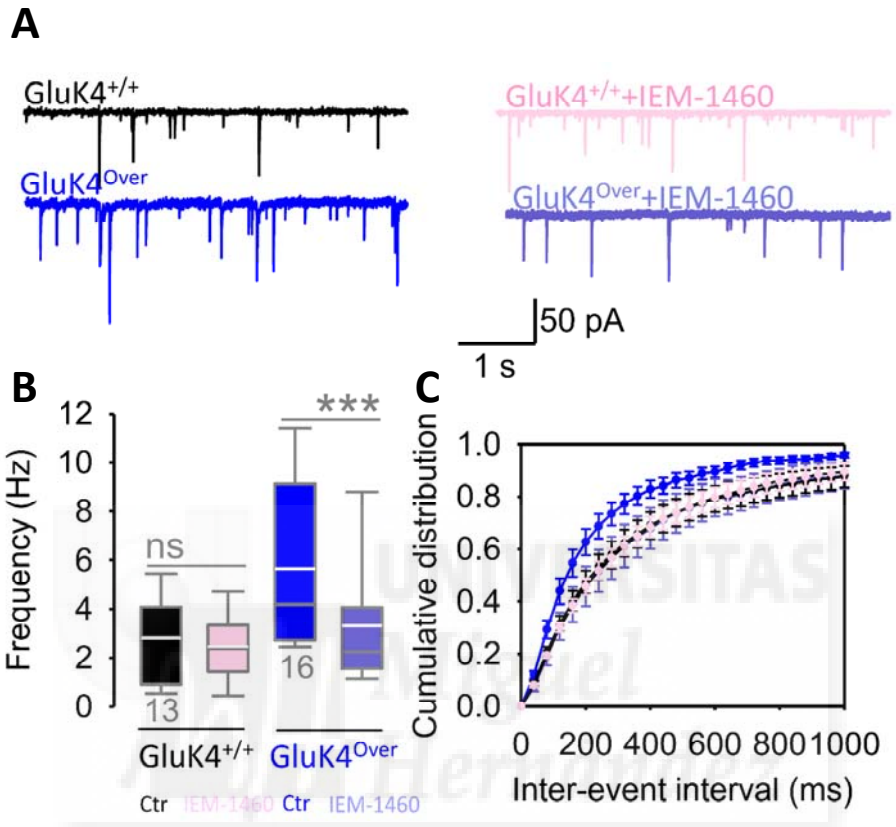

Figure 31: **The presence of presynaptic Ca^{2+}-permeable KARs is assessed by IEM-1460.A)** Representative AMPARs/KARs-mediated mEPSCs (Vm=-75 mV) in CA3 pyramidal cells in each genotype before and after application of IEM-1460 (50µM). **B)** IEM-1460 (50 µM, light pink bars) had no effect on transmission at synapses in $GluK4^{+/+}$, but significantly decreased frequency of $mEPSC_{AMPARs/KARs}$ in $GluK4^{Over}$ slices. **C)** Cumulative distributions of both $mEPSC_{AMPARs/KARs}$ frequency illustrating the differences between the two genotypes and the effect of IEM-1460 on them. (13 neurons/slices from 4 WT mice; 16 neurons/slices from 5 $GluK4^{Over}$ mice). In the box plots, horizontal grey lines denote the median and white lines represent the mean. ***p<0.001; ANOVA on ranks.

Similarly, paired stimuli were applied to evoke MFs-EPSCs and PPR were calculated at 40 ms interstimulus interval, before and after applying IEM-1460 for 10 minutes in the perfusion fluid. These data showed a restoration of $GluK4^{Over}$ PPR values to those observed in $GluK4^{+/+}$ mice (Fig.32).

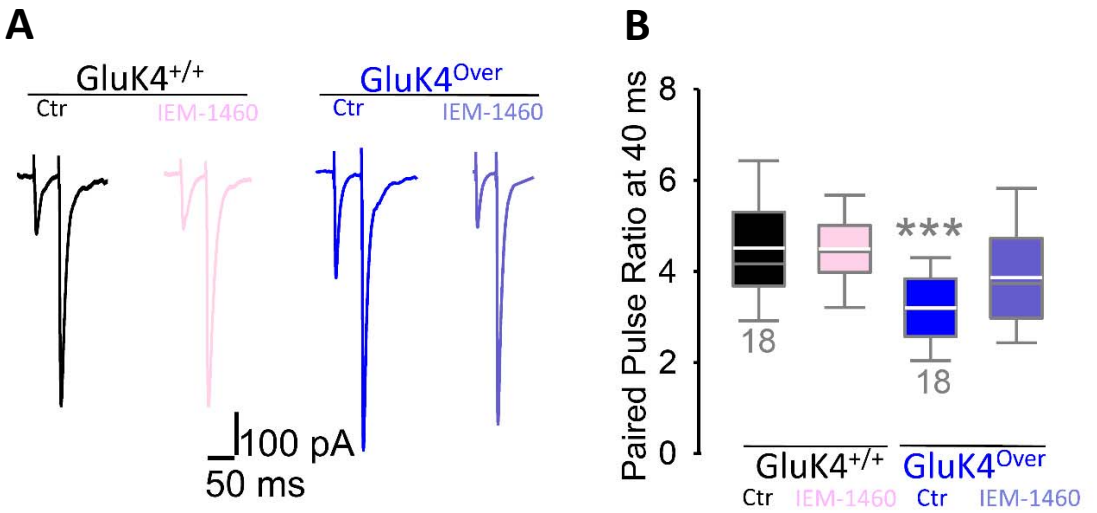

Figure 32: **IEM-1460 restores PPR in GluK4^{Over} mice**. **A)** Representative examples of paired pulse responses with 40 ms of interval in GluK4$^{+/+}$ and GluK4^{Over} before and after 10 minutes of IEM-1460 (50 μM) application. **B)** Grouped data of paired pulse ratios indicating IEM-1460 (50 μM, pink bar) had no effect on transmission at synapses in GluK4$^{+/+}$, but increases PPR in GluK4^{Over} slices (violet bar). *** p<0.001; ANOVA on ranks. 18 neurons/slices were recorded from 6 WT mice; 18 neurons/slices recorded from 8 GluK4^{Over} mice).

Taken together, these results showed that GluK4 overexpression led to a significant decreased of both kind of short-term synaptic plasticity, PPF and FF (Fig. 25, 26). The finding that both paired-pulse ratio and frequency facilitation are restored by UBP310 led us to conclude that tonic activation of GluK4-containing KARs at presynaptic terminals are responsible for the decreased facilitation observed in GluK4^{Over} mice. This was also justified by the effect of LY382884 on mEPSC$_{AMPARs/KARs}$ frequency. Additionally, we find out that presynaptic GluK4-containing KARs do allow Ca^{2+} entry into the MFs terminals.

3.6.5 Long-term synaptic plasticity in GluK4^{Over} mice

Synaptic plasticity at the MFs-CA3 synapses is unusual for several reasons, including low basal release probability, pronounced frequency facilitation and presynaptic forms of long-term potentiation (LTP) and depression (LTD), manifested as long-term changes in the probability of glutamate release. For that reason, we studied the well characterized NMDARs-independent LTP and LTD at MFs-CA3 cell synapses to see if there was an impairment of these kind of synaptic plasticity in GluK4 overexpressing mice. High-frequency stimulation

(100Hz for 1 sec) of MFs afferents onto CA3 pyramidal cells results in NMDARs–independent LTP, while low-frequency stimulation (1Hz for 15 min) induced LTD at MFs-CA3 cell synapses. D-APV was perfused during the time of each experiment and field EPSPs (fEPSPs) were recorded from CA3 region stimulating the MFs pathway.

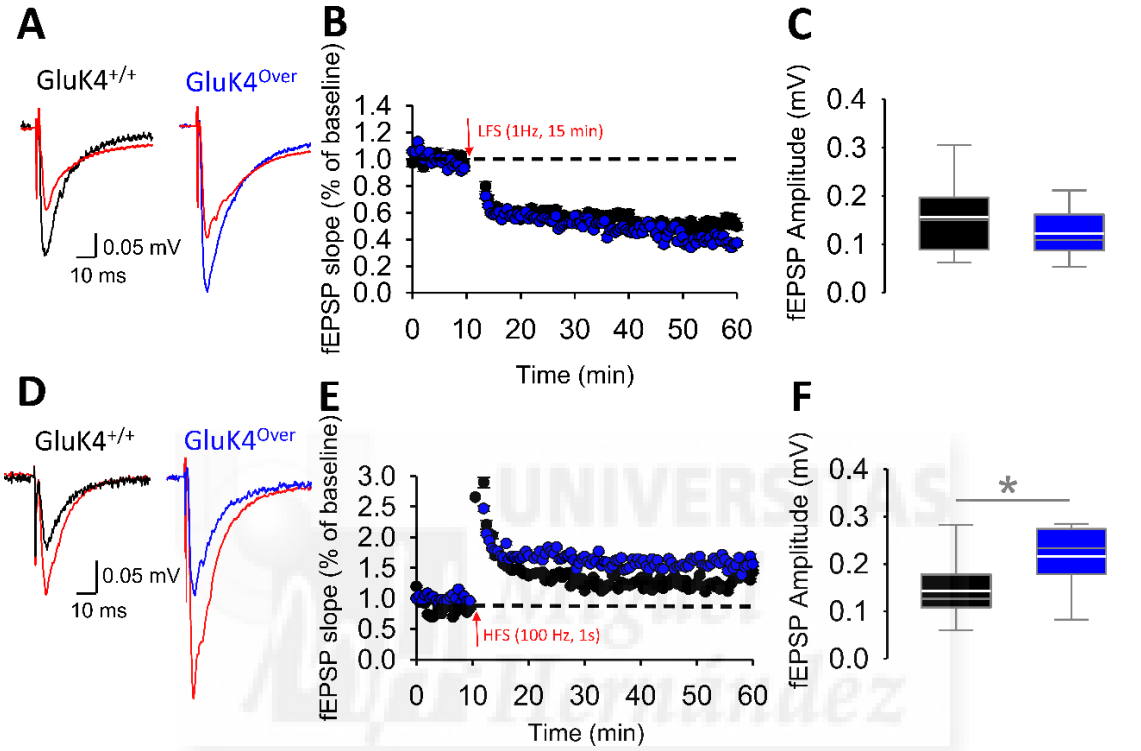

Figure 33: **NMDARs-indipendent LTP, but not LTD is changed in GluK4^{Over} mice. A)** Representative examples of fEPSCs in GluK4$^{+/+}$ and GluK4^{Over} mice during baseline period (black lines for WT mice and blu lines for GluK4^{Over} mice) and 20 – 30 min post-induction (red lines)**. B)** Pooled data of normalized fEPSPs plotted as function of time (mean± SEM, *n*=16 for GluK4$^{+/+}$ and *n*=12 for GluK4^{Over} mice; black and blue circles respectively). A Low Frequency Stimulation protocol (red arrow) induced LTD in both genotypes at the same degree. **C)** Averages of fEPSPs values at GluK4$^{+/+}$ and GluK4^{Over} MFs-CA3 synapses during 10 min (from 20 to 30 min). GluK4$^{+/+}$ and GluK4^{Over} show the same degree of depression. **D)** Representative examples of fEPSCs in GluK4$^{+/+}$ and GluK4^{Over} mice during baseline period and 20 – 30 min post-induction (red lines). **E)** Pooled data of normalized fEPSPs plotted as function of time (mean± SEM, *n*=10 slices from 2 GluK4$^{+/+}$ mice and *n*=7 slices from 2 GluK4^{Over} mice; black and blue circles respectively). A High Frequency Stimulation protocol (red arrow) induced LTP in both genotypes. **F)** Averages of fEPSPs values at GluK4$^{+/+}$ and GluK4^{Over} MFs-CA3 synapses during 10 min (from 20 to 30 min). GluK4^{Over} mice show increased fEPSPs amplitudes compared to GluK4$^{+/+}$ mice.* p<0.05; Student's t-test.

Data reported in Fig. 33 show the absence of impairment in LTD, but a significant increase in long-term synaptic potentiation confirming the initial idea of an involvement of GluK4-containing KARs in long-term presynaptic changes. During high-frequency tetanic stimulation of MFs terminals, presynaptic GluK4-KARs activation provides calcium entry into the presynaptic terminals, resulting in the long-lasting enhancement of evoked glutamate release. This further clarifies

GluK4-KARs function in the facilitation of glutamate release in both short and long-term phenomena, manifested as short and long term changes in the probability of glutamate release.

3.7 GluK4 OVEREXPRESSION IS REGULATING THE Ca^{2+}-PERMEABLE AMPARs INSERTION INTO THE POST SYNAPTIC DENSITY (PSD)

3.7.1 ANTAGONIZING KARS PRESERVES THE DIFFERENCE IN $mEPSC_{AMPAR}$ CONDUCTANCE

The increased amplitude of both evoked and miniature $EPSC_{AMPARs/KARs}$ and their faster decay time may be explained in several ways. However, both the increase in the probability of release (as already shown in Fig. 20) and the increased density of KARs and CP-AMPARs at postsynaptic site in mature neurons could explain these changes. Therefore, we tested this latter hypothesis by a number of strategies. A supplemental and important observation from the study of $mEPSC_{AMPARs/KARs}$ in the presence of LY382884, already shown in Fig. 30, was that LY382884 significantly decreased $mEPSC_{AMPARs/KARs}$ amplitudes (before 47.1 pA±3.8 pA and after 35.5 pA±2.7 pA LY382884 application, n = 12; $p<0.05$) in $GluK4^{Over}$, but it had no significant effect on $mEPSC_{AMPARs/KARs}$ amplitude in control $GluK4^{+/+}$ animals (before 28.2 pA±2.9 pA and after 24.5 pA±2.3 pA LY382884 application, n = 11). As we already showed, presynaptic GluK4-KARs provide Ca^{2+} entry into the cell, provoking a synchronous released of synaptic quanta with a consequent increase of the mEPSCs amplitudes. The effect of the KARs-antagonist LY382884 on spontaneous synaptic transmission was also studied at 0.2 mM Ca^{2+}, to better understand if the action of the compound was on pre and/or postsynaptic KARs. As Fig 34 shows, LY382884 had no significant effect on the mean amplitude of mEPSC in both $GluK4^{+/+}$ mice (before 21.5 pA±2.9 pA and after 19.1 pA±1.7 pA treatment) and $GluK4^{Over}$ mice (before 35.0 pA±1.8 pA and after 30.2 pA±1.9 pA treatment). Moreover, the mean frequency values were 1.2±0.2 Hz (before treatment) and 1.0±0.1 Hz (after treatment) in $GluK4^{+/+}$ neurons and 3.0±0.4 Hz (before treatment) and 2.3±0.4 Hz (after treatment) in $GluK4^{Over}$ neurons.

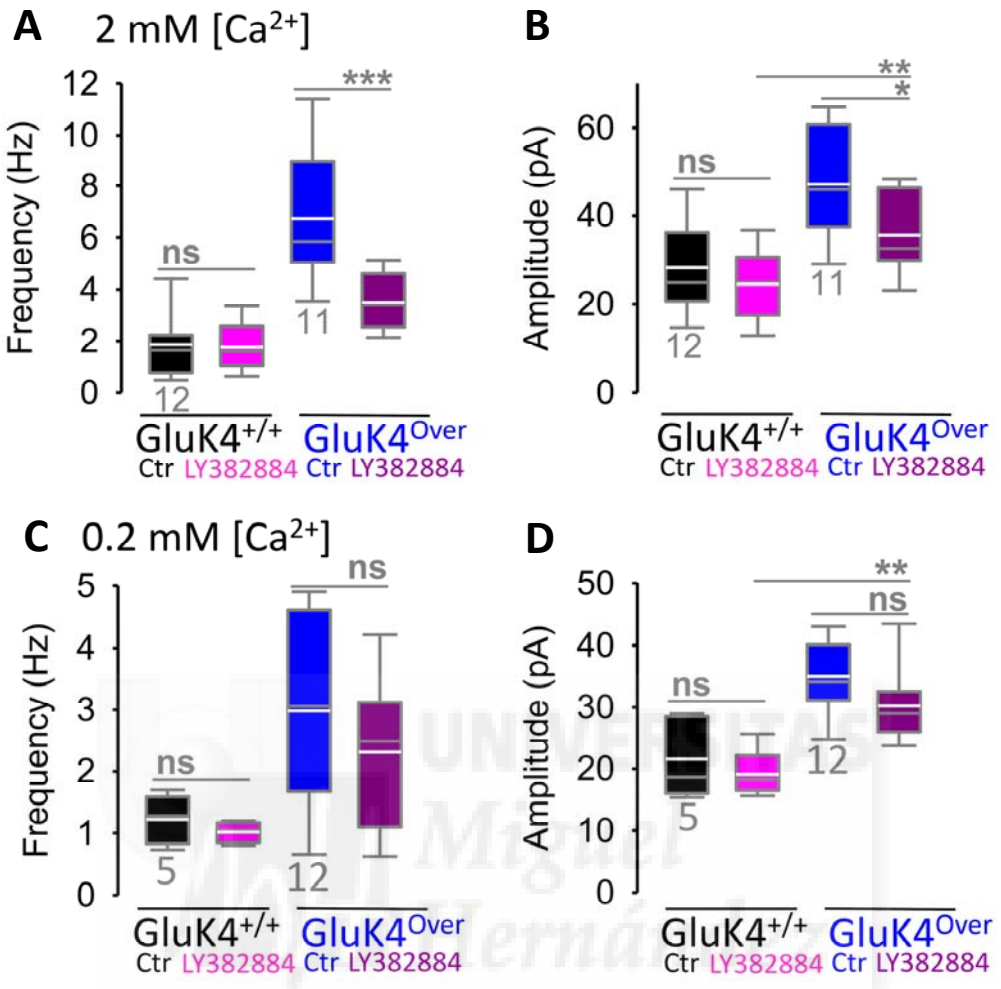

Figure 34: Ca^{2+}-dependent effect of LY382884. A) Summary plot showing $mEPSC_{AMPARs/KARs}$ had higher mean frequency in the $Glu4^{Over}$ mice compared to $GluK4^{+/+}$ mice; LY382884 application significantly decreases the frequency of events in $GluK4^{Over}$ mice **B)** LY382884 application had no effect on $mEPSC_{AMPARs/KARs}$ amplitude in $GluK4^{+/+}$ mice, whereas it significantly decreased these values in $GluK4^{Over}$ mice. **C)** Effects of LY382884 (10 μM) application at 0.2 mM Ca^{2+} on $mEPSC_{AMPARs/KARs}$ frequency and **D)** amplitude. LY382884 application did not affect these values on both genotypes. The number under the bars indicate the number of the cells, one for each slice. * p<0.05, ** p<0.01, *** p<0.001 one-way ANOVA test.

These results might be explained considering that the KARs antagonist LY382884 is exclusively decreasing the multivesicular glutamate release, via the blockade of presynaptic KARs, which depends on extracellular Ca^{2+} concentration. The Ca^{2+}-dependent effect of LY382884 led us to conclude that its effect on the $mESPC_{AMPARs/KARs}$ amplitude, observed at 2 mM Ca^{2+} but not at 0.2 mM Ca^{2+}, is the consequence of the presynaptic KARs block instead of any kind of postsynaptic receptors antagonism.

Furthermore, after blocking KARs, AMPARs-mediated currents still contribute to enhancing mEPSCs amplitude (see pink and dark bars) at 2 mM Ca^{2+}, and even at lower Ca^{2+}, a condition excluding any influence of glutamate release on the postsynaptic amplitude.

We concluded that GluK4 overexpression is causing, in addition to the increase in the number of postsynaptic KARs, coherent with the already shown increased $sEPSC_{KARs}$ amplitude (Fig. 19C), also an increase in the AMPARs-conductance, in agreement with the presence of CP-AMPARs in $GluK4^{Over}$ mice (Paragraph 3.5.3).

3.7.2 Block of EPSCs by IEM-1460 correlates with rectification

In mature $GluK4^{+/+}$ mice the greatest population of AMPARs is Ca^{2+}-impermeable, CI (Fig. 24). To further confirm that GluK4 overexpression provokes an increase in the percentage of CP-AMPARs localized in the postsynaptic terminal, the effect of IEM-1460, an open channel blocker of CP-AMPARs was further studied. Evoked $EPSC_{AMPARs}$ were recorded and rectification index calculated as already described. EPSCs evoked by stimulation of the MFs pathway evidenced the ability of IEM-1460 to decrease $EPSC_{AMPARs}$ amplitude of $GluK4^{Over}$ mice without affecting $EPSC_{AMPARs}$ amplitude of $GluK4^{+/+}$ mice. The capability of IEM-1460 to decrease $EPSC_{AMPARs}$ amplitudes correlated with their rectification properties in $GluK4^{Over}$ mice, providing evidence for postsynaptic localization of CP-AMPARs in our transgenic animals.

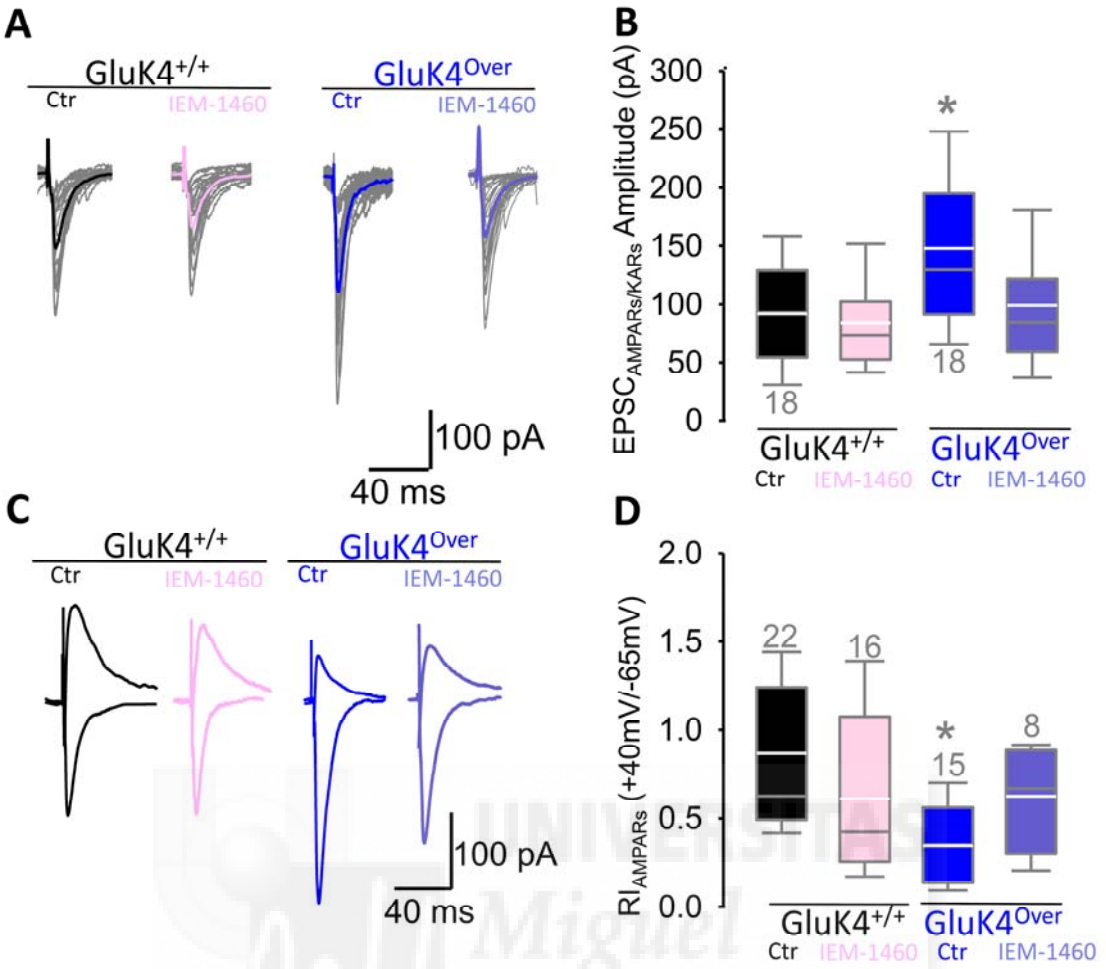

Figure 36: **IEM-1460 decreases $EPSC_{AMPAR}$ amplitudes and reverts RI_{AMPAR} in $GluK4^{Over}$ mice. A)** Representative examples of EPSCs (Vm=-65 mV) recorded in the same CA3 pyramidal cell of each genotype in control and in the presence of IEM-1460 (50 μM). **B)** Quantification of all cells recorded in each condition. Inward rectification and blockade by IEM-1460 50 μM. **C)** Representative recordings of individual EPSC evoked by MFs stimulation at -65 mV and +40 mV; **D)** set of data showing the null effect of IEM-1460 50 μM (light pink bars) on RI of $GluK4^{+/+}$cells, but increased values on $GluK4^{Over}$ neurons. The number under the boxes indicate the number of the cells (one for each slice) recorded from 3 mice for each genotype *p<0.05; ANOVA on ranks.

These data highlight that GluK4 overexpression is affecting the number and the type of AMPARs at postsynaptic sites and confirm that new CP-AMPARs are inserted in the PSD in the transgenic mice.

3.8 THE SIGNALING MECHANISM MEDIATED BY GluK4-CONTAINING KARs

3.8.1 PRESYNAPTIC PKC ACTIVATION IS DOWNSTREAM OF Ca^{2+} INFLUX MEDIATED BY GLUK4-KARS

In order to find out the cellular mechanism activated by GluK4-containing KARs at both pre- and postsynaptic side, we decided to test whether a possible G-protein–mediated cascade was activated by GluK4-KARs. CP-AMPARs insertion into the postsynaptic membrane is regulated by phosphorylation via a Ca^{2+}/calmodulin-dependent protein kinase II (CaMKII) (Guire et al., 2008), protein kinase C (PKC)-dependent (Yang et al., 2010; Boehm et al., 2006), and PKA-dependent (Esteban et al., 2003) mechanisms. To understand how new CP-AMPARs are inserting in $GluK4^{Over}$ mice we decided to study the effect of Calphostin-C, a highly specific inhibitor of PKC, in MFs-CA3 synapses synaptic transmission. A general rule seems to be that activity-dependent phosphorylation of GluA1, by PKC, delivers AMPARs to synapses in LTP (Boehm et al., 2006), whereas GluA1 dephosphorylation is a signal for internalization and LTD. In contrast, PKC phosphorylation of GluA2 promotes AMPARs internalization and its dephosphorylation is important in synaptic retention (Steinberg et al., 2006). We studied the effects of Calphostin-C on $mEPSC_{AMPARs/KARs}$. After 5 minutes of baseline recording, Calphostin-C (0.5 μM) was perfused for 7 minutes and the last 3 minutes of traces recordings. The initial set of experiment was carried out in 2 mM extracellular Ca^{2+} concentration. Comparing the $mEPSC_{AMPARs/KARs}$ between slices of the different genotype groups, we detected significant differences. The inhibition of PKC abolished the increase in $mEPSC_{AMPARs/KARs}$ frequencies in $GluK4^{Over}$ mice (5.17±0.71 Hz, and 2.32±0.4 Hz before and after Calphostin-C treatment, respectively; *n* = 20) and slightly, but not significantly, decreases $mEPSC_{AMPARs/KARs}$ frequencies in $GluK4^{+/+}$ mice (before 1.80± 0.29 Hz, and after 1.00±0.12 Hz Calphostin-C treatment; *n* = 16). The inhibition of PKC also decreased $mEPSC_{AMPARs/KARs}$ amplitudes in $GluK4^{Over}$ mice (42.4±2.5 pA and 24.4±1.8 pA before and after Calphostin-C treatment, respectively; *n* = 20), without affecting $GluK4^{+/+}$ $mEPSC_{AMPARs/KARs}$ amplitudes (25.7±1.7 pA, and 17.5±1.7 pA before and after Calphostin-C treatment, respectively; *n* = 16).

These results led us to investigate in more detail the mechanism activated by GluK4-KARs at MFs-CA3 synapses. Thinking about a possible extracellular Ca^{2+}-dependence of PKC activation, we decided to record $mEPSC_{AMPARs/KARs}$ lowering the extracellular Ca^{2+} concentration to 0.2 mM: As we can see in Fig. 38, at 0.2 mM $[Ca^{2+}]_e$ we observed a significant decrease in the frequency of elementary events in both genotypes (1.69±0.18 Hz at 2 mM $[Ca^{2+}]_e$ *vs* 0.85±0.09 Hz at 0.2 mM $[Ca^{2+}]_e$ for GluK4$^{+/+}$ mice and 5.95±0.51 Hz at 2 mM $[Ca^{2+}]_e$ *vs* 1.91±0.32 Hz at 0.2 mM $[Ca^{2+}]_e$ for GluK4^{Over} mice), meaning that the probability of glutamate release depends on the $[Ca^{2+}]_e$. Furthermore, at 0.2 mM $[Ca^{2+}]_e$, the action of Calphostin-C is occluded and does not affect any further the frequency of $mEPSC_{AMPARs/KARs}$ in GluK4^{Over} mice (1.91±0.32 Hz and 1.33 ±0.25 Hz before and after Calphostin C treatment, respectively; *n* = 14) (Fig. 38C), suggesting that the activation of PKC is activated by the Ca^{2+} entry into the cell mediated by Ca^{2+}-permeable GluK4-KARs.

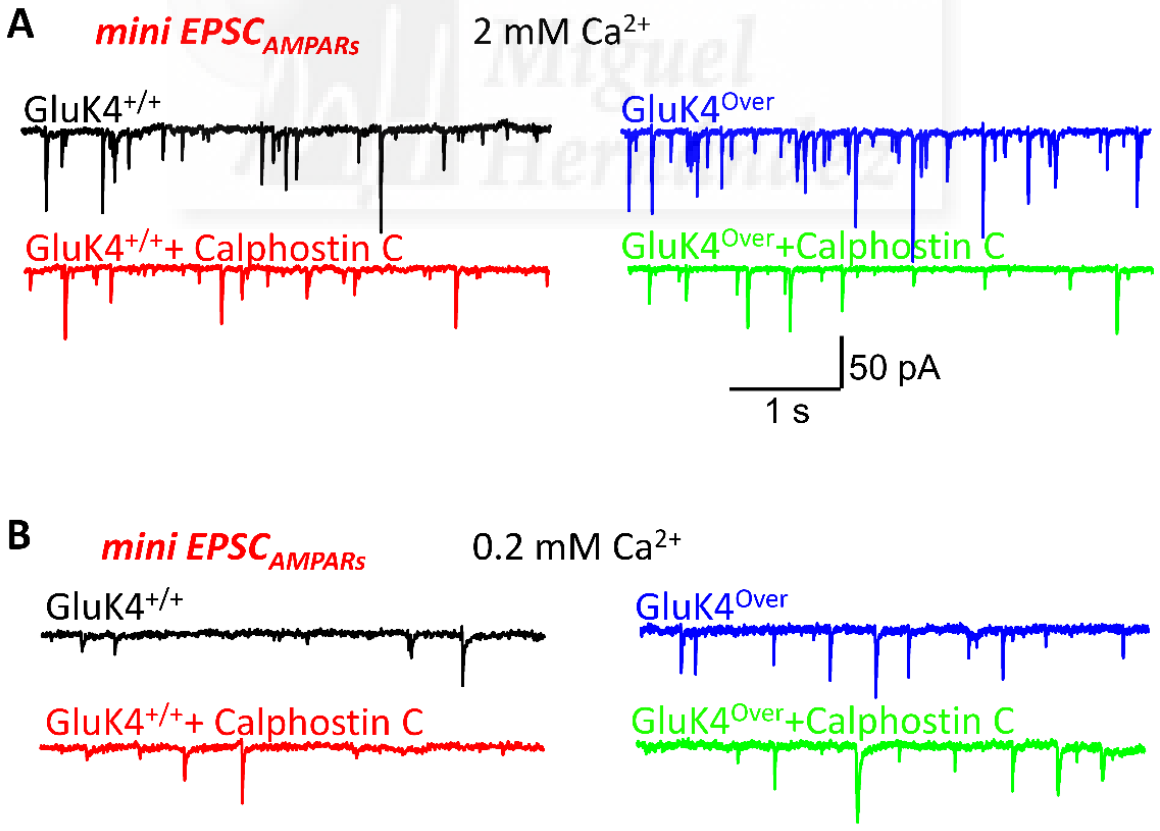

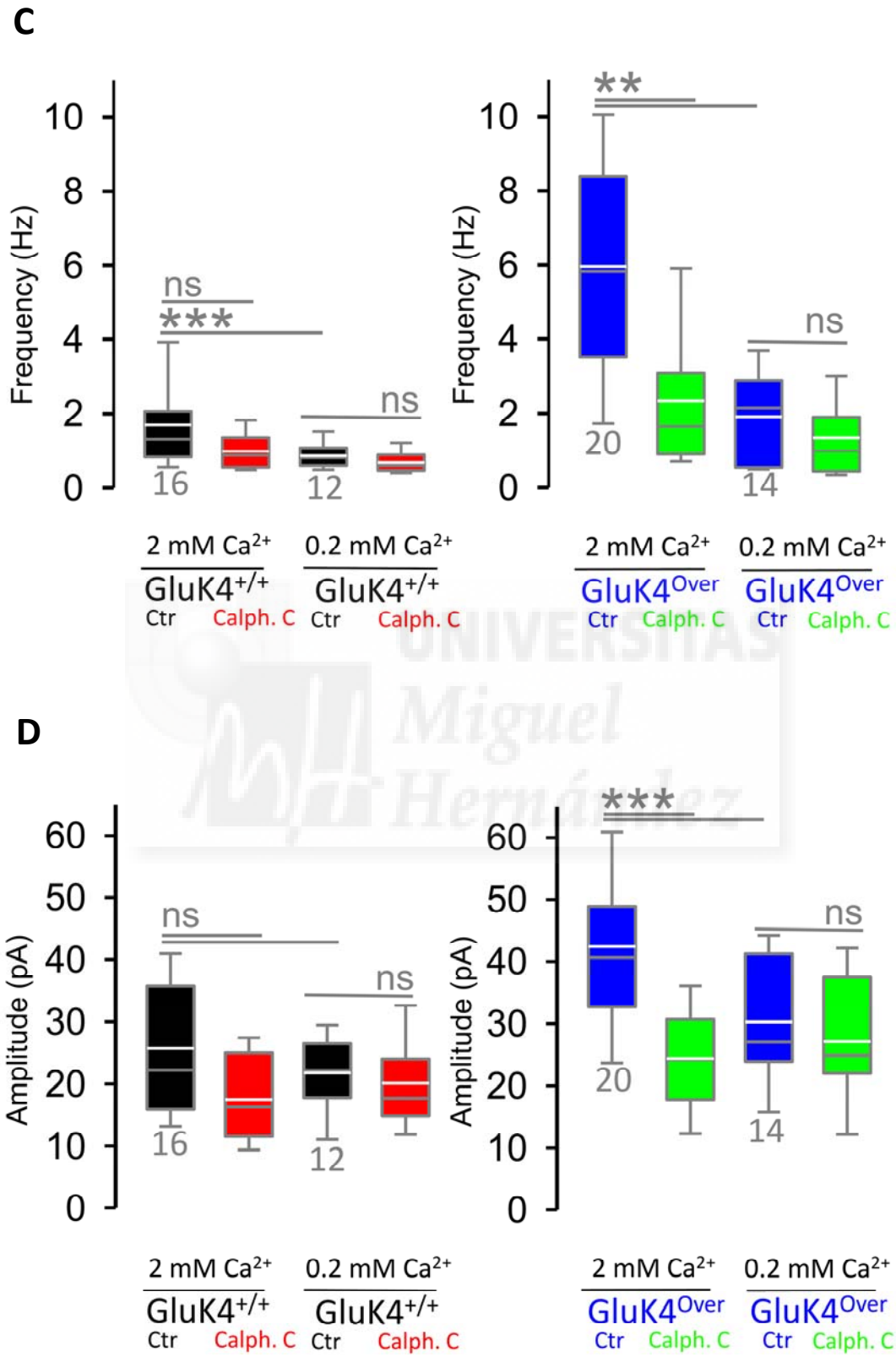

Figure 38: PKC inhibition of mEPSC$_{AMPARs/KARs}$ by Calphostin C. A) Examples trace of mEPSC$_{AMPARs/KARs}$ before and after Calphostin C treatment at 2 mM Ca^{2+}. **B)** Examples trace of mEPSC$_{AMPARs/KARs}$ before and after Calphostin C treatment at 0.2 mM Ca^{2+} **C)** and **D)** Summary plot on the

effect of Calphostin C on frequencies and amplitudes of $mEPSC_{AMPARs/KARs}$. The numbers under the boxes indicate the number of cells (one for each slice) recorded from 3 mice for each genotype at 2 mM Ca^{2+} and from 2 mice for each genotype at 0.2 mMCa^{2+}. ***p*<0.01; *** p<0.001 ANOVA on ranks.

As Fig.38D shows, the amplitudes of $mEPSC_{AMPARs/KARs}$ recorded at 0.2 mM $[Ca^{2+}]_e$ were significantly decreased only in $GluK4^{Over}$ mice (42.4±2.5 pA at 2 mM$[Ca^{2+}]_e$ and 30.3±2.5 pA at 0.2 mM $[Ca^{2+}]_e$). Furthermore this amplitude at 0.2 mM $[Ca^{2+}]_e$ was not reduced by Calphostin-C treatment (30.3±2.5 pA and 27.1±2.5 pA before and after Calphostin-C treatment, respectively; *n* = 14 for $GluK4^{Over}$ mice).

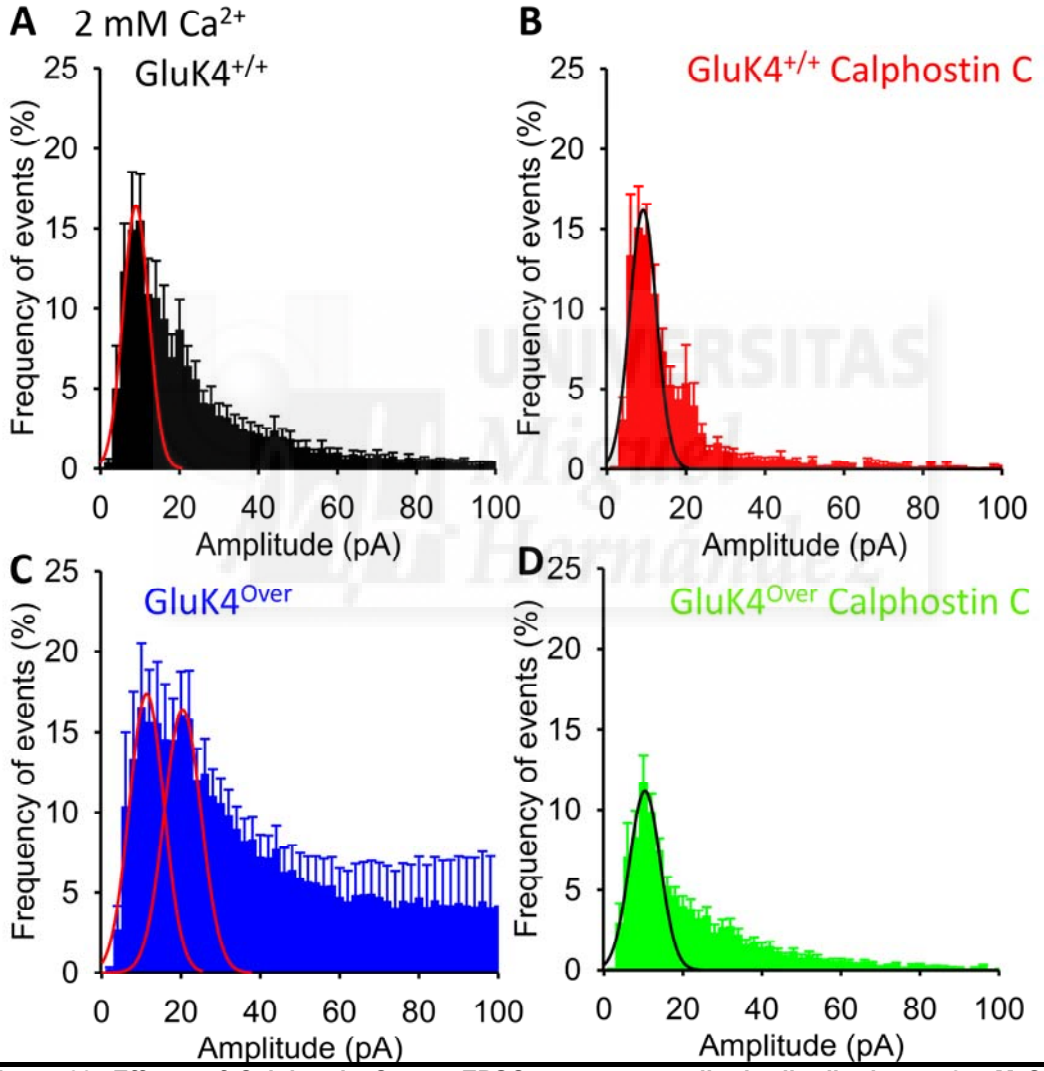

Figure 39: Effects of Calphostin C on $mEPSC_{AMPARs/KARs}$ amplitude distribution at 2 mM Ca^{2+}. A) Amplitude histograms of $mEPSC_{AMPARs/KARs}$ before and **B)** after Calphostin C treatment in $GluK4^{+/+}$ mice show the same Gaussian fit. **C)** Amplitude histograms of $mEPSC_{AMPARs/KARs}$ before and **D)** after Calphostin C treatment in $GluK4^{Over}$ mice**.** Note a spread distribution with only 1 pick after Calphostin-C treatment**.** Histograms are the average amplitude distributions of 16 cells (3 mice) for $GluK4^{+/+}$ and of 20 cells (3 mice) for $GluK4^{Over}$.

PKC-inhibition at 2 mM Ca^{2+} did not change the amplitude distribution of $mEPSC_{AMPARs/KARs}$ in $GluK4^{+/+}$ mice: Gaussian fit was 8.9 pA±3.2 pA and 9.1 pA

±3.4 pA before and after Calphostin-C application respectively for the GluK4$^{+/+}$ distribution; whereas one of the two curves evidenced in GluK4^{Over} amplitude distribution (11.3 pA±4.3 pA and 20.4 pA±4.6 pA) almost disappeared after Calphostin-C application leaving only one pick with a value of 10.4 pA±3.9 pA. However we can still observe a quite dispersed distribution of mEPSC$_{AMPARs/KARs}$ amplitude compared to GluK4$^{+/+}$ (Fig. 39).

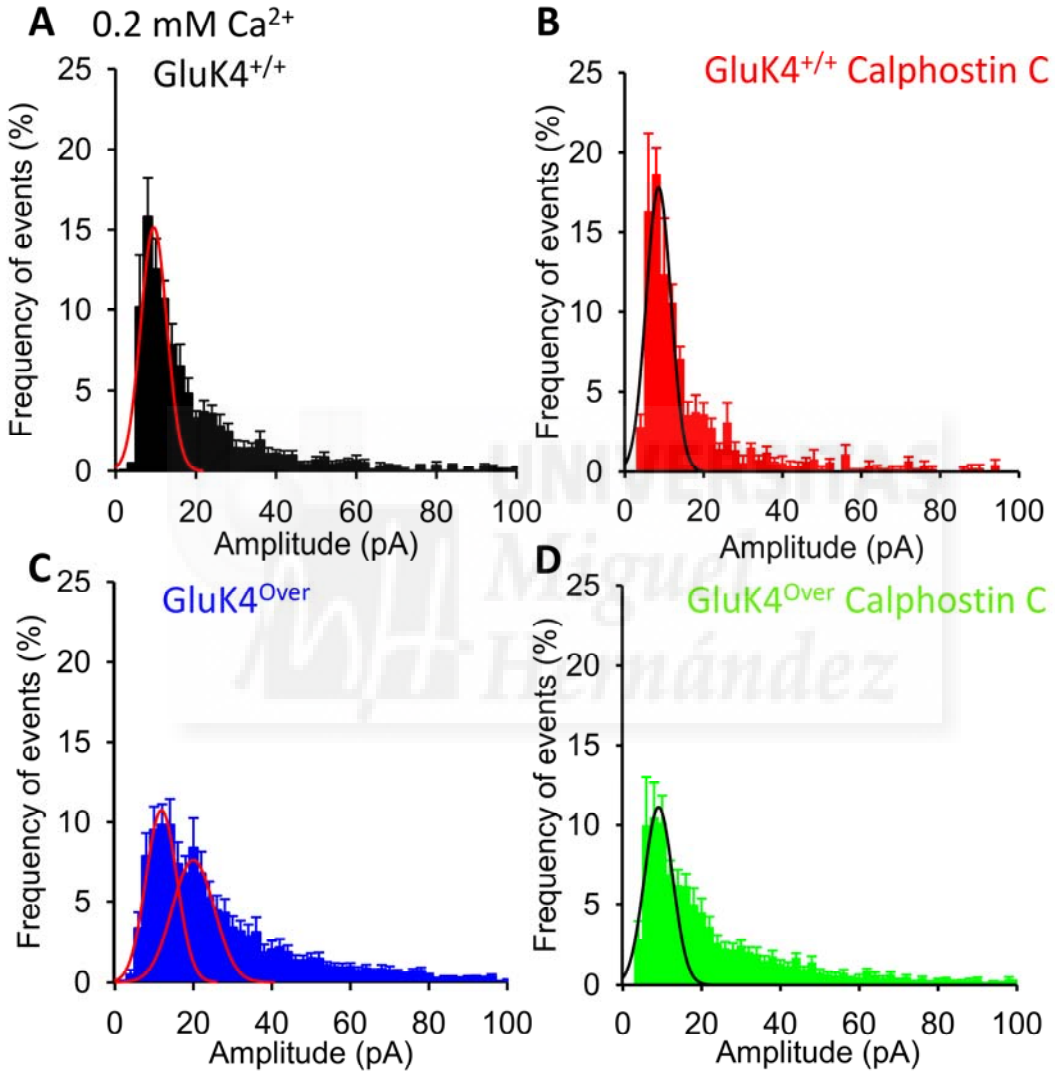

Figure 40: Effects of Calphostin C on mEPSC$_{AMPARs/KARs}$ amplitude distribution at 0.2 mM Ca^{2+}. A) Amplitude histograms of mEPSC$_{AMPARs/KARs}$ before and **B)** after Calphostin C treatment in GluK4$^{+/+}$ mice show the same Gaussian fit. **C)** Amplitude histograms of mEPSC$_{AMPARs/KARs}$ before and **D)** after Calphostin C treatment in GluK4^{Over} mice**.** Note a spread distribution with only 1 pick after Calphostin-C treatment**.** Histograms are the average amplitude distributions of 12 cells (2 mice) for GluK4$^{+/+}$ and of 14 cells (2 mice) for GluK4^{Over}**.**

The same tendency was observed in the amplitude distributions of mEPSC$_{AMPARs/KARs}$ recorded at 0.2 mM Ca^{2+} (Fig.40). Calphostin-C application

did not determine significant changes in GluK4$^{+/+}$ mice (9.5 pA±3.2 pA and 8.6 pA±3.1 pA before and after Calphostin-C application respectively), instead Gaussian fit yields two mean value for the distribution before the treatment (11.9 pA±3.9 pA and 19.9 pA±5.3 pA) and one value (9.1 pA±3.6 pA) after the treatment for GluK4^{Over} mice. Also in this latter case, as at 2 mM Ca^{2+}, we can still appreciate a spread amplitude distribution in GluK4^{Over} mice after Calphostin-C application.

These data suggest that the effect of Calphostin-C on mEPSC$_{AMPARs/KARs}$ amplitudes recorded at 2 mM $[Ca^{2+}]_e$ is predominately due to an indirect effect on the multivesicular release process, therefore presynaptic GluK4-containing KARs trigger a mechanism involving PKC which may be induced by the Ca^{2+} flow into the presynaptic terminal, modulating the glutamate release machinery to increase the glutamate release.

Moreover, considering that the effect of Calphostin-C on mEPSC$_{AMPARs/KARs}$ amplitudes in GluK4^{Over} mice recorded at 0.2 mM $[Ca^{2+}]_e$, a condition where the presynaptic effect of KARs on postsynaptic amplitudes are negligible (as we showed), did not revert completely to the respective value observed in GluK4$^{+/+}$ mice, as well as the presence of a spread amplitude distribution after Calphostin-C treatment, we can also think that a postsynaptic GluK4-containing KARs-dependent and Ca^{2+}-independent mechanism could be accountable for the insertion of new CP-AMPARs at postsynaptic CA3 neurons. Further experiments need to be carried out to discover which possible mechanism could be responsible for the insertion of new CP-AMPARs at CA3 cell after overexpressing GluK4 subunit.

3.9 GluK4 OVEREXPRESSION DOES NOT ALTER SYNAPTIC TRANSMISSION AT Shaffer Collateral -CA1 SYNAPSES

After having consistently highlighted the physiological consequences of overexpressing *grik*4 in the mouse forebrain, showing more efficient information transfer through the MFs-CA3 connections, we wondered how this information could flow throughout the hippocampal circuit. Therefore, we studied synaptic

transmission also at Schaffer-Collateral to CA1 pyramidal cells synapses. CA1 pyramidal neurons were patched and kept at -65 mV and GABARs and NMDARs were blocked to isolate glutamatergic AMPARs-mediated events. Stimulating electrode was placed in the Shaffer collateral pathway and eEPSCs were recorded. Paired-pulse stimulation (40 ms interval) was also applied to induce short-term synaptic plasticity of evoked excitatory responses which was assessed by measuring the PPR. Rectification properties were also studied, recording at -65 mV and at +40 mV.

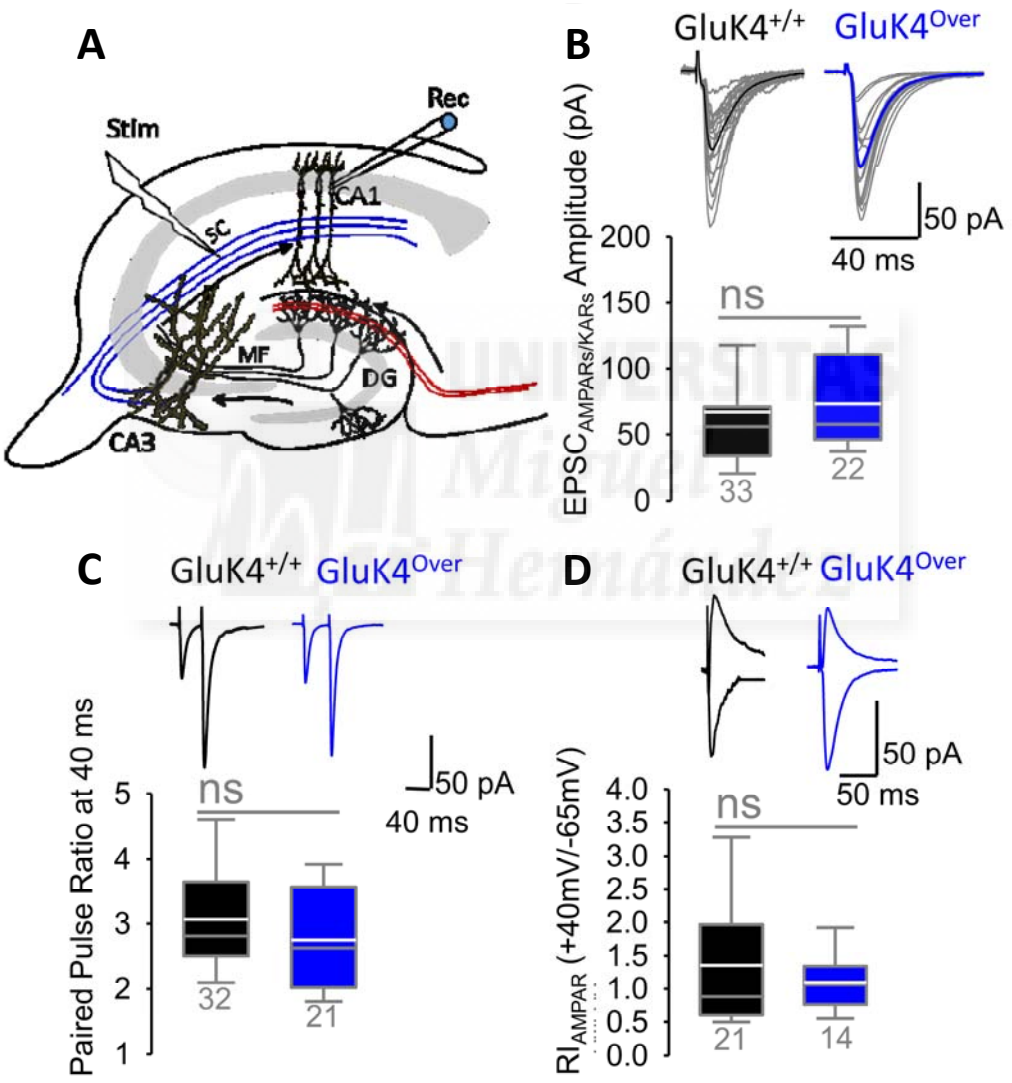

Figure 41: **Synaptic transmission at SC-CA1 pyramidal cells is not altered in GluK4^{Over} mice. A)** Hippocampal slice scheme showing recording (Rec) electrode in a CA1 pyramidal cell and stimulating pipette placed in the Shaffer collateral pathway, originating from CA3 cells to contact CA1 cells. Synaptic transmission from Schaffer collateral to CA1 pyramidal cells. Examples recording of at 30 traces with their respective averages showing no difference between GluK4^{Over} (blue line) and GluK4$^{+/+}$ (black line) eEPSC amplitude **(B)**, PPR **(C)** and RI **(D)**. Grouped data proving no difference in EPSC$_{AMPA}$ amplitude, PPR and RI between the two genotypes. The numbers under the box indicate cells recorded from 2 mice for each genotype. Mann-Whitney rank-test.

We found that GluK4 overexpression does not affect synaptic information transfer from Shaffer Collateral to CA1 pyramidal cells, leading us to conclude that the alterations caused by GluK4 overexpression are restricted to the MFs-CA3 synapses discarding the involvement of associational-commissural ipsi and contralateral projections from CA3 neurons.

3.10 THE ATYPICAL ANTIDEPRESSANT Tianeptine REVERTS THE SYNAPTIC CHANGES IN GluK4^{Over} MICE

Based on the observation that Tianeptine, an antidepressant structurally similar to tricyclic antidepressant but with a different pharmacological profile, reverted some of the behavioral deficits affecting GluK4^{Over} mice like anhedonia, and depression (Aller et al., 2015), we decided to investigate the effects of exposing hippocampal slices in vitro to 100 μM Tianeptine.

Slices were incubated for one hour before studying synaptic transmission at MFs-CA3 synapses. Significant differences were observed between GluK4^{Over} and their wildtype siblings when hippocampal slices were exposed to Tianeptine.

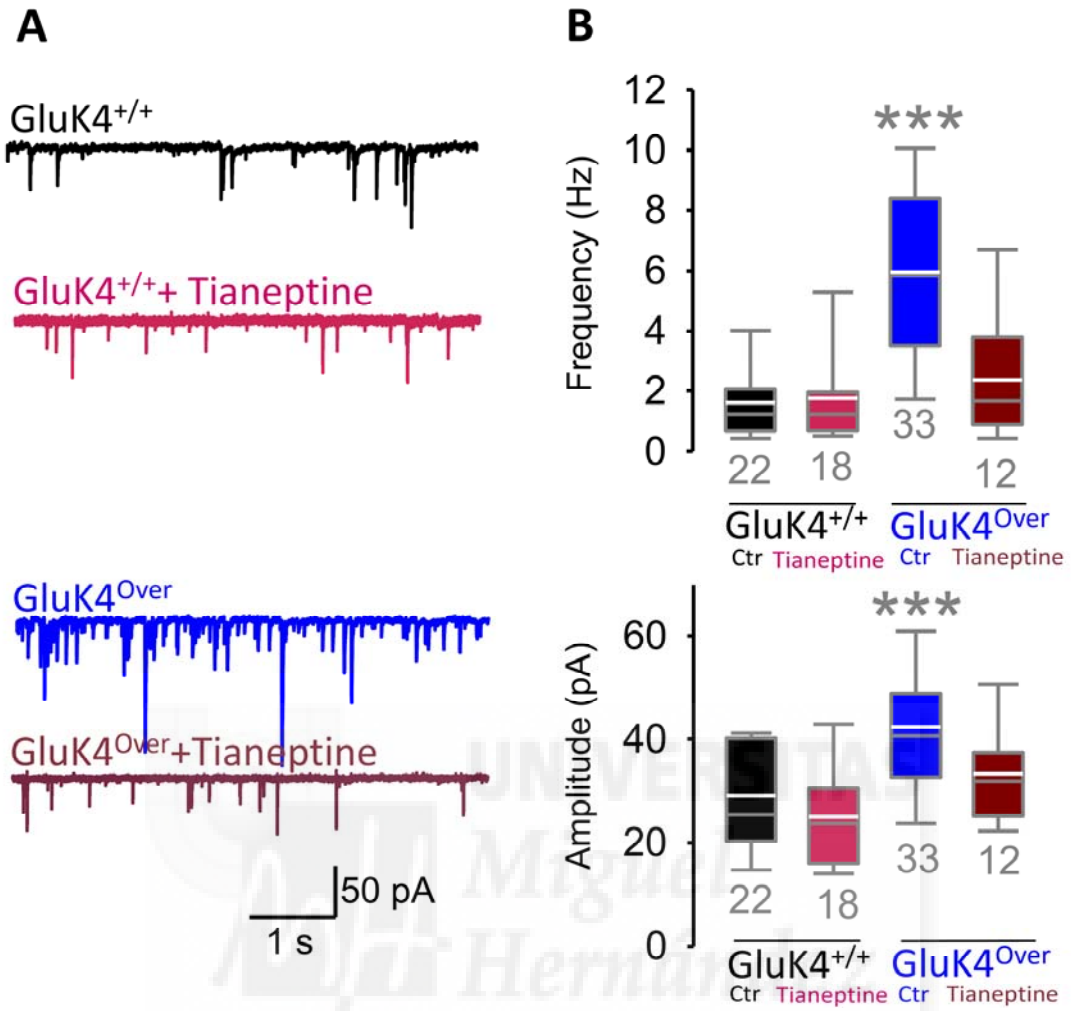

Figure 42: **Tianeptine 1h-exposure restores both mEPSC$_{AMPARs/KARs}$ frequencies and amplitudes in GluK4^{Over} mice. A)** Representative examples of mEPSC$_{AMPARs/KARs}$ traces (Vm=-75 mV) recorded in CA3 pyramidal cell of each genotype in both control and Tianeptine treatment conditions. **B)** Quantification of all recordings shows the restoration of frequency and amplitude values by Tianeptine exposure of GluK4^{Over}, but not GluK4$^{+/+}$ slices. The numbers under the box indicate cells/slices recorded from 3 mice for each genotype in each condition. ***p<0.001; ANOVA on ranks.

The treatment with Tianeptine normalized both the frequency of mEPSC$_{AMPAR/KARs}$ (5.96±0.51Hz *vs* 2.37±0.61Hz in GluK4^{Over} without and with Tianeptine, respectively; n = 12; Fig.42) and PPR values (3.20±0.13 *vs* 4.58±0.23 in GluK^{Over} without and with Tianeptine, respectively; n = 25, Fig. 43) in GluK4^{Over} slices having no action on WT mice.

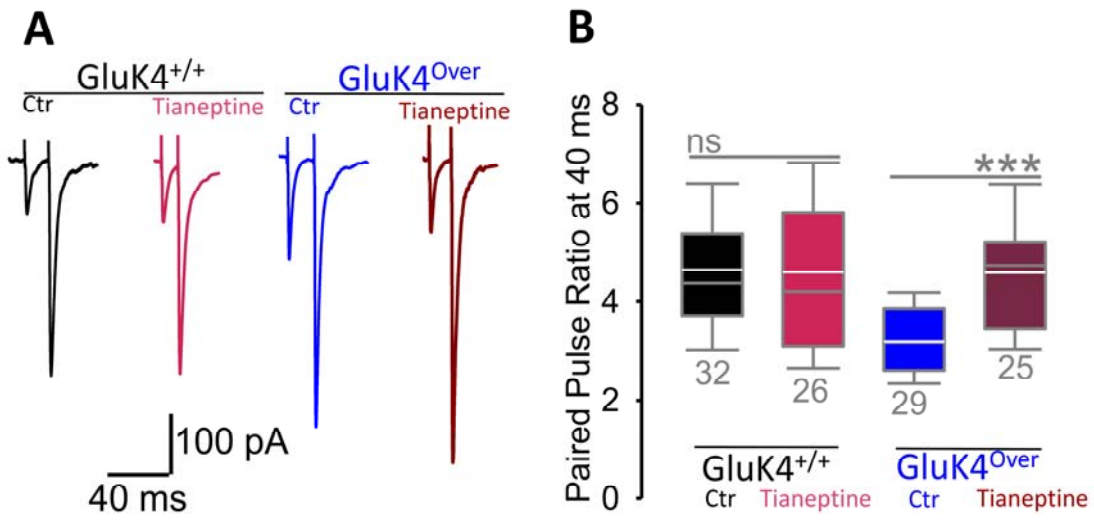

Figure 43: Presynaptic effects of Tianeptine. A) Paired pulse recordings showing the effect of Tianeptine on both genotypes**. B**) Pool data result in the increase of PPR in GluK4^{Over} mice after Tianeptine incubation, but no effects on GluK4$^{+/+}$ mice. The numbers under the box indicate cells/slices recorded from 3 mice for each genotype in each condition. ***p<0.001; ANOVA on ranks.

Tianeptine also restored amplitudes of mEPSC$_{AMPAR/KARs}$ in GluK^{Over} (42.4±2.5 pA *vs* 33.3±2.8 pA without and with Tianeptine, respectively; n = 12, Fig. 42). Interestingly, the RI$_{AMPAR}$ was also restored to normality (0.34±0.21 in GluK^{Over} *vs* 0.63±0.70 without and with Tianeptine, respectively; n = 21, Fig. 44), indicating a postsynaptic action as well.

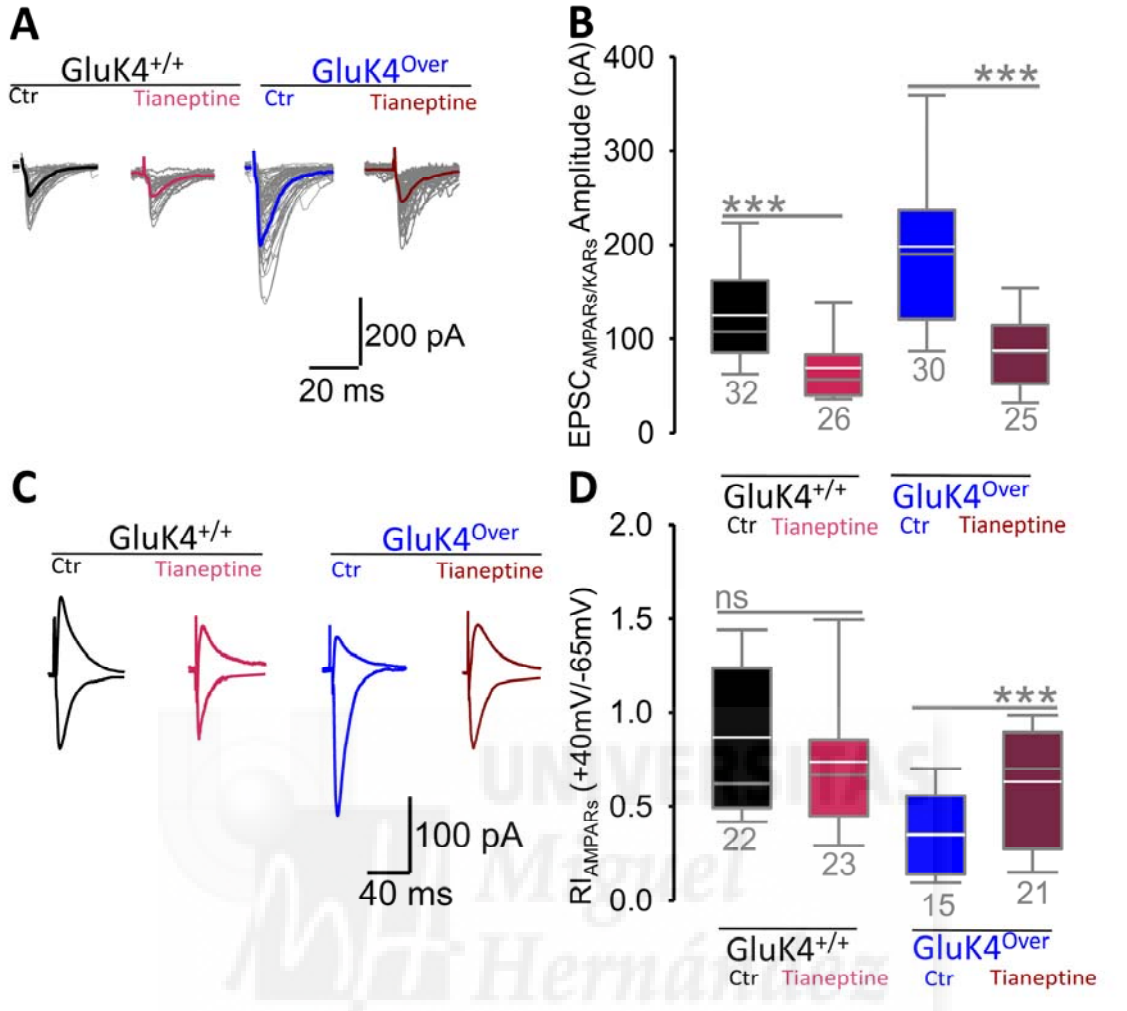

Figure 44: Postsynaptic effect of Tianeptine. A) Tianeptine re-establishes the $EPSC_{AMPARs}$ amplitude in $GluK4^{Over}$ mice, restoring the AMPARs subunit composition as shown by the Rectification Index increase **D)**, without any effect on $GluK4^{+/+}$ mice. The numbers under the box indicate cells/slices recorded from 3 mice for each genotype in each condition. ***p<0.001; ANOVA on ranks.

In order to discard any direct effect of Tianeptine on either KARs or AMPARs channel activity, we also studied the acute effects of Tianeptine. Application of Tianeptine while recording synaptic responses did not produce any alteration of frequency or amplitude of synaptic responses in WT nor $GluK4^{Over}$ as illustrated below (Fig. 45).

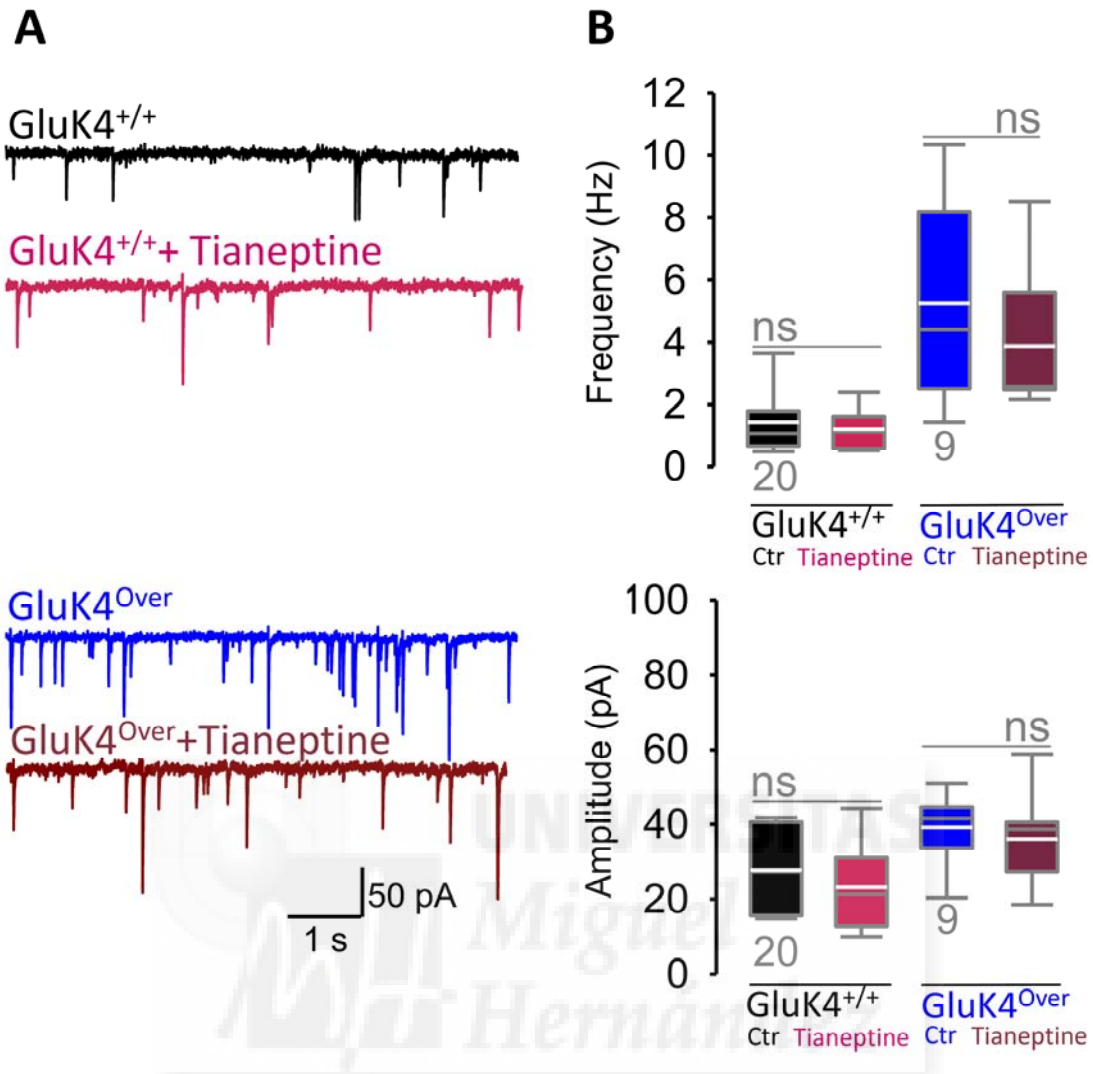

Figure 45: **A)** Representative examples of $mEPSC_{AMPARs/KARs}$ traces (Vm=-75 mV) recorded in CA3 pyramidal cell of each genotype in both control and Tianeptine acute treatment. **B)** Quantification of all recordings shows any effects on frequency values (upper panel) and amplitude values (lower panel) by Tianeptine perfusion in both $GluK4^{Over}$ and $GluK4^{+/+}$ slices. The numbers under the box indicate cells/slices recorded from 3 $GluK4^{+/+}$ mice and 2 $GluK4^{Over}$ mice. ANOVA on ranks.

Taken together these results illustrate the possible mechanism by which Tianeptine reverted depression in $GluK4^{Over}$ mice.

3.11 THE EFFECT CAUSED BY THE OVEREXPRESSION OF GluK4 IS MAINTAINED IN DIFFERENT TRANSGENIC MICE LINES

To discard any action of the insertion point of *grik4* containing the transgene, C57BL/6J-Tg(camk2-grik4)2, another mouse line overexpressing GluK4 protein with a similar level of expression of GluK4 in the forebrain to the previously analyzed, was studied. This was done to assure that the random insertion site of the *grik*4 transgene was no other genes related to the observed phenotypic

changes. For this purpose, we performed the same battery of initial experiments. Spontaneous EPSCs mediated by KARs were recorded to confirm the existence of functional KARs containing exogenous GluK4. Coherent with previous observations relative to the principal mouse line, these mice showed larger $sEPSC_{KARs}$ amplitude in CA3 pyramidal neurons than their wild type siblings (5.08±0.44 pA, *n* = 10 and 3.75±0.22 pA, *n* = 10 for $GluK4^{Over}$ and $GluK4^{+/+}$, respectively; p<0.01), and the events presented faster deactivation rates (64.2±8.45 ms and 41.4±4.1 ms for $GluK4^{+/+}$ and $GluK4^{Over}$, respectively; p<0.05) (Fig. 46).

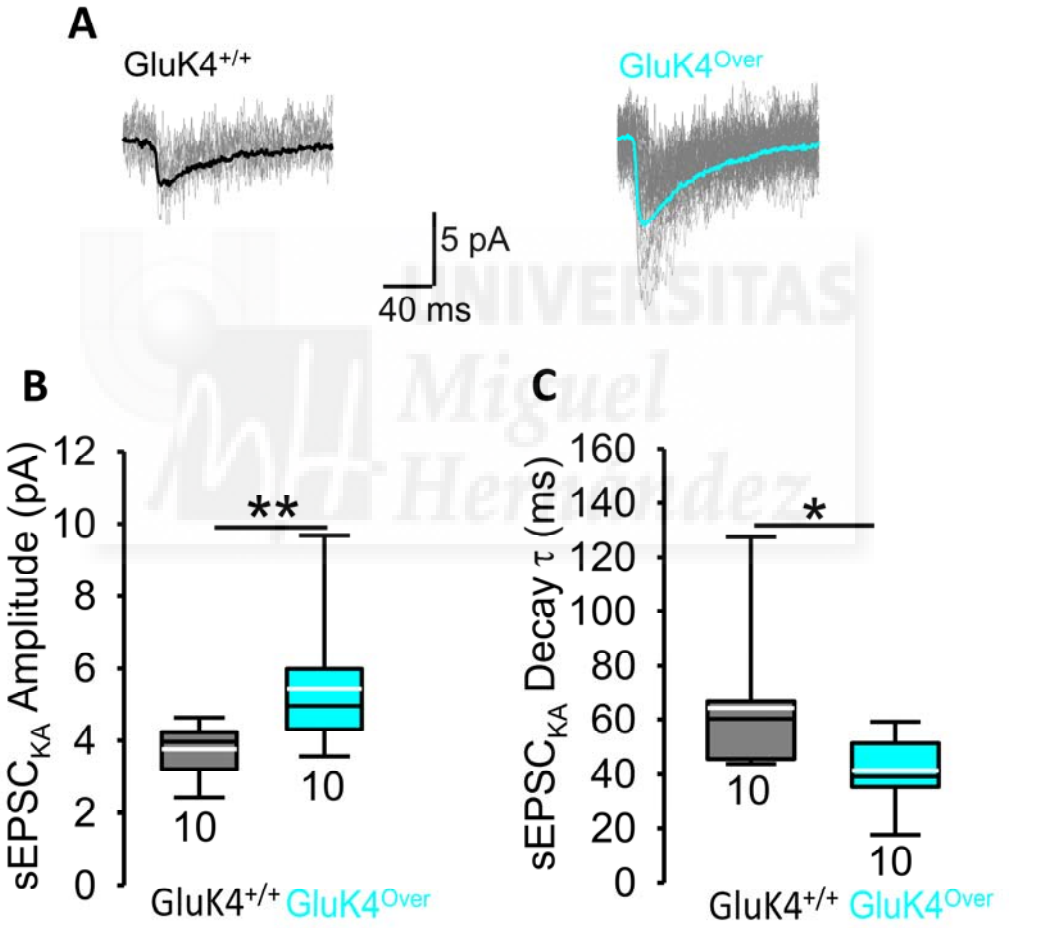

Figure 46: **$sEPSC_{KARs}$ are increased in their amplitudes and frequency in C57BL/6J-Tg(camk2-grik4)2 mouse line. A)** Examples of 20 $sEPSC_{KARs}$ traces for each genotype; mean amplitude of $GluK4^{Over}$ mice (blue line) is larger than the mean amplitude of $GluK4^{+/+}$ mice (black line); **B)** pooled data from 10 cells of each genotype showing a significant difference between $GluK4^{Over}$ and $GluK4^{+/+}$; $GluK4^{Over}$ cells show faster kinetic compared to $GluK4^{+/+}$ cells. **p*<0.05 ***p*<0.01; Mann-Whitney rank-test.

AMPARs-mediated transmission was studied observing the same changes as in the other $GluK4^{Over}$ mouse line: GluK4 overexpression settles higher values for EPSCs amplitudes (176.7±14.9 pA for $GluK4^{Over}$ *vs* 99.5±7.0 pA for $GluK4^{+/+}$) and

lower values for both PPR (3.19±0.13 for GluK4^{Over} *vs* 5.08±0.44 pA for GluK4$^{+/+}$) and FF (345.5±39.4 pA for GluK4^{Over} *vs* 515.5±52.7 pA for GluK4$^{+/+}$).

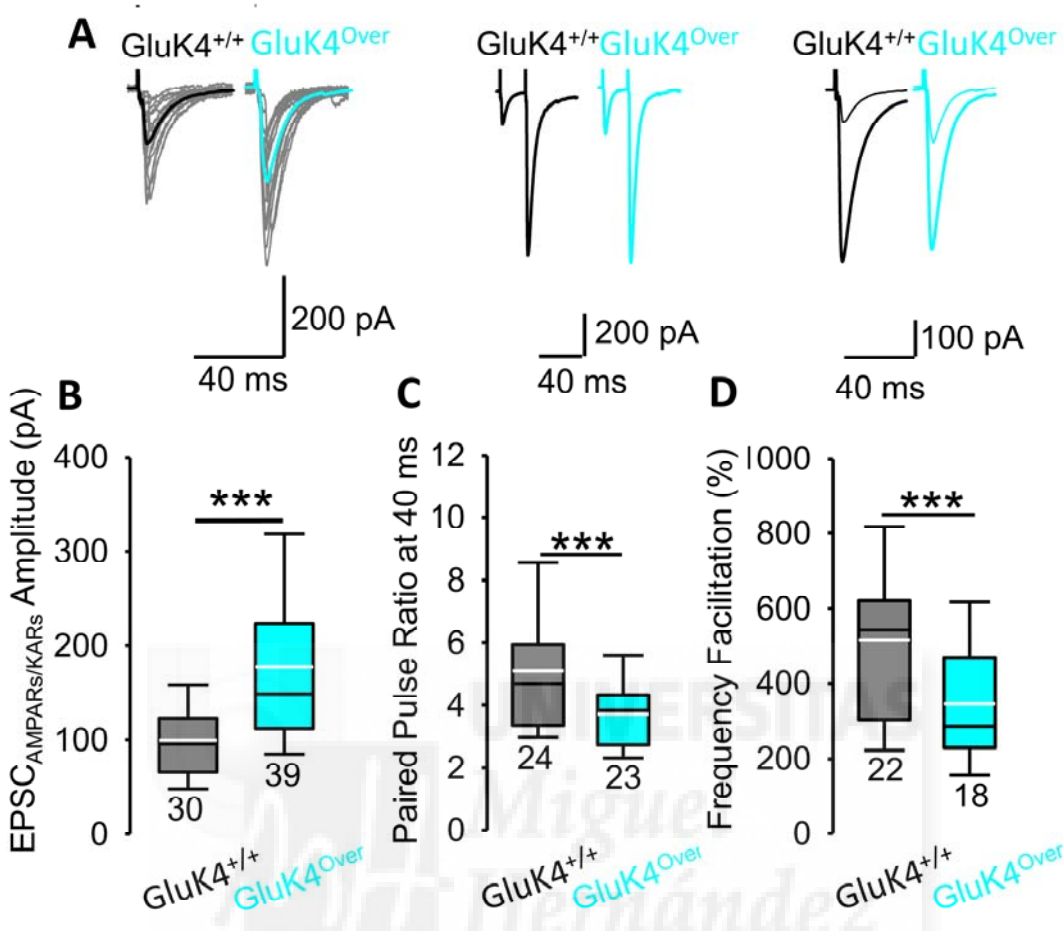

Figure 47: **C57BL/6J-Tg(camk2-grik4)2 mouse line shows the same phenotypic changes of C57BL/6J-Tg(camk2-grik4)2 mouse line. A)** from the left to the right, representative recordings of $EPSC_{AMPARs}$ PPR and FF from GluK4^{Over} (cyan) mice and GluK4$^{+/+}$ (black) mice, where GluK4^{Over} neurons have higher $EPSC_{AMPARs}$, decreased PPR and FF compared to wild type mice. ***p<0.001; Mann-Whitney rank-test.

These data confirm that the GluK4^{Over} phenotype studied is exclusively linked to the alteration in GluK4 protein level in our transgenic mice.

3.12 SYNAPTIC CHANGES IN GluK4^{Over} MICE ARE COMPLETELY RESCUED AFTER RESTORING THE EXPRESSION OF *grik4* GENE

To examine whether restoring the levels of GluK4 could rescue the functional alterations observed in the transgenic mice, we crossed GluK4^{Over} mice with GluK4$^{-/-}$ mice. The GluK4^{RCV} mice obtained by this cross restored the expression level of GluK4 protein. The Western blot in Fig. 48A shows that the exogenous

GluK4 protein was exclusively expressed in GluK4^{RCV}, somehow restoring the levels of the protein towards the normal situation.

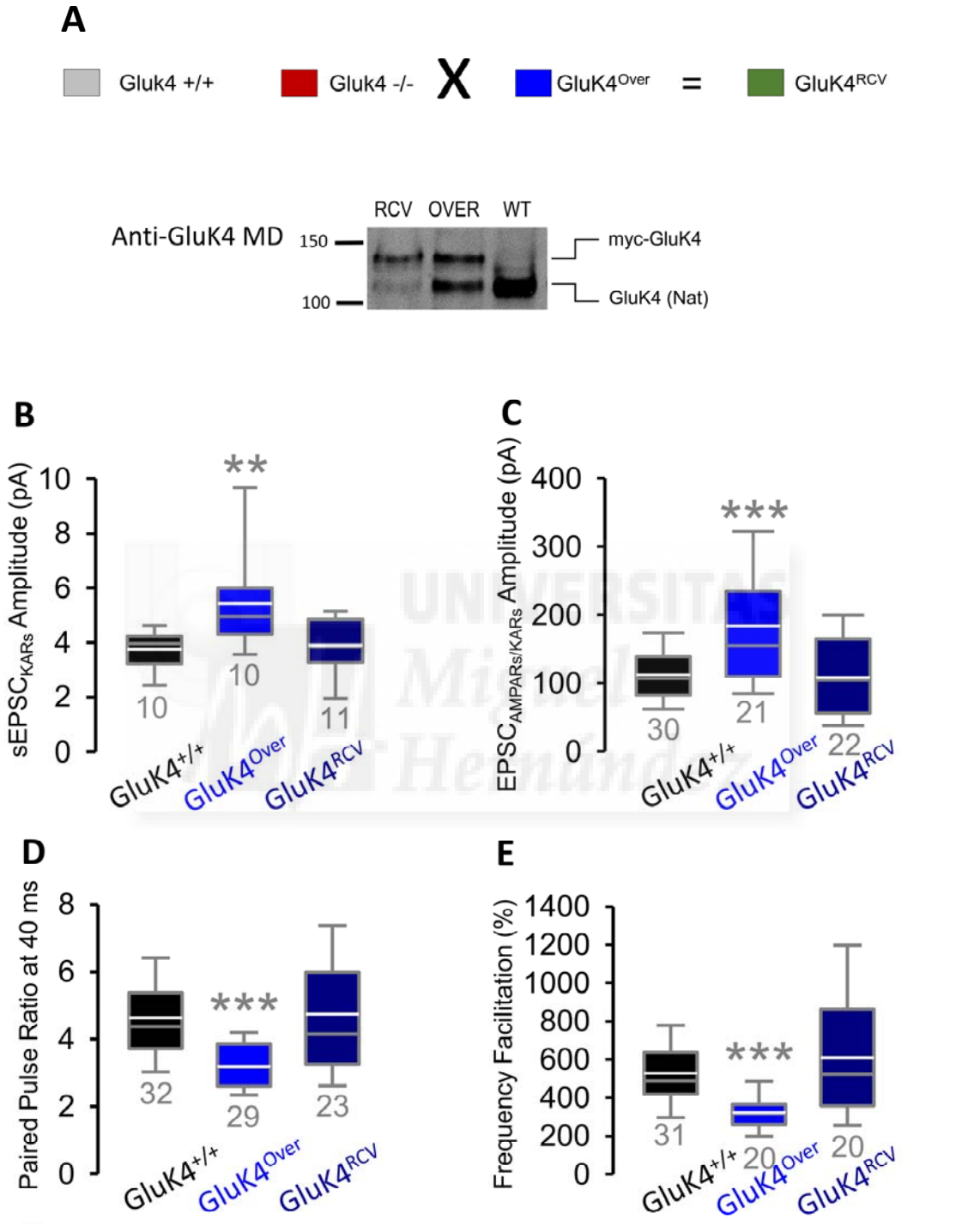

Figure 48: Restoring the normal levels of GluK4 protein and synaptic alterations in GluK4^{RCV} mice. **A)** GluK4^{RCV} results in restoration of GluK4 protein level. **B)** GluK4^{RCV} results in restoration of sEPSC$_{KARs}$ **(C)**, EPSC$_{AMPARs}$ **(D)** PPR and **(E)** FF. The numbers under the box indicate cells from 3 mice for each genotype. **p<0.01, ***p<0.001; ANOVA on ranks.

Normalization of GluK4 protein levels rescued the normal synaptic phenotype inthat GluK4^{RCV} showed normal WT values in sEPSC$_{KAR}$, EPSC$_{AMPARs}$ amplitude, PPR and FF as shown in Fig. 48.

These results confirm again that altering dosage of a single gene of the glutamatergic system is enough to alter the synaptic information transfer through MFs-CA3 synapses.

UNIVERSITAS
Miguel
Hernández

4. Discussion

UNIVERSITAS
Miguel
Hernández

In this work we aimed to delineate the role played by KARs by using a novel transgenic mouse overexpressing one of the high-affinity subunits of these receptors, GluK4. We showed that *grik4* overexpression results in an extensive change in the glutamatergic system, causing a complex and diversified alteration of synaptic function in the hippocampus, where the overexpressed GluK4 protein determines more efficient information transfer through the MFs-CA3 synapses in a specific manner, without altering Schaffer Collateral-CA1 connection. The altered synaptic information flow in MFs-CA3 cells synapses was massive and reflected by remarkable changes in the properties and number of KARs, AMPARs, and NMDARs.

Moreover, through this functional approach, we found that *grik4* overexpressing mouse may be considered a mouse model to directly address circuit dysfunctions associated with autism spectrum disorders (ASDs), given that these mice recapitulate the behavioral symptomatology of autism spectrum disorder, as we already showed in a previous work (Aller et al., 2015).

4.1 EXOGENOUS GluK4 PROTEIN LOCALIZES PRE- AND POSTSYNAPTICALLY AND TAKES PART OF FUNCTIONAL KARs AT MFs-CA3 CELL SYNAPSES

Expression of the GluK4 receptor subunit is restricted to few regions of the brain, with a high level in the CA3 area of the hippocampus and dentate gyrus region, where GluK4 associates with GluK2 but not GluK3 (Darstein et al., 2003), and where KARs are known to modulate circuit activity and synaptic plasticity.

We characterized the myc-GluK4 expression, given that mice overexpressing *grik4* gene were tagged with 5 *myc* epitopes. In particular, two different mouse lines were chosen for their characterization and an exhaustive investigation of *myc-grik4* expression was carried out on them. First, western blots revealed that *grik4* overexpression led to an excess of GluK4 protein content just doubling endogenous levels in the neocortex, and increasing them by ~50% in the hippocampus. Second, *in situ* hybridization of both *grik4* overexpressing mouse lines confirmed the presence of this transgene in the DG and CA3 area of the

hippocampal formation. Third, immunocytochemical studies evidenced exogenous GluK4 expressed on both sides of the MFs-CA3 synapses. Similarly, evaluation of synaptic transmission in the hippocampal CA3 revealed that the presence of more GluK4 protein increased the amplitudes and frequencies of KARs-mediated spontaneous EPSCs, confirming that GluK4 protein participated of new functional KARs at both presynaptic and postsynaptic terminals. These new GluK4-containing KARs showed faster kinetics of deactivation, a property which likely affects KARs synaptic function and neurotransmission in the hippocampal circuitry. A possible explanation for the faster kinetics of the new GluK4-containg KARs could be the stoichiometry of functional KARs, which could incorporate more GluK4 subunits conferring new biophysical properties to GluK4-containing KARs receptors in GluK4 overexpressing mice.

Concerning other KAR subunits, we found that GluK4^{Over} mice present reduced protein levels of GluK5. Surprisingly, we also detected a subtle not significant, decrease in the GluA2/3 protein levels in GluK4^{Over} animals. Therefore, a kind of down-regulation happens for these subunits upon overexpression of GluK4. We could not analyze GluK1 because of the unavailability of a specific antibody. Since GluK4 and GluK5 only form functional receptors in combination with GluK1, GluK2 or GluK3, it can be suggested that the presence of an excess of GluK4 is replacing at some extent GluK5 subunits, therefore reducing their expression, and forming new GluK4-KARs at both sides of the MFs-CA3 cells synapse. Considering the expression of GluK2 and GluK1 in CA3 (Paternain et al., 2000), we can assume that presynaptically new GluK2/GluK4 and/or GluK1/GluK4 receptors could be formed. Postsynaptically, we can assume that heteromeric combinations of GluK2/GluK4 are also produced.

4.2 GluK4-CONTAINING KARs PROVIDE A POSITIVE FEEDBACK IN THE GLUTAMATE RELEASE

At most central synapses, transmitter release can be modulated by various ionotropic and metabotropic presynaptic receptors (Engelman and MacDermott, 2004; Miller, 1998). When terminals express receptors for their own neurotransmitter, an autoregulatory loop is formed that may facilitate (positive feedback) or inhibit (negative feedback) transmitter release, and thereby

contributes to activity-dependent forms of short-term plasticity (Zucker and Regehr, 2002). The hippocampal MFs pathway has proved to be an ideal system for studying the properties of presynaptic ionotropic neurotransmitter receptors and, in particular, it is well accepted that the kainate subtype of ionotropic glutamate receptor is abundant at MFs. Presynaptic, KARs at MFs are reportedly activated by endogenous glutamate (Schmitz et al., 2000) and thus contribute to the robust use-dependent facilitation of transmitter release observed during increased presynaptic activity (Contractor et al., 2001; Lauri et al., 2001, 2003; Pinheiro et al., 2007). Additionally, several studies have suggested that presynaptic KARs may facilitate the induction of MFs-CA3 long-term potentiation (LTP) (Bortolotto et al., 1999; Contractor et al., 2001; Lauri et al., 2001, 2003; Pinheiro et al., 2007, Schmitz et al., 2003). However, the subunit composition of presynaptic KARs as well as how and when they exactly modulate glutamate release remain still controversial. Here, we provide evidence that GluK4-containing KARs are responsible for increasing glutamate release from MFs contacting CA3 pyramidal neurons upon their activation by ambient glutamate. Higher frequencies of AMPARs/KARs-mediated mEPSCs support the idea that the overexpression of *grik4* gene determines an increase of the probability of glutamate release, although the alteration in the number of release sites could not be excluded. This was even clearer when we looked at the amplitude distributions of $mEPSC_{AMPARs/KARs}$ recorded at 0.2 mM Ca^{2+}. In fact, when extracellular Ca^{2+} was reduced, $mEPSC_{AMPARs/KARs}$ frequency fell abruptly to about half the control value in $GluK4^{Over}$ mice and the larger events were almost eliminated, meaning that a Ca^{2+}-dependent mechanism is responsible for the altered probability of glutamate release in our transgenic mice, which promotes a multivesicular release responsible of the largest events. Importantly, the reduction of $mEPSC_{AMPARs/KARs}$ frequency by the application of LY382884, a specific KARs antagonist, and the Ca^{2+}-dependent effect of this compound, lead us to conclude that Ca^{2+}-permeable KARs directly contribute to modify synaptic transmitter release at MFs-CA3 cells synapses. The new KARs with a different stoichiometry incorporating GluK4 would have a higher affinity for glutamate becoming susceptible to activation by ambient glutamate. It is generally assumed that the balance between release and uptake mechanisms determines the concentration of neurotransmitter in the extracellular space of the CNS and that

between each episode of synaptic activation the neurotransmitter concentration within and outside the cleft is maintained at very low levels, preventing continuous activation or desensitization of receptors. In our case, receptors with higher affinity can bind glutamate at a lower concentration and through their tonic activation increase the basal probability of release. This is further confirmed by the fact that GluK4^{Over} mice presented markedly altered functional properties though to reflect presynaptic mechanisms, such as PPR and FF, which magnitude is inversely related to the initial probability of release. Results with KARs antagonist UBP310, which rescued both PPR and FF in GluK4^{Over} but not in GluK4$^{+/+}$ mice, are entirely consistent with this idea. Originally developed as a GluK1-selective antagonist (Dolman et al., 2007), UBP310 potently antagonizes GluK3 homomers (Perrais et al., 2009) and recombinant GluK2/5 and likely GluK2/GluK4 receptors. It has been shown that UBP does not have any effect on presynaptic wild-type MFs terminals (Perrais et al., 2009). Its action in the GluK4^{Over} mice indicates that presynaptic receptors in these mice are enriched with GluK4.

A functional assay showed that LY382884 acts as an antagonist of heteromeric KARs containing a GluK1 subunit, such as GluK1/GluK2 and GluK1/GluK5 with similar potency to that for GluK1 alone (Bortolotto et al., 1999; 2001). The sensitivity of glutamate release modulation to these two KARs antagonist, UBP310 and LY382884, evidenced that GluK4 overexpressing mice have presynaptic receptors also incorporating GluK1 whose function is to provide a positive feedback in the glutamate release. Thus, GluK4-containing KARs finely tune transmitter release affecting the properties of synaptic information flow from DG and in a subtle and complex way they influence the CA3 network activity.

4.3 LONG-TERM PLASTICITY CHANGES IN GluK4^{Over} MICE

There is a general agreement about that long-term changes in MFs-CA3 are presynaptic (both LTP and LTD), meaning they depend neither on postsynaptic NMDARs and AMPARs activation nor on postsynaptic Ca^{2+}-influx. In this case, Hebbian rules are violated, in that the activation of the presynaptic terminal will alter the synaptic strength at all of its postsynaptic contacts, independent of

postsynaptic coordinated activity. Instead, there is strong evidence for an involvement of presynaptic Ca^{2+}-channels. And it has been shown that presynaptic mGluRs and KARs might have a role in, but are not essential for, the induction of LTP at MFs–CA3 pyramidal cell synapses (Kapur et al., 2001; Contractor et al., 2001; Lauri et al., 2001, 2003; Bortolotto et al., 2003). These presynaptic forms of LTP and LTD are manifested as long-term changes in the probability of glutamate release. As proven in earlier studies and given that GluK4^{Over} mice displayed a higher probability of glutamate release, we wondered how GluK4 overexpression might affect long-term synaptic changes. Our experiments inducing NMDARs-independent LTP showed that GluK4-overexpression set a higher value for MFs potentiation compared to the wild type case, although they shared the same degree of depression. These results are consistent with studies from GluK4 knockout mice showing reduced LTP (Catches et al., 2012), confirming the idea that our synaptic phenotype, directly linked to *grik4* gene, is characterized by potentiated MFs-CA3 synapses where GluK4-containing KARs are the central pivot. In this scenario, enhanced MFs long-term plasticity may over-activates the same CA3 circuit pattern, generating an improper information transfer process.

4.4 GluK4 OVEREXPRESSION IS REGULATING AMPARs TRAFFICKING IN GluK4^{Over} MICE

Postsynaptic KARs have been shown to regulate synaptic transmission in MFs to CA3 pyramidal neurons (Castillo et al., 1997; Vignes and Collingridge, 1997). Postsynaptic KARs mediate EPSCs with slow kinetic in CA3 pyramidal cells, providing a temporal summation of synaptic signals and integration of excitatory circuits. GluK4^{Over} mice presented, together with an increase in the number of postsynaptic GluK4-containing KARs, a change in the AMPARs-mediated currents. Firstly, both the quantal content, evidenced by the $mEPSC_{AMPARs/KARs}$ amplitude distributions, and evoked $EPSC_{AMPARs/KARs}$ amplitudes were increased in GluK4^{Over} animals. We showed that lowering the extracellular Ca^{2+} caused a huge decrease in the probability to get events with the largest amplitude. Therefore, higher probability of release must affect the mean overall amplitude of

$mEPSC_{AMPARs/KARs}$ in GluK4^{Over} mice. However, we were still able to observe a difference in $mEPSC_{AMPARs/KARs}$ amplitude between the two genotypes under a condition that minimize the appearance of large synaptic events. We attributed this change mainly to an increase in the AMPARs conductance in GluK4^{Over} neurons, considering that the contribution of new postsynaptic GluK4-KARs to the overall $mEPSC_{AMPARs/KARs}$ amplitude was low. Indeed, the frequency and amplitude of these events was tenfold lower than those observed for AMPARs-mediated events. The decrease of the $mESPC_{AMPARs/KARs}$ mean amplitude caused by the application of LY382884 can be also explained as an indirect effect of this compound on presynaptic GluK1/GluK4 KARs on the probability of release and thus on the postsynaptic current. In addition, after antagonist treatment, $mEPSC_{AMPARs/KARs}$ amplitudes were still higher in GluK4^{Over} than GluK4$^{+/+}$ mice. Thus, new postsynaptic GluK4–KARs are contributing not only to the increased $sEPSC_{KARs}$ but also indirectly to the enhancement of AMPARs-mediated transmission. The lower rectification index of AMPARs currents in GluK4^{Over} mice led us to conclude that new CP-AMPARs, with higher conductance, are inserted at the postsynaptic membrane in these mice. An additional proof in favor of this conclusion is the restoration of evoked-$EPCS_{AMPARs/KARs}$ amplitudes upon the application of IEM-1460, an open channel blocker of CP-AMPARs and KARs. The rectification index was rescued by this compound which strongly indicates that new CP-AMPARs were inserted at postsynaptic terminals of GluK4^{Over} animals. Considering the RI values and the single channel conductance values for the different AMPARs subunit combinations, we conclude that CP-AMPARs replace CI-AMPARs, through the removal of GluA2 containing CI-AMPARs at the same time as the addition of CP-AMPARs. Although this could result in no net increase in total receptor number, it could still lead to a synaptic potentiation, because of the higher conductance of CP-AMPARs. In contrast to the normal physiological prevalence of Ca^{2+}-impermeable AMPARs at mature hippocampal MFs-CA3 pyramidal neuron synapses (Ho et al., 2007), GluK4^{Over} CA3 neurons rather contain Ca^{2+}-permeable AMPARs contributing to the fast excitatory glutamatergic transmission.

4.5 GluK4^{Over} MICE SHOW SOME IMPAIRED/ DELAYED FUNCTIONAL PROPERTIES IN THE GLUTAMATERGIC TRANSMISSION

Several aspects of our results account for an impaired or delayed maturation of MFs-CA3 synapses. First of all, KARs tonic activity is responsible for enhancing the probability of release from MFs terminals in GluK4^{Over} mice. KARs are developmentally regulated, and their temporal and spatial expression in some brain regions is compatible with their crucial functions in controlling the maturation of neuronal networks. For instance, at developing MFs-CA3 synapses, presynaptic KARs facilitate glutamate release and promote induction of LTP during high-frequency transmission (Schmitz et al., 2001). It is well established that presynaptic KARs tonic activity is a hallmark of the immature brain and it is switched off during development in an activity-dependent manner as a result of the loss of high-affinity receptors (Lauri et al., 2006).

Another point reinforcing our idea of an immature synapse is the Ca^{2+} permeability of KARs autoreceptors, provided by the action of IEM-1460 on $mEPSC_{AMPARs/KARs}$ frequencies and paired pulse ratios. It should be remembered that, during early development, a high proportion of GluK1 and GluK2 KARs subunits are unedited at the Q/R site and hence calcium permeable (Bernard et al., 1999; Lee et al., 2001) and calcium flux via KARs may facilitate release at the MFs pathway during early development (Pinheiro et al., 2007; Lauri et al., 2003). Another example of the developmentally regulated Ca^{2+} permeability of KARs is represented by their presence at DRG neurons from late embryonic and newborn rats, being predominantly Ca^{2+}-permeable but becoming fully Ca^{2+}-impermeable later in the first postnatal week (Lee et al., 2001).

In our case, the excess of the high-affinity subunit GluK4 generates presynaptic Ca^{2+}- permeable KARs, incorporating also GluK1, which persist until adult age.

The presence of GluA2-lacking, CP^{-}AMPARs in GluK4^{Over} CA3 pyramidal cells provide another feature indicating the immature nature of MFs-CA3 neuron synapses because AMPARs that lack the GluA2 subunit have traditionally been associated with early development, and have been shown to be Ca^{2+}-permeable

(Geiger et al., 1995; Gu et al., 1996; Washburn et al., 1997). The larger amplitude observed both in the elementary $EPSC_{AMPARs/KARs}$ and in the evoked $EPSC_{AMPARs/KARs}$ as well as their faster kinetics could be, in part, accounted for the insertion of AMPARs lacking GluA2 in $GluK4^{Over}$ mice instead of AMPARs containing GluA2. The presence of CP-AMPARs was also revealed in $GluK4^{Over}$ mice by their different degree of current rectification. In fact, $GluK4^{Over}$ mice showed a lower rectification index, compared to control mice, with values closely to values observed in $GluK4^{+/+}$ juvenile (P13/P14) mice. Recovery of the evoked $EPSC_{AMPARs}$ and, most importantly, the rescued of the rectification index by the application of the Ca^{2+}-channel blocker IEM-1460 confirmed the insertion of new CP-AMPARs in the postsynaptic density of $GluK4^{Over}$ CA3 cells.

Finally, the NMDA hypofunction observed in $GluK4^{Over}$ mice, evidenced by smaller NMDARs-mediated EPSCs, likely is the result of these receptors incorporating a higher amount of NR2B subunit. This is inferred from the slower kinetics that NMDARs-mediated current presented in $GluK4^{Over}$ mice. Typically, NR2B subunits are abundant at early developmental stages and are progressively replaced by NR2A during development (Monyer et al., 1994). The general assumption is that synapses at earlier stages of development contain NMDARs with higher levels of NR2B.
Taking all together, we can conclude that overexpression of *grik4* gene impedes the proper functional maturation of MFs-CA3 cells synapses.

4.6 MOLECULAR MECHANISMS REGULATING CHANGES IN $GluK4^{Over}$ MICE ARE PKC-DEPENDENT

The developmental switch in KARs function in the hippocampus is also associated with a change in their downstream signaling. Numerous studies provided evidence for KARs action mediated by PKC. For instance, in interneurons, KARs modulate the GABA release via a second messenger cascade where PKC is participating (Rodriguez Moreno and Lerma, 1998). In addition, in the hippocampus, the PKC dependence of presynaptic KARs signaling has been also shown in the CA3-CA1 connections (Lauri et al., 2005, 2006).

Here, we show that tonic activation of presynaptic GluK4-containing KARs increases the probability of glutamate release in the overexpressing mice. Treatment with Calphostin-C reverted $mEPSC_{AMPARs/KARs}$ frequency to normality. However, this happened only at normal extracellular Ca^{2+} concentration (2 mM). When the extracellular Ca^{2+} concentration was lowered to 0.2 mM, the tonically increased probability of glutamate release was not observed, allowing us to consider the following scenario: GluK4-containing KARs are affecting the probability of glutamate release thanks to their ionotropic activity and their Ca^{2+} permeability, which permits the increase in intracellular Ca^{2+} in the MFs terminals favouring PKC activation, which it is well known to produce an enhancement of Ca^{2+}-channel current and a subsequent increase in transmitter release.

On the other hand, the concomitant postsynaptic gain observed in $GluK4^{Over}$ mice reflected both the huge increase in the probability of release but also the insertion of new GluK4-containing KARs and CP-AMPARs, as already described. Taking into account that AMPARs are highly mobile proteins that undergo constitutive and activity-dependent translocation to, and removal from, the synapses, we thought on the possibility that GluK4-containing KARs could modify such a trafficking by activating intracellular cascades involving PKC. The activation of PKC may phosphorylate AMPARs subunits in a way determining a change in the AMPARs subunits composition, coherent with previous studies showing the involvement of PKC in the trafficking of AMPARs and their dynamic from extrasynaptic and synaptic sites (Henley et al., 2011).

For this reason, we investigated how GluK4-cointaining KARs were affecting the CP-AMPARs insertion into the postsynaptic membrane. In light of the reversal effects of the Calphostin-C application on amplitudes of $mEPSC_{AMPARs/KARs}$, we initially thought on a mechanism mediated by protein phosphorylation. Instead, the results obtained from $mEPSC_{AMPARs/KARs}$ recordings at 0.2 mM extracellular Ca^{2+} indicated that the effect of PKC inhibition on $mESPC_{AMPARs/KARs}$ amplitude was predominantly due to the indirect presynaptic reduction of the probability of release. In addition application of Calphostin-C at both $[Ca^{2+}]_e$ did not revert completely $mEPSC_{AMPARs/KARs}$ amplitudes in $GluK4^{Over}$ mice to the respective values observed in $GluK4^{+/+}$ mice, not totally reshaping the amplitude distribution.

This left unanswered the question as to whether GluK4-KARs at postsynaptic sides could trigger the insertion of new CP-AMPARs. Further experiments are needed to figure out which possible mechanism could be responsible for the insertion of new CP-AMPARs at CA3 cell after overexpressing GluK4 subunit.

4.7 GluK4 OVEREXPRESSION RECREATES AUTISM-LIKE PHENOTYPES

KARs have been linked to several brain disorders such as epilepsy, schizophrenia, and autism spectrum disorder (ASDs). A diagnosis of ASDs is determined from the presence of core and profound deficits in social interaction and communication, restricted interests, and inappropriate repetitive activity being easily measured in rodent models (Korff, 2006; Lewis, 2007). Other abnormalities include high prevalence of mental retardation and clinically important common co-morbidities, such as anhedonia, depression, anxiety, epilepsy, and intellectual disabilities. Close to the behavioral features, autism mouse models elucidated also abnormality in synaptic plasticity and neurotransmission. For instance, disruption in the balance between excitation and inhibition is a commonly proposed disease mechanism in ASD, as well as in the common ASDs co-morbid epilepsy (Orekhova et al., 2007; Polleux and Lauder, 2004). There is strong evidence that glutamate receptors are affected in ASDs, like the metabotropic glutamate receptor type 5 (mGluR5), which appears to be an effective pharmacologic target in a number of models of ASDs and there is also evidence of a role for KARs, NMDARs, and AMPARs in the neurophysiology of ASDs, though the relationship between dysfunction in those receptors and ASDs-associated phenotypes is not well understood. Several mouse models have been used to investigate this complex and multigenic disorder leading to long list of candidate genes for autism susceptibility. Our data allowed us to include *grik4* gene in this list, in both direct and indirect way on glutamate receptors-mediated synaptic transmission in the hippocampus.

It has been recently shown that *de novo* copy number variation (deletion or duplication of a chromosomal region) of the human *GRIK4* gene is directly implicated as a risk factor for autism or mental retardation (Griswold et al., 2012). In line with that, we recently showed that mice overexpressing *grik4* in the forebrain displayed several behavioral deficits relevant to all core ASDs-like symptoms, including decreased social interaction, increased anxiety and depression, important common co-morbidities to ASDs. Furthermore, mice without *grik4* showed a totally contrasting phenotype to *grik4* overexpressing mice. While a gain of function of this gene (i.e., GluK4^{Over} mice) induced severe depression and anxiety, loss of GluK4 function (i.e., GluK4 knock-out) caused anxiolytic and antidepressant-like behaviors (Aller et al., 2015; Catches et al., 2012). This antagonistic effect strongly indicates a direct link between autistic like behavior and GluK4 levels in the forebrain, putting the mentioned protein at the level of another KARs subunit, GluK2 subunit, already identified as a likely contributor to ASDs (Jamain et al., 2002; Shuang et al., 2004). GluK4 overexpression alters the synaptic properties of the hippocampal transmission flow, changing the filter properties of MFs-CA3 cells synapses. For this reason, we can speculate that deficits in this mechanism may be one of the causes of the altered behavioral phenotype characterizing these transgenic mice. In favor of this idea, it has been shown that an altered information transfer may not only impact cognition, but also contribute to anxiety disorders, as ASDs, by impairing the ability to discriminate between safe and fearful context with the resulting inability to respond appropriately to situations that have different emotional valence, leading to the generalization observed in certain anxiety disorders.
To give more weight to the GluK4 involvement in ASDs and near to its direct link to ASDs, here, we also showed several indirect effects on other glutamate receptors than KARs and on synaptic glutamatergic transmission caused by *grik4* overexpression. The reported pieces of evidence enriched the already existing studies linking a large family of candidate genes for ASDs, which are involved in the plasticity, maintenance, and development of excitatory synapses.

Considering the upregulation of GluA1 as the mainly determinant of the insertion of new CP-AMPARs in GluK4^{Over} CA3 cells, our data agree with other recent studies linking GluA1 abnormality to ASD's phenotypes. Different ASD-mice

model showed increased AMPARs-mediated EPSC as well as increased expression of GluA1 subunit. For instance naïve excitatory synapses on hippocampal pyramidal neurons from a Rett syndrome mice model have larger AMPARs-mediated evoked EPSCs and mEPSCs, larger AMPAR/NMDAR ratio, reduced inward rectification of AMPAR-mediated EPSCs, and higher surface levels of GluA1 at synapses (Wei et al., 2016). Furthermore, postmortem studies find that humans with ASDs have specific abnormalities in AMPARs, such as the increased levels of GluA1, which may be directly involved in the disease pathogenesis (Purcell et al., 2001).

Downregulation of GluA2 subunit is one of the possible causes determining the presence of CP-AMPAR in our GluK4^{Over} mice and in this case our finding are also consistent with a previous study in which Ramanathan et al. (2004) identified a 19 mb deletion of chromosome 4q in an ASDs child, which included the gene encoding the glutamate receptor GluA2 subunit. In another ASDs mouse model, with Shank3 mutation it has also been shown reduced GluA2 protein levels (Zhou et al., 2016). This latter ASDs mouse model presented also reduced NMDARs-mediated transmission, as our GluK4^{Over} mice do. Regarding the alteration in the NMDARs function, we observed a NMDARs hypofunction coherent with another study, showing that reduced NMDARs function, with consequent decreased NMDAR/AMPAR, contributed to ASD-like behavior in Shank2 mutant mice (Won et al., 2012).

These data first established a theme that glutamatergic dysfunction may primarily impact specific symptom domains within the core- and associated-ASDs features. These include behavioral features like social interaction, anxiety and depression and physiological dysfunction in the glutamate receptors manifested by a complex alteration in the glutamatergic transmission system. Thus, our studies may provide a significant contribution to understand how the ASDs-associated behaviors may be generated by glutamatergic-associated changes within a network where a broader set of aetiologies and phenotypes co-occur and to develop therapeutics to treat glutamate receptor dysfunction in the autistic brain.

4.8 RESCUE OF THE SYNAPTIC PHENOTYPE BY REESTABLISHMENT OF GluK4 LEVEL PROTEIN AND BY Tianeptine TREATMENT

Overexpression of the *grik4* gene in our mouse model resulted in synaptic alterations and autistic-like behaviors including anxiety, social interaction deficits, and depression, leading us to delineate a relationship between ASDs related phenotypes and GluK4-containing KARs. We also found that the same synaptic defects are present in another GluK4–overexpressing mouse line suggesting that the *grik4* gene variation specifically accounts for the changes in the glutamatergic network occurring in the hippocampal MFs-CA3 synapses. We generated a novel mouse model, GluK4^{RCV}, obtained by crossing GluK4$^{-/-}$ with GluK4^{Over} mice, and then showed that setting back to normal the levels of *grik4* gene expression in adult mice led to the restoration of glutamatergic synaptic transmission in the MFs-CA3 area of the hippocampus. We also provided evidence that abnormalities observed in the glutamatergic system, such as mEPSC$_{AMPARs/KARs}$ frequencies and amplitudes, RI and PPR could be rescued by one hour exposure of GluK4^{Over} slices to Tianeptine, an atypical antidepressant. Given the lack of acute effects, this antidepressant is regulating somehow the aberrant downstream intracellular mechanism activated by GluK4-containing KARs and therefore correcting behavioral abnormalities, including depression.

Taking all results together, we propose GluK4^{Over} mice as a powerful tool to understand synaptic dysfunctions and aberrant neurotransmission in ASDs and to provide a helpful advance for preclinical drug development targeting abnormal GluK4-KARs mediated activity in ASDs.

UNIVERSITAS
Miguel
Hernández

5. Conclusions

UNIVERSITAS
Miguel
Hernández

The results obtained in the course of this study are of pioneering nature. Through the analysis of KARs function in the hippocampus, we revealed that overexpression of the GluK4 subunit led to influential changes in the synaptic transmission at MFs-CA3 pyramidal cells synapses highlighting the essential role of the high-affinity GluK4 subunit for the normal ionotropic function of neuronal KARs. In base to these results, the following conclusions may be raised:

1. Overexpression of *grik*4 leads to increased GluK4 protein at synapses, where it takes part of functional KARs.

2. GluK4-containing KARs modulate glutamate release at MFs when activated by ambient glutamate, increasing the gain of those synapses.

3. The overexpression of GluK4 makes adult synapses to retain properties of neonatal synapses, highlighting the central role of GluK4 in the hippocampal circuit development.

4. Some antidepressants (e.g. tianeptine) are effective in restoring to normal altered synaptic gain.

5. These studies enriched the information about the role of GluK4 subunit in KARs physiology and proposed GluK4^{Over} mice as a powerful tool to understand synaptic dysfunctions and aberrant neurotransmission in ASDs to provide a rational approach for pharmacologic drug development targeting abnormal glutamatergic synaptic transmission.

UNIVERSITAS
Miguel
Hernández

6. BIBLIOGRAPHY

UNIVERSITAS
Miguel
Hernández

Abbott LF, Regehr WG (2004). Synaptic computation. Nature 431: 796–803.

Acsády L, Kamondi A, Sik A, Freund T, Buzsaki G (1998). GABAergic cells are the major postsynaptic targets of mossy fibers in the rat hippocampus. J. Neurosci.18: 3386–3403.

Aller MI, Pecoraro V, Paternain AV, Canals S, Lerma J (2015). Increased dosage of high-affinity kainate receptor gene GRIK4 alters synaptic transmission and reproduces Autism Spectrum Disorder feature. J Neurosci. 35: 13619-13628.

Amaral DG and Witter MP (1989). The three-dimensional organization of the hippocampal formation: a review of anatomical data. Neuroscience 31: 571-591.

Amaral DG, Ishizuka N, Claiborne B. Neurons, numbers and the hippocampal network. (1990). Prog Brain Res. 83:1–11.

Bahn S, Volk B, Wisden W. (1994). Kainate receptor gene expression in the developing rat brain. J Neurosci. 14:5525–5547.

Barry MF, Ziff EB (2002). Receptor trafficking and the plasticity of excitatory synapses. Curr Opin Neurobiol 12: 279 –286.

Begni S, Popoli M, Moraschi S, Bignotti S, Tura GB, Gennarelli M (2002). Association between the ionotropic glutamate receptor kainate 3 (*GRIK3*) ser310ala polymorphism and schizophrenia. Mol Psychiatry 7:416–418.

Bernard A, Ferhat L, Dessi F, Charton G, Represa A, Ben Ari Y, Khrestchatisky M (1999). Q/R editing of the rat GluR5 and GluR6 kainate receptors in vivo and in vitro: evidence for independent developmental, pathological and cellular regulation. Eur J Neurosci.11:604–616.

Bliss TV, Lomo T (1973). Long-lasting potentiation of synaptic transmission in the dentate area of the anaesthetized rabbit following stimulation of the perforant path. J. Physiol. 232: 331–356.

Boehm J, Kang MG, Johnson RC, Esteban J, Huganir RL, Malinow R (2006). Synaptic incorporation of AMPA receptors during LTP is controlled by a PKC phosphorylation site on GluR1. Neuron. 51:213-25.

Bortolotto ZA, Clarke VR, Delany CM, Parry MC, Smolders I, Vignes M, Ho KH, Miu P, Brinton BT, Fantaske R, Ogden A, Gates M, Ornstein PL, Lodge D, Bleakman D, Collingridge GL (1999). Kainate receptors are involved in synaptic plasticity. Nature 402, 297–301.

Bortolotto ZA, Lauri S, Isaac JTR, and Collingridge GL (2003). Kainate receptors and the induction of mossy fibre long-term potentiation. Philosophical Transactions of the Royal Society B: Biological Sciences 358: 657–666.

Boulter J, Hollmann M, O'Shea-Greenfield A, Hartley M, Deneris E, Maron C, Heinemann S (1990). Molecular cloning and functional expression of glutamate receptor subunit genes. Science 249:1033–1037.

Breustedt J, Schmitz D (2004). Assessing the Role of GLUK5 and GLUK6 at Hippocampal Mossy Fiber Synapses. J Neurosci. 24:10093–10098.

Bureau I, Bischoff, Heinemann, SF, and Mulle C (1999). Kainate receptor-mediated responses in the CA1 field of wild-type and GluR6-deficient mice. J. Neurosci. 19, 653-663.

Bureau I, Dieudonne S, Coussen F, Mulle C (2000). Kainate receptor-mediated synaptic currents in cerebellar Golgi cells are not shaped by diffusion of glutamate. Proc. Natl.Acad. Sci. U. S. A. 97: 6838–6843.

Burgess N, Maguire EA, O'Keefe J. (2002). The human hippocampus and spatial and episodic memory. Neuron 35: 625-641.

Caiati MD, Sivakumaran S, Cherubini E (2010). In the Developing Rat Hippocampus, Endogenous Activation of Presynaptic Kainate Receptors Reduces GABA Release from Mossy Fiber Terminals. J Neurosci. 30: 1750–1759.

Castillo PE, Malenka RC, and Nicoll RA (1997). Kainate receptors mediate a slow postsynaptic current in hippocampal CA3 neurons. Nature 388: 182–186.

Catches JS, Xu J, and Contractor A. (2012). Genetic ablation of the GluK4 kainate receptor subunit causes anxiolytic and antidepressant-like behavior in mice. Behav. Brain Res. 228: 406–414.

Chittajallu R, Vignes M, Dev KK, Barnes JM, Collingridge GL, Henley JM (1996). Regulation of glutamate release by presynaptic kainate receptors in the hippocampus. Nature 379: 78–81.

Christensen JK, Paternain AV, Selak S, Ahring PK, Lerma J (2004). A mosaic of functional kainate receptors in hippocampal interneurons. J Neurosci. 24:8986–8993.

Contractor A, Swanson GT, Sailer A, O'Gorman S & Heinemann SF (2000). Identification of the kainate receptors subunit underlying modulation of excitatory synaptic transmission in the CA3 region of the hippocampus. J Neurosci. 20: 8269–8278.

Contractor A, Swanson G, Heinemann SF (2001). Kainate receptors are involved in short- and long-term plasticity at mossy fiber synapses in the hippocampus. Neuron 29:209 –216.

Contractor A, Sailer AW, Darstein M, et al. (2003). Loss of kainate receptor–mediated heterosynaptic facilitation of mossy-fiber synapses in KA2$^{-/-}$ mice. J Neurosci. 23:422–429.

Cossart R, Epsztein J, Tyzio R, et al. (2002). Quantal release of glutamate generates pure kainate and mixed AMPA/kainate EPSCs in hippocampal neurons. Neuron 35:147–159.

Darstein M, Petralia RS, Swanson GT, Wenthold RJ, Heinemann SF (2003). Distribution of kainate receptor subunits at hippocampal mossy fiber synapses. J Neurosci. 22:8013-9.

De Rubeis S, He X, Goldberg AP, Poultney CS, Samocha K, Cicek AE, Kou Y, Liu L, Fromer M, Walker S, Singh T, Klei L, Kosmicki J, Shih-Chen F, Aleksic B, Biscaldi M, Bolton PF, Brownfeld JM, Cai J, Campbell NG, et al. (2014). Synaptic, transcriptional and chromatin genes disrupted in autism. Nature 515:209 –215.

Dingledine R, Borges K, Bowie D, Traynelis SF (1999). The glutamate receptor ion channels. Pharmacol. Rev. 51: 7–61.

Dobrunz LE and Stevens CF (1999). Response of hippocampal synapses to natural stimulation patterns. Neuron 22:157-166.

Dolman NP, More JCA, Alt A, Knauss JL, Pentikäinen OT, Glasser CR, Bleakman D, Mayer ML, Collingridge GL, Jane DE (2007). Synthesis and pharmacological characterization of N3-substituted willardiine derivatives: role of the substituent at the 5-position of the uracil ring in the development of highly potent and selective GLUK5 kainate receptor antagonists. J. Med. Chem. 50, 1558–1570.

Dutta S, Das S, Guhathakurta S, Sen B, Sinha S, Chatterjee A, Ghosh S, Ahmed S, Ghosh S, and Usha R (2007). Glutamate receptor 6 gene (GluR6 or GRIK2) polymorphisms in the Indian population: a genetic association study on autism spectrum disorder. Cell. Mol. Neurobiol. 27: 1035–1047.

Ekstrom AD, Kahana MJ, Caplan JB, Fields TA, Isham EA, Newman EL & Fried I (2003). Cellular networks underlying human spatial navigation. Nature 425: 184-188.

Engelman HS, MacDermott AB (2004). Presynaptic ionotropic receptors and control of transmitter release. Nat Rev Neurosci. 5:135-45.

Esteban JA, Shi SH, Wilson C, Nuriya M, Huganir RL, Malinow R (2003). PKA phosphorylation of AMPA receptor subunits controls synaptic trafficking underlying plasticity. Nat Neurosci. 6:136-43.

Evstratova A and Tóth K (2014). Information processing and synaptic plasticity at hippocampal mossy fiber terminals. Front. Cell. Neurosc.

Feng G, Mellor RH, Bernstein M, Keller-Peck C, Nguyen QT, Wallace M, Nerbonne JM, Lichtman JW, SanesJR (2000). Imaging neuronal subsets in transgenic mice expressing multiple spectral variants of GFP. Neuron 28:41–51.

Fernandes HB, Catches JS, Petralia RS, Copits BA, Xu J, Russell TA, Swanson GT, Contractor A (2009).High-affinity kainate receptor subunits are necessary for ionotropic but not metabotropic signaling. Neuron 63:818–829.

Fioravante D, Regehr WG (2011). Short-term forms of presynaptic plasticity. Curr Opin Neurobiol. 2: 269-74.

Fisahn A, Heinemann SF, McBain CJ (2005). The kainate receptor subunit GluR6 mediates metabotropic regulation of the slow and medium AHP currents in mouse hippocampal neurones. J Physiol. 1:199–203.

Foster KA, Kreitzer AC, Regehr WG (2002). Interaction of postsynaptic receptor saturation with presynaptic mechanisms produces a reliable synapse. Neuron 36: 1115–1126.

Foster KA, Crowley JJ, Regehr WG (2005). The influence of multivesicular release and postsynaptic receptor saturation on transmission at granule cell to Purkinje cell synapses. J Neurosci. 25: 11655–1166.

Frerking M, Malenka RC, Nicoll RA (1998). Synaptic activation of kainate receptors on hippocampal interneurons. Nat. Neurosci. 1: 479–486.

Geiger JR, Melcher T, Koh DS, Sakmann B, Seeburg PH, Jonas P, Monyer H (1995). Relative abundance of subunit mRNAs determines gating and Ca^{2+} permeability of AMPA receptors in principal neurons and interneurons in rat CNS. Neuron 15:193–204.

Gerges NZ, Backos DS, Rupasinghe CN, Spaller MR, Esteban JA (2006). Dual role of the exocyst in AMPA receptor targeting and insertion into the postsynaptic membrane. EMBO J. 25:1623-34

Gilman SR, Iossifov I, Levy D, Ronemus M, Wigler M, Vitkup D (2011). Rare de novo variants associated with autism implicate a large functional network of genes involved in formation and function of synapses. Neuron 70:898 –907.

Gratacòs M, Costas J, de Cid R, Bayés M, González JR, Baca-García E, de Diego Y, Fernández-Aranda F, Fernández-Piqueras J, and Guitart M et al. (2009) Identification of new putative susceptibility genes for several psychiatric disorders by association analysis of regulatory and non-synonymous SNPs of 306 genes involved in neurotransmission and neurodevelopment. Am J Med Genet B Neuropsychiatr Genet 150: 808–816.

Griswold AJ, Ma D, Cukier HN, Nations LD, Schmidt MA, Chung RH, et al. (2012). Evaluation of copy number variations reveals novel candidate genes in autism spectrum disorder-associated pathways. Hum. Mol. Genet. 21: 3513–3523.

Gu JG, Albuquerque C, Lee CJ, Mac Dermott AB (1996). Synaptic strengthening through activation of Ca 2-permeable AMPA receptors. Nature 381:793–796.

Guire ES, Oh MC, Soderling TR, Derkach VA (2008). Recruitment of calcium-permeable AMPA receptors during synaptic potentiation is regulated by CaM-kinase I.J. Neurosci. 28: 6000–6009.

Hallermann S, Feitova A, Schmidt H, Wehersmuller A, Silver RA, Gundelfinger ED, Eilers J (2010). Bassoon speeds vesicle reloading at a central excitatory synapse. Neuron 68:710-723.

Henley JM, Barker EA, Glebov OO (2011). Routes, destinations and delays: recent advances in AMPA receptor trafficking. Trends Neurosci. 34: 258–268.

Henneberger C, Papouin T, Oliet SH, Rusakov DA (2010). Long-term potentiation depends on release of D-serine from astrocytes. Nature 463:232–236.

Henze DA, Card JP, Barrionuevo G, and Ben-Ari Y (1997). Large amplitude miniature excitatory postsynaptic currents in hippocampal CA3 pyramidal neurons are of mossy fiber origin. J Neurophysiol 77: 1075–1086.

Henze DA, Wittner L, Buzsáki G (2002). Single granule cells reliably discharge targets in the hippocampal CA3 network in vivo. Nature Neuroscience. 5:790–795.

Herb A, Burnashev N, Werner P, Sakmann B, Wisden W, and Seeburg PH (1992). The KA-2 subunit of excitatory amino acid receptors shows widespread expression in brain and forms ion channels with distantly related subunits. Neuron 8: 775–785.

Ho MT, Pelkey KA, Topolnik L, Petralia RS, Takamiya K, Xia J, Huganir RL, Lacaille JC, McBain CJ (2007). Developmental expression of Ca^{2+}-permeable AMPA receptors underlies depolarization-induced long-term depression at mossy fiber CA3 pyramid synapses. J Neurosci. 27:11651– 11662.

Jamain S, Betancur C, Quach H, Philippe A, Fellous M, Giros B, Gillberg C, Leboyer M, Bourgeron T (2002). Linkage and association of the glutamate receptor 6 gene with autism. Mol Psychiatry 7: 302–310.

Jones MV, Westbrook GL (1996). The impact of receptor desensitization on fast synaptic transmission. Trends Neurosci. 19:96–101.

Jung MW and McNaughton BL (1993). Spatial selectivity of unit activity in the hippocampal granular layer. Hippocampus 3: 165–182.

Juuri J, Clarke VR, Lauri SE, Taira T (2010). Kainate receptor induced ectopic spiking of CA3 pyramidal neurons initiates network bursts in neonatal hippocampus. J Neurophysiol. 104:1696–1706.

Kamiya H, and Ozawa S (1999). Dual mechanism for presynaptic modulation by axonal metabotropic glutamate receptor at the mouse mossy fibre- CA3 synapse. J Physiol. 518: 497–506.

Kapur A, Yeckel M, and Johnston D (2001). Hippocampal mossy fiber activity evoques Ca2+ reléase in CA3 pyramidal neurons via a metabotropic glutamate receptor pathway. Neuroscience 107: 59-69.

Kidd FL, Isaac JT (1999). Developmental and activity-dependent regulation of kainate receptors at thalamocortical synapses. Nature 400: 569–573.

Knight HM, Walker R, James R, Porteous DJ, Muir WJ, Blackwood DHR, and Pickard BS (2012). GRIK4/KA1 protein expression in human brain and correlation with bipolar disorder risk variant status. Am. J. Med. Genet. B. Neuropsychiatr. Genet. 159: 21–29.

Kobayashi K, Manabe T, and Takahashi T (1996). Presynaptic long-term depression at the hippocampal mossy fiber-CA3 synapse. Science 273: 648–650.

Korff S, Harvey BH (2006). Animal models of obsessive-compulsive disorder: rationale to understanding psychobiology and pharmacology. Psychiatr Clin North Am. 29: 371–390.

Lai IC, Liou YJ, Chen JY, Wang YC (2005). No association between the ionotropic glutamate receptor kainate 3 gene ser310ala polymorphism and schizophrenia. Neuropsychobiology 51:211–213.

Lau CG, Zukin RS (2007). NMDA receptor trafficking in synaptic plasticity and neuropsychiatric disorders. Nat. Rev. Neurosci. 8:413–426.

Lauri SE, Bortolotto ZA, Bleakman D, Ornstein PL, Lodge D, Isaac JT, and Collingridge GL (2001). A critical role of a facilitatory presynaptic kainate receptor in mossy fiber LTP. Neuron 32: 697–709.

Lauri SE, Bortolotto ZA, Nistico R, Bleakman D, Ornstein PL, Lodge D, Isaac JT, Collingridge GL (2003). A role for Ca 2^{+} stores in kainate receptor-dependent synaptic facilitation and LTP at mossy fiber synapses in the hippocampus. Neuron 39:327–341.

Lauri SE, Segerstrale M, Vesikansa A, Maingret F, Collingridge GL, Isaac JTR, Taira T (2005). Endogenous activation of kainate receptors inhibits glutamatergic transmission and modulates network activity in the developing hippocampus. J Neurosci. 25: 4473–4484.

Lauri SE, Vesikansa A, Segerstrale M, Collingridge GL, Isaac JT, Taira T. (2006). Functional maturation of CA1 synapses involves activity-dependent loss of tonic kainate receptor-mediated inhibition of glutamate release. Neuron 50:415–429.

Lee CJ, Kong H, Manzini MC, Albuquerque C, Chao MV, Macdermott AB (2001). Kainate receptors expressed by a subpopulation of developing nociceptors rapidly switch from high to low Ca^{2+} permeability. J Neurosci. 21:4572–4581.

Lerma J, Zukin RS & Bennet MVL. (1990). Glycine decreases desensitization of N-methyl-D-aspartate (NMDA) receptors expressed in Xenopus oocytes and is required for NMDA responses. Proceedings of the National Academy of Sciences of the USA 87: 2354-23585.

Lerma J, Paternain AV, Rodriguez-Moreno A, Lopez-Garcia JC (2001). Molecular physiology of kainate receptors. Physiol. Rev. 81:971–998.

Lerma J (2003). Roles and rules of kainate receptors in synaptic transmission. Nat. Rev. Neurosci. 4: 481–495.

Levy D, Ronemus M, Yamrom B, Lee YH, Leotta A, Kendall J, Marks S, Lakshmi B, Pai D, Ye K, Buja A, Krieger A, Yoon S, Troge J, Rodgers L, Iossifov I, WiglerM (2011). Rare de novo and transmitted copy-number variation in autistic spectrum disorders. Neuron 70:886–897.

Lewis MH, Tanimura Y, Lee LW, Bodfish JW (2007). Animal models of restricted repetitive behavior in autism. Behav Brain Res. 176: 66–74.

Le Duigou C, Savary E, Kullmann DM, Miles R (2015). Induction of Anti-Hebbian LTP in CA1 Stratum Oriens Interneurons: Interactions between Group I Metabotropic Glutamate Receptors and M1 Muscarinic Receptors. J Neurosci. 35: 13542-13554.

Li JM, Zeng YJ, Peng F, Li L, Yang TH, Hong Z, Lei D, Chen Z, Zhou D (2010). Aberrant glutamate receptor 5 expression in temporal lobe epilepsy lesions. Brain Res. 1311: 166–174.

Lowry ER, Kruyer A, Norris EH, Cederroth CR, and Strickland, S (2013). The GluK4 kainate receptor subunit regulates memory, mood, and excitotoxic neurodegeneration. Neuroscience 235: 215–225.

Lucifora S, Willcockson HH, Lu CR, Darstein M, Phend KD, Valtschanoff JG, Rustioni A (2006). Presynaptic low- and high-affinity kainate receptors in nociceptive spinal afferents. Pain 120:97–105.

Lyon L, Borel M, Carrión M, Kew JN, Corti C, Harrison PJ, Burnet PW, Paulsen O, Rodríguez-Moreno A (2011).Hippocampal mossy fiber long-term depression in Grm2/3 double knockout mice. Synapse 65: 945–954.

Malenka RC (1994). Synaptic plasticity in the hippocampus: LTP and LTD. Cell 78: 535–53810.

Malinow R, Malenka RC (2002) AMPA receptor trafficking and synaptic plasticity. Annu. Rev. Neurosci. 25: 103–126.

Marchal M, Mulle C (2004). Postnatal maturation of mossy fibre excitatory transmission in mouse CA3 pyramidal cells: a potential role for kainite receptors. J Physiol. 561:27-37.

McNaughton BL, Morris RGM. (1987). Hippocampal synaptic enhancement and information storage within a distributed memory system.Trends Neurosci. 10: 408–415.

Melyan Z, Wheal HV, Lancaster B (2002). Metabotropic mediated kainate receptor regulation of IsAHP and excitability in pyramidal cells. Neuron 34: 107–114.

Miller RJ (1998). Presynaptic receptors. Annu Rev Pharmacol Toxicol. 38:201-27.

Milner B, Squire LR and Eric R. Kandel ER (1998). Cognitive Neuroscience and the Study of Memory. Neuron 20: 445–468.

Minelli A, Scassellati C, Bonvicini C, Perez J, Gennarelli M (2009). An association of GRIK3 Ser310Ala functional polymorphism with personality traits. Neuropsychobiology 59:28–33.

Monyer H, Burnashev N, Laurie DJ, Sakmann B, Seeburg PH (1994). Developmental and regional expression in the rat brain and functional properties of four NMDA receptors. Neuron 3:529-40.

Motazacker MM, Rost BR, Hucho T, Garshasbi M, Kahrizi K, Ullmann R, Abedini SS, Nieh SE, Amini SH, Goswami C, et al. (2007). A defect in the ionotropic

glutamate receptor 6 gene (GRIK2) is associated with autosomal recessive mental retardation. Am. J. Hum. Genet. 81: 792–798.

Mulle C, Sailer A, Perez-Otano I, et al. (1998). Altered synaptic physiology and reduced susceptibility to kainate-induced seizures in GluR6-deficient mice. Nature 392:601–605.

Neher E. (1998). Vesicle pools and Ca^{2+} microdomains: new tools for understanding their roles in neurotransmitter release. Neuron 20:389–399.

Neves G, Cooke SF and Bliss TV (2008). Synaptic plasticity, memory and the hippocampus: a neural network approach to causality. Nat. Rev. Neurosci. 9: 65-75

Nicoll RA, Schmitz D (2005). Synaptic plasticity at hippocampal mossy fibre synapses. Nat. Rev. Neurosc. 6: 863–876.

O'Keefe j, DJ (1971). The hippocampus as a spatial map. Preliminary evidence from unit activity in the freely-moving rat.Brain Research 34: 171–175.

Orekhova EV, Stroganova TA, Nygren G, Tsetlin MM, Posikera IN, Gillberg C, Elam M (2007). Excess of high frequency electroencephalogram oscillations in boys with autism. Biological psychiatry 62: 1022–1029.

Orth A, Tapken D, Hollmann M, (2013). The delta subfamily of glutamate receptors: characterization of receptor chimeras and mutants. Eur. J. Neurosci. 37: 1620–1630.

Oswald RE, Ahmed A, Fenwick MK, and Loh AP (2007). Structure of glutamate receptors. Current Drug Targets 8: 573–582.

Overstreet LS, Jones MV, Westbrook GL (2000). Slow Desensitization Regulates the Availability of Synaptic GABAA Receptors. J Neurosci. 20:7914–7921.

Paternain AV, Morales M, Lerma J. (1995). Selective antagonism of AMPA receptors unmasks kainate receptor-mediated responses in hippocampal neurons. Neuron 14:185–189.

Paternain AV, Herrera MT, Nieto MA, and Lerma J (2000).GluR5 and GluR6 kainate receptor subunits coexist in hippocampal neurons and coassemble to form functional receptors. J Neurosci. 20: 196–205.

Pellegrini-Giampietro DE, Zukin RS, Bennet MV, Cho S, and Pulsinelli WA (1992). Switch in glutamate receptor subunit gene expression in CA1 subfield of hippocampus following global ischemia in rats. Proc. Natl. Acad. Sci. 89: 10499–10503.

Pereda AE (2014). Electrical synapses and their functional interactions with chemical synapses. Nat. Rev. Neurosci. 15: 250–263.

Perrais D, Pinheiro PS, Jane DE, and Mulle C (2009). Antagonism of recombinant and native GluK3-containing kainate receptors. Neuropharmacology 56:131–140.

Pickard BS, Malloy MP, Christoforou A, Thomson PA, Evans KL, Morris SW, Hampson M, Porteous DJ, Blackwood DH, Muir WJ (2006). Cytogenetic and genetic evidence supports a role for the kainate-type glutamate receptor gene, GRIK4, in schizophrenia and bipolar disorder. Mol. Psychiatry 11:847– 857.

Pickard BS, Knight HM, Hamilton RS, Soares DC, Walker R, Boyd JK, Machell J, Maclean A, McGhee KA, Condie A, Porteous DJ, St Clair D, Davis I, Blackwood DH, Muir WJ (2008). A common variant in the 3'UTR of the GRIK4 glutamate receptor gene affects transcript abundance and protects against bipolar disorder. Proc Natl Acad Sci U S A. 105:14940-5.

Pinheiro P and Mulle C (2006). Kainate receptors. Cell Tissue Res. 326: 457–482.

Pinheiro PS, Perrais D, Coussen F, Barhanin J, Bettler B, Mann JR, Malva JO, Heinemann SF, Mulle C (2007). GluR7 is an essential subunit of presynaptic kainate autoreceptors at hippocampal mossy fiber synapses. Proc. Natl. Acad. Sci. U. S. A. 104: 12181–12186.

Polleux F, Lauder JM (2004). Toward a developmental neurobiology of autism. Ment Retard Dev Disabil Res Rev. 10: 303–317.

Purcell AE, Jeon OH, Zimmerman AW, et al. (2001). Postmortem brain abnormalities of the glutamate neurotransmitter system in autism. Neurology 57: 1618–1628.

Ramanathan S, Woodroffe A, Flodman PL, Mays LZ, Hanouni M, Modahl CB, Steinberg-Epstein R, Bocian ME, Spence MA and Smith M (2004). A case of autism with an interstitial deletion on 4q leading to hemizygosity for genes

encoding for glutamine and glycine neurotransmitter receptor sub-units (AMPA2, GLRA3, GLRB) and neuropeptide receptors NPY1R, NPY5R. BMC Medical Genetics 5: 10.

Rodríguez-Moreno A, Herreras O, Lerma J (1997). Kainate receptors presynaptically downregulate GABAergic inhibition in the rat hippocampus. Neuron 19: 893–901.

Rodriguez-Moreno A, Lerma J (1998). Kainate receptor modulation of GABA release involves a metabotropic function. Neuron 20:1211–1218.

Rollenhagen A., Sätzler K., Rodriquez EP, Jonas P, Frotscher M, Lübke JHR (2007).Structural determinants of transmission at large hippocampal mossy fiber synapses. J. Neurosci. 27: 10434–10444.

Rolls ET, Kesner RP (2006). A computational theory of hippocampal function, and empirical tests of the theory. Prog. Neurobiol.79: 1–48.

Rolls ET, Treves A (1998). Neural Networks and Brain Function. Oxford: Oxford University Press

Rozas JL, Paternain AV, Lerma J (2003). Noncanonical signaling by ionotropic kainate receptors. Neuron 39:543-53.

Ruiz A, Sachidhanandam S, Utvik JK, Coussen F, Mulle C (2005). Distinct subunits in heteromeric kainate receptors mediate ionotropic and metabotropic function at hippocampal mossy fiber synapses. J Neurosci. 25:11710-8.

Segerstråle M, Juuri J, Lanore F, Piepponen P, Lauri SE, Mulle C, Taira T (2010). High firing rate of neonatal hippocampal interneurons is caused by attenuation of afterhyperpolarizing potassium currents by tonically active kainate receptors. J Neurosci. 30: 6507–6514.

Salin PA, Scanziani M, Malenka RC, Nicoll RA (1996). Distinct short-term plasticity at two excitatory synapses in the hippocampus. Proc Natl Acad Sci U S A 93:13304–13309.

Scarr E, Beneyto M, Meador-Woodruff JH, and Dean B (2005). Cortical glutamatergic markers in schizophrenia. Neuropsychopharmacology 30: 1521–1531.

Schmitz D, Frerking M, Nicoll RA (2000). Synaptic activation of presynaptic kainate receptors on hippocampal mossy fiber synapses. Neuron 27: 327–338.

Schmitz D, Mellor J, and Nicoll RA (2001). Presynaptic kainate receptor mediation of frequency facilitation at hippocampal mossy fiber synapses. Science 291: 1972–1976.

Schmitz D, Mellor J, Breustedt J, Nicoll RA (2003) Presynaptic kainate receptors impart an associative property to hippocampal mossy fiber longterm potentiation. Nat. Neurosci. 6:1058–1063.

Segerstråle M, Juuri J, Lanore F, Piepponen P, Lauri SE, Mulle C, Taira T (2010). High firing rate of neonatal hippocampal interneurons is caused by attenuation of afterhyperpolarizing potassium currents by tonically active kainate receptors. J Neurosci. 30: 6507–6514.

Shuang M, Liu J, Jia MX, Yang JZ, Wu SP, Gong XH, Ling YS, Ruan Y, Yang XL, and Zhang D (2004). Family-based association study between autism and glutamate receptor 6 gene in Chinese Han trios. Am. J. Med. Genet. B. Neuropsychiatr. Genet. 131: 48–50.

Simmons RM, Li DL, Hoo KH, Deverill M, Ornstein PL, Iyengar S. (1998). Kainate GluR5 receptor subtype mediates the nociceptive response to formalin in the rat. Neuropharmacology 37:25–36.

Song I, Huganir RL (2002). Regulation of AMPA receptors during synaptic plasticity. Trends Neurosci. 25: 578 –588.

Steinberg JP, Takamiya K, Shen Y, Xia J, Rubio ME, Yu S, et al. (2006). Targeted in vivo mutations of the AMPA receptor subunit GluR2 and its interacting protein PICK1 eliminate cerebellar long-term depression. Neuron 49: 845–860.

Sutton MA, Ito HT, Cressy P, Kempf C, Woo JC, Schuman EM (2006). Miniature neurotransmission stabilizes synaptic function via tonic suppression of local dendritic protein synthesis. Cell 125: 785–799.

Takenouchi T, Hashida N, Torii C, Kosaki R, Takahashi T, Kosaki K (2014). 1p34.3 deletion involving GRIK3: Further clinical implication of GRIK family glutamate receptors in the pathogenesis of developmental delay. Am J Med Genet A 164: 456–460.

Tashiro A, Dunaevsky A, Blazeski R, et al. (2003). Bidirectional regulation of hippocampal mossy fiber filopodial motility by kainate receptors: a two-step model of synaptogenesis. Neuron 38:773–784.

Thiagarajan TC, Lindskog M, Tsien RW (2005). Adaptation to synaptic inactivity in hippocampal neurons. Neuron 47: 725–737.

Toth K, Suares G, Lawrence JJ, Philips-Tansey E, McBain CJ (2000). Differential mechanisms of transmission at three types of mossy fiber synapse. J Neurosci. 20: 8279–8289.

Tzounopoulos T, Janz R, Sudhof TC, Nicoll RA, Malenka RC (1998) A role for cAMP in long-term depression at hippocampal mossy fiber synapses. Neuron 21:837–845.

Vignes M, and Collingridge GL (1997). The synaptic activation of kainate receptors. Nature 388: 179–182.

Whalley HC, Pickard BS, McIntosh AM, Zuliani R, Johnstone EC, Blackwood DHR, Lawrie SM, Muir WJ and Hall J (2009). Modulation of hippocampal activation by genetic variation in the GRIK4 gene. Mol Psychiatry.14: 465.

Washburn MS, Numberger M, Zhang S, Dingledine R (1997). Differential dependence on GluR2 expression of three characteristic features of AMPA receptors. J Neurosci. 17: 9393–9406.

Wei L. et al., (2016). Excitatory synapses are stronger in the hippocampus of Rett syndrome mice due to altered synaptic trafficking of AMPA-type glutamate receptors. J Neurosci. 35:13542-54.

Werner P, Voigt M, Keinänen K, Wisden W, and Seeburg PH (1991). Cloning of a putative high-affinity kainate receptor expressed predominantly in hippocampal CA3 cells. Nature 351: 742–744.

Whalley HC, Pickard BS, McIntosh AM, Zuliani R, Johnstone EC, Blackwood DH, Lawrie SM, Muir WJ, Hall J (2009). A GRIK4 variant conferring protection against bipolar disorder modulates hippocampal function. Mol Psychiatry 14:467– 468.

Won H, Lee HR, Gee HY, Mah W, Kim JI, Lee J, Ha S, Chung C, Jung ES, Cho YS, Park SG, Lee JS, Lee K, Kim D, Bae YC, Kaang BK, Lee MG, Kim E (2012). Autistic-like social behaviour in Shank2-mutant mice improved by restoring NMDA receptor function. Nature 486: 261-5.

Yan D, Yamasaki M, Straub C, Watanabe M, Tomita S (2013). Homeostatic control of synaptic transmission by distinct glutamate receptors. Neuron 78: 687–699.

Yang Y, Wang XB, Zhou Q (2010). Perisynaptic GluR2-lacking AMPA receptors control the reversibility of synaptic and spines modifications. Proc. Natl. Acad. Sci. U S A 107: 11999–12004.

Yokoi M, Kobayashi K, Manabe T, Takahashi T, Sakaguchi I, Katsuura G, Shigemoto R, Ohishi H, Nomura S,Nakamura K, Nakao K, Katsuki M, Nakanishi S (1996). Impairment of hippocampal mossy fiber LTD in mice lacking mGluR2. Science 273:645–647.

Zhou Y, Kaiser T, Monteiro P, Xiangyu Zhang X, Van der Goes MS, Wang D et al. (2016). Mice with Shank3 Mutations Associated with ASD and Schizophrenia Display Both Shared and Distinct Defects. Neuron 89: 147–162.

Zucker RS, Regehr WG. (2002). Short-term synaptic plasticity. Annu. Rev. Physiol. 64:355–405.